

**Advanced techniques for postharvest disease
detection, control, and quality enhancement in papaya:
electronic nose analysis and chitosan-zinc oxide
nanoparticle coatings**



By Ayesha Ashraf Khan

**A thesis submitted in fulfilment of the requirement for the degree of Masters of
Research**

**School of Biosciences, Faculty of Science, The University of Nottingham Malaysia
Campus, March 2024**

Abstract

Papaya (*Carica papaya*), a valuable tropical fruit in Malaysia, is highly susceptible to postharvest fungal diseases that can severely affect its quality and lead to economic losses. To address these challenges, this study explored a novel, non-destructive approach using electronic nose (EN) technology, a biosensor capable of detecting quiescent fungal infections by sensing changes in volatile composition, thereby avoiding the invasiveness of traditional methods. Additionally, an eco-friendly and cost-effective edible coating has been investigated as a means to control fungal diseases, providing a comprehensive solution to reduce postharvest losses in papaya.

EN was first investigated for its ability to differentiate between papaya ripening stages. Using the case-based reasoning (CBR) classification method, EN effectively detected differences in odour profiles across different storage days. The similarity percentages were 84.25% between days 1 and 3, 82.81% between days 1 and 5, and 94.19% between days 3 and 5—all below the 98% threshold, confirming distinct changes in volatiles over time. GC-MS analysis validated these findings by identifying potential biomarkers for each stage, including vinyl butyrate on day 1, acetone on day 3, and cyclobutanol on day 5, demonstrating EN's accuracy and sensitivity of EN in tracking papaya ripening.

EN technology was then investigated to determine how early and accurately it could detect quiescent fungal diseases in papayas, focusing on pathogens such as *Colletotrichum gloeosporioides* (CG), *Fusarium solani* (FS), and *Lasiodiplodia theobromae* (BC). EN successfully distinguished volatile profiles between healthy and infected samples, with CG-infected samples showing 94.36% similarity between days 1 and 3, and 91.58% similarity between days 1 and 5, reflecting disease progression. By day 5, BC-infected papayas exhibited distinct profiles with only 83.40% similarity to CG, and GC-MS identified specific potential biomarkers for each pathogen, further supporting EN's pathogen differentiation capability.

Finally, an eco-friendly edible coating combining chitosan with green-synthesised zinc oxide nanoparticles (ZnO NPs) from pandan leaf extract was tested for its efficacy in controlling anthracnose disease in papaya. Increasing concentrations of ZnO NPs in the chitosan solution demonstrated a trend of progressively reduced disease incidence, with 2.5 g/L of ZnO NPs emerging as the optimal concentration. Papayas treated with this chitosan-2.5 g/L ZnO NP coating showed a 63% reduction in disease incidence compared to those treated with chitosan alone. Moreover, the disease severity was reduced by 36.5%, highlighting the effectiveness of the coating in delaying anthracnose onset.

This study highlights EN technology as a rapid, non-destructive tool for detecting ripening stages and fungal infections in papayas, complemented by an eco-friendly ZnO-chitosan coating that offers a sustainable solution to mitigate postharvest losses by delaying onset of infections and extending shelf life, particularly in tropical regions where papaya is economically vital.

Acknowledgment

First and foremost, I want to extend my thanks to the University of Nottingham Malaysia for providing the necessary resources and assistance for completing this research, including financial support and the Research Assistantship (RA).

I am deeply grateful to my supervisor, Prof Asgar Ali, whose consistent guidance, supervision, and encouragement have been invaluable throughout this lengthy process. Without his support, this would not have been achievable. I also extend my heartfelt appreciation to my co-supervisor, Prof Kasturi Muthoosamy, for her steadfast support and scholarly guidance during the research period.

Furthermore, I would like to express my gratitude to the laboratory technicians and my colleagues, Tan Guang Heng and Saran Anandan at the Centre of Excellence for Postharvest Biotechnology lab, as well as the lab technicians at the Engineering Research Building and my peers from the Faculty of Engineering, Newton Lo Well and Adriel Tan Yan Sheng at the University of Nottingham Malaysia for their tireless assistance.

Above all, I want to thank my parents and friends for their unwavering love and support throughout my research journey. A special acknowledgment goes to my friend, Sadheedh Umar Jiffry, for his consistent encouragement and checking my work. Thank you to everyone involved.

Supervisory Committee

Asgar Ali, PhD

Professor

Director of Centre of Excellence for Postharvest Biotechnology

The University of Nottingham Malaysia

(Principal Supervisor)

Kasturi Muthoosamy, PhD

Professor

Foundation in Engineering

(Co-Supervisor)

Declaration

I hereby declare that the thesis is based on my original work except for the quotations and citations, which have been duly acknowledged. I also declare that it has not been previously submitted or concurrently submitted for any other degree at the University of Nottingham Malaysia or other institutions.

Ayesha Ashraf Khan

Date: 26/03/2024

List of Figures

Figure 1.1: Antimicrobial activity and mechanism of bionanocomposite films on fruits (Jafarzadeh et al., 2021)

Figure 2.1: Schematic of the working principle of the electronic nose in characterising the volatile organic compounds released by fruit for early detection and quality monitoring analysis (Graphic created with Microsoft Word software).

Figure 2.2: Schematic of typical electronic nose sensor signal processing for data acquisition (Graphic created with Microsoft Word software).

Figure 2.3: Flowchart of pattern recognition systems available for early detection analysis via EN (Graphic created with Microsoft Word software).

Figure 2.4: Flowchart of early detection tool using an electronic nose for postharvest diseases and postharvest quality (Graphic created with Microsoft Word software).

Figure 2.5: Green synthesis of ZnO NPs using plant extract (Zeghoud et al., 2022)

Figure 2.6: Antifungal activity of ZnO NPs. (a) Fungal cell wall, (b) mechanism of action, (A) destruction of fungal cell wall, (B) DNA disruption, (C) inhibition of protein synthesis, and (D) mitochondrial disruption (Lakshmeesha et al., 2020).

Figure 2.7: Chitosan structure (Ibrahim and Zairy, 2015)

Figure 2.8: Different methods of preparing chitosan–metal nanoparticle solutions and the formation of chitosan shells around the nanoparticles (Frank et al., 2020).

Figure 3.1: Electronic nose principle and experimental setup. (Graphics were designed using the Canva software).

Figure 3.2: Graph of normalized data after averaging all the raw sensor values (Sr1, Sr2, Sr3, Sr4) measured on days 1, 2 and 3 (D1, D3, D5).

Figure 3.3: Loading plot of the first two principal components of PCA for healthy papaya fruit after 5 days of incubation. The numbers indicate the number of replicates. PC1 and PC2 accounted for 70 and 17 % of the variance, respectively.

Figure 4.1: Percentage of papaya samples showing disease symptoms for the control group (H) and each of the four inoculation treatments (CG, GF, BC, and CFB) after 5 days of storage.

Figure 4.2: Percentage of disease severity calculated for the control group (H) and each of the four inoculation treatments (CG, GF, BC, and CFB) after five days of storage.

Figure 4.3: Loading plot of the first two principal components of PCA for papaya fruit samples infected by *Colletotrichum gloeosporioides* (CG) over 5 days (D1–D5) of incubation. The numbers following the label “R” indicate the number of replicates. PC1 and PC2 accounted for 20.8% and 39% of variance, respectively. The coloured circle highlights the grouping based on similarity in the volatile profile, where yellow indicates group 1, blue indicates group 2, and red indicates group 3.

Figure 4.4: Loading plot of the first two principal components of PCA for papaya fruit samples infected with *Lasiodiplodia theobromae* (BC) over 5 days (D1–D5) of incubation. The numbers following the label “R” indicate the number of replicates. PC1 and PC2 accounted for 60 and 73% of the variance, respectively.

Figure 4.5: Loading plot of the first two principal components of PCA for papaya fruit samples infected with *Fusarium solani* (FS) over 5 days (D1–D5) of incubation. The numbers following the label “R” indicate the number of replicates. PC1 and PC2 accounted for 30.8% and 49.3% of variance, respectively.

Figure 4.6: Loading plot of the first two principal components of PCA for papaya fruit samples infected with combination diseases over five days (D1–D5) of incubation. The numbers following the label “R” indicate the number of replicates. PC1 and PC2 accounted for 21.0% and 77.5% of variance, respectively.

Figure 5.1: Illustration of application of Chitosan (CS)-ZnO NPs coatings on papaya for in vivo antifungal assay. Graphic created using Canva software.

Figure 5.2: SEM photographs of ZnO NPs of (a) dry powder at x10000 magnification (b) dry powder at x20000 magnification (c) powder dispersed in water at x50000 magnification.

Figure 5.3: EDX spectrograph of green synthesized ZnO NPs

Figure 5.4: Average size, PDI, and size distribution graph of the green-synthesised ZnO NPs obtained from Zetasizer.

Figure 5.5: Zeta potential graph of green synthesized ZnO NPs obtained from Zetasizer.

List of Tables

Table 2.1: Summary of early detection of postharvest related diseases based on volatiles biomarker of different disease infections from various produce using electronic nose sensors.

Table 2.2: Summary of quality monitoring applications based on key volatile components detected from different crops using electronic nose sensors.

Table 2.3: Recent studies on the preparation procedure of green synthesized ZnO NPs.

Table 2.4: Recent studies on the application of Chitosan-ZnO NPs coating on fresh produce.

Table 3.1: Gas sensor array of the EN system.

Table 3.2: In the table above, 1000 data measurements were collected from 5 repeated experiments for every sample. Sr1, Sr2, Sr3 and Sr4 indicate sensor 1, sensor 2, sensor 3 and sensor 4 respectively. DM represents the data measurement for papaya samples.

Table 3.3: Average of all raw data from 4 sensors after normalisation collected on days 1, 3 and 5 (D1, D3, D5). The highest sensor reading for all samples is at Sr1, hence the values are 1 after normalization.

Table 3.4: Similarity percentages between samples measured on the same day. A percentage similarity of over 99 % indicate that the two samples are significantly similar to each other. Values below 99 or 98 % showed a significantly weak difference.

Table 3.5: Similarity percentages of samples on different days. A percentage similarity of over 99 % shows that the two samples are significantly similar to each other. Values below 99 or 98 % showed a significantly weak difference.

Table 3.6. The overall potential biomarkers of healthy papaya fruit after five days of incubation were determined by GC-MS analysis.

Table 3.7: Mean values (with standard deviations) of quality indices for papaya samples during 5 days of storage. Different letters for the same parameter indicate significant differences between storage days according to ANOVA ($p < 0.05$).

Table 3.8: Spearman correlation between EN sensors and quality indices of papaya.

Table 4.1: Average of all raw data from the four sensors after normalisation from the control group (H), fruit infected with CG, FS, BC, and CFB collected on days 1, 3, and 5 (D1, D3, and D5). Sr1, Sr2, Sr3, and Sr4 denote sensors 1, 2, 3, and 4, respectively. The highest sensor reading for all samples was obtained at Sr1; hence, the values were 1 after normalisation.

Table 4.2: Similarity of each treatment group (CG, FS, BC, and CFB) between different storage days. The average values of replicates from each group were compared. A percentage similarity of over 99% shows that the two samples are significantly similar to each other. Values below 99 or 98% showed a significant weak difference.

Table 4.3: Percentage similarity between papaya samples inoculated with different fungi (CG, FS, BC, and CFB) on days 1, 3, and 5. The average values of replicates from each group were compared. A percentage similarity of over 99% shows that the two samples are significantly similar to each other. Values below 99 or 98% showed a significant weak difference.

Table 4.4: Percentage similarity between each treatment sample (CG, FS, BC, and CFB) and healthy control samples on days 1, 3, and 5 (D1, D3, and D5). The average values of replicates from each group were compared. A percentage similarity of over 99% shows that the two samples are significantly similar to each other. Values below 99 or 98% showed a significant weak difference.

Table 4.5: Disease incidence % measured for the healthy control group (H) and all four fungal inoculation treatments (CG, FS, BC, and CFB).

Table 4.6: Disease severity % measured for the healthy control group (H), and all four different fungal inoculation treatments (CG, FS, BC, and CFB) after 5 days of storage.

Table 4.7: Pictures of disease progression in papaya samples inoculated with different fungi (CG, FS, BC, and CFB) and stored for 5 days.

Table 4.8. Potential biomarkers for papaya (*cv. Sekaki*) fruit infected with CG after 5 d of incubation, based on GC-MS analysis. The number under the area percentage indicates the day of incubation.

Table 4.9. Potential biomarkers for papaya (*cv. Sekaki*) fruit infected with *Lasiodiplodia theobromae* after 5 days of incubation, based on GC-MS analysis. The number under the area percentage indicates the day of incubation.

Table 4.10. Potential biomarkers for papaya (*cv. Sekaki*) fruit infected with *Fusarium solani* after 5 days of incubation, based on GC-MS analysis. The number under the area percentage indicates the day of incubation.

Table 4.11. Potential biomarkers for papaya (*cv. Sekaki*) fruit infected with a combination of diseases after 5 days of incubation, based on GC-MS analysis. The number under the area percentage indicates the day of incubation.

Table 5.1: Photographs of colonies of *Colletotrichum sp.* subjected to different treatments during 7 days incubation: control and ZnO NPs of concentrations 0.5g/L, 1.2g/L and 2.0g/L

Table 5.2. Average fungal growth area (and standard deviations) of *Colletotrichum sp.* and percentage inhibition relative to the control across three treatments over the seven-day

measurement period. Values in the same column with different letters are significantly different, ($p < 0.05$).

Table 5.3. Disease severity average for each treatment group recorded for tested papayas over the storage of 12 days.

Table 5.4: Photographs of papaya samples showing significant differences in disease symptoms under different concentrations of ZnO NPs-0.5g/L, 1.5g/L, 2g/L, 0g/L (Chitosan only) and control, from 8 to 12th day of storage.

List of Abbreviations

1. **ANOVA** - Analysis of Variance
2. **AMB** - Aerobic mesophilic bacteria
3. **BC** - *Botrytis Cinerea*
4. **BPNN** - Backpropagation Neural Network
5. **CBR** - Case-Based Reasoning
6. **CFB** - Combination of Fungal Blends
7. **CFU/g** - Colony Forming Units per gram
8. **CG** - *Colletotrichum gloeosporioides*
9. **CAR** - Carboxen
10. **DVB** - Divinylbenzene
11. **EDX** - Energy-dispersive X-ray spectroscopy
12. **EN** - Electronic Nose
13. **FEM** - Finite Element Method
14. **FDA** - Food and Drug Administration
15. **FESEM** - Field Emission Scanning Electron Microscopy
16. **FS** - *Fusarium solani*
17. **FOX** - Fast Olfaction X (commercial electronic nose)
18. **GC-MS** - Gas Chromatography-Mass Spectrometry
19. **HPLC** - High-performance Liquid Chromatography
20. **HS SPME** - Headspace Solid-phase Micro-extraction
21. **LAMP** - Loop-mediated Isothermal Amplification
22. **LDA** - Linear Discriminant Analysis
23. **MCP** - Methylcyclopropene
24. **MLP** - Multilayer Perceptron
25. **MOS** - Metal Oxide Semiconductors
26. **MOSFET** - Metal Oxide Semiconductor Field-Effect Transistors

27. **NASBA** - Nucleic acid sequence-based amplification
28. **NIR** - Near-Infrared Spectroscopy
29. **PDA** - Potato Dextrose Agar
30. **PDI** - Polydispersity Index
31. **PCR** - Polymerase Chain Reaction
32. **PCA** - Principal Component Analysis
33. **PC-LDA** - Principal Component-Linear Discriminant Analysis
34. **PLS-DA** - Partial Least Squares Discriminant Analysis
35. **PLSR** - Partial Least Squares Regression
36. **PDMS** - Polydimethylsiloxane
37. **RBFNN** - Radial Basis Function Neural Network
38. **SEM** - Scanning Electron Microscopy
39. **SNV** - Standard Normal Variate
40. **SPSS** - Statistical Package for the Social Sciences
41. **SVM** - Support Vector Machine
42. **TA** - Titratable Acidity
43. **TSS** - Total Soluble Solids
44. **SSC** – Soluble solids concentration
45. **VOC** - Volatile Organic Compounds
46. **ZnO NPs** - Zinc Oxide Nanoparticles
47. **L*** - Lightness (a component of the CIELAB color space)
48. **a*** - Red/Green chromaticity (positive a* values indicate red, and negative values indicate green)
49. **b*** - Yellow/Blue chromaticity (positive b* values indicate yellow, and negative values indicate blue)

Table of contents

Advanced techniques for postharvest disease detection, control, and quality enhancement in papaya: electronic nose analysis and chitosan-zinc oxide nanoparticle coatings	1
Abstract	2
Acknowledgment	4
Supervisory Committee	5
Declaration.....	6
List of Figures	7
List of Tables	8
List of Abbreviations.....	11
Table of contents	13
Chapter 1: Introduction	17
Chapter 2: Literature Review	22
Electronic nose as a tool for quality monitoring and early detection of postharvest diseases.....	22
2.1 Fundamental principles of EN.....	22
2.1.1. Sensory array materials	22
2.1.2 Odour sampling.....	25
2.1.3 Disease detection and quality characterization	26
2.1.4 Data acquisition and pattern recognition	27
2.2 EN for early detection of postharvest diseases.....	28
2.3 EN for postharvest quality monitoring.....	37
2.3.1 Freshness quality.....	44
2.3.2 Ripening quality	47
2.3.4 Sensory quality.....	48
2.3.5 Other quality parameters.....	48
Combination of green synthesized ZnO NPs with chitosan as edible coatings to control postharvest fungal diseases.....	50

2.4 Green synthesis of ZnO- NPs using plant extract	50
2.4.1 A general mechanism of the synthesis of ZnO NPs using plant extract	51
2.4.2 Antifungal properties of ZnO NPs	60
2.5 Chitosan as a carrier for metal-oxide nanoparticles to form an edible coating.	62
2.6 Papaya as the crop for this study	74
Chapter 3: Electronic Nose to accurately monitor ripening stages of papaya during post-harvest storage.	77
3.1 Introduction	77
3.2 Methodology	78
3.2.1 Sample preparation	78
3.2.2 Volatile profiling of papaya ripening using EN	78
3.2.3 Volatile profiling of papaya ripening using GC-MS.....	80
3.2.4 Analysis of physicochemical properties of papaya during ripening	81
3.3 Data analysis	82
3.3.1 Data analysis and pattern recognition of EN sensor readings.....	82
3.3.2 EN data preprocessing.....	83
3.3.3 Intelligent classification with Case Based Reasoning method (CBR)	83
3.3.4 Determination of VOCs composition during papaya ripening with GC-MS readings	84
3.3.5 Statistical analysis of physicochemical test results during papaya ripening.....	84
3.4 Results and discussion	85
3.4.1 Change in VOCs profile during papaya ripening detected with EN.	85
3.4.2 Distinguishing the different ripening stages of papaya using CBR classification.....	86
3.4.3 Identifying potential volatile biomarkers at different stages of papaya ripening using GC-MS.....	88
3.4.4 Changes in physicochemical properties during papaya ripening and their correlation with EN readings.	92
3.5 Chapter conclusion	97
Chapter 4: Early detection and classification of major post-harvest fungal diseases in papaya fruit using Electronic Nose	98

4.1 Introduction	98
4.2 Methodology	98
4.2.1 Sample preparation	98
4.2.2 Inoculation	98
4.2.3 Volatile profiling of inoculated papaya samples with EN and GC-MS.....	99
4.3 Data analysis	99
4.3.1 Data analysis and pattern recognition of EN sensor readings and the determination of VOCs composition using GC-MS	99
4.3.2 Disease incidence and disease severity	99
4.4 Results and discussion	100
4.4.1 Distinguishing volatile odour from different papaya fungal infections with EN ...	100
4.4.2 EN to detect the disease progression in papayas during 5 days of storage.	101
4.4.3 EN to distinguish between papayas infected with different fungi.	101
4.4.4 EN to distinguish between infected and healthy papayas during 5 days of storage.	102
4.4.5 Disease incidence and disease severity percentage.....	103
4.4.6 GC-MS analysis of papaya fruit inoculated with CG over 5 days of storage.....	106
4.4.7 GC-MS analysis of papaya fruit inoculated with BC over 5 days of storage.	108
4.4.8 GC-MS analysis of papaya fruit inoculated with FS over 5 days of storage.....	111
4.4.9 GC-MS analysis of papaya fruit inoculated with CFB over 5 days of storage.	113
4.4.10 Relationship between EN sensor responses and GC-MS results.....	116
4.5 Chapter conclusion	117
Chapter 5: Application of chitosan combined with green synthesized ZnO NPs as edible coating to control anthracnose disease in papaya during postharvest storage	118
5.1 Introduction	118
5.2 Materials and methodology	118
5.2.1 Materials.....	118
5.2.2 Pandan (<i>Pandanus amaryllifolius</i>) leaves as the leaf extract	119
5.2.3 Preparation of leaf extract	119
5.2.4 Preparation of ZnO NPs	119

5.2.5 Characterization of nanoparticles.....	120
5.2.6 In vitro antifungal assay of ZnO NPs against Colletotrichum gloeosporioides	120
5.2.7 Preparation of chitosan-ZnO NPs coating treatments	120
5.2.8 Preparation of spore suspensions	121
5.2.9 In vivo antifungal assay of chitosan-ZnO NPs coating against Colletotrichum gloeosporioides	121
5.2.10 Evaluation of disease Incidence and severity	122
5.3 Statistical analysis.....	122
5.4 Results and discussion	123
5.4.1. Characteristics of nanoparticles	123
5.4.2 In vitro antifungal effect of ZnO NPs	125
5.4.3 In vivo antifungal effect of Chitosan-ZnO NPs coating to control anthracnose disease in papayas.....	128
5.5 Chapter conclusion	133
Limitations and Future Directions.....	134
Conclusion	136
List of Publications.....	137
References	138

Chapter 1: Introduction

The postharvest period, spanning from harvesting to consumption, is critical for tropical fruits like bananas, mangoes, and papayas. These fruits are sensitive to environmental conditions, have rapid metabolic rates, and are highly susceptible to pathogens (Israfi et al., 2022). Unlike temperate fruits, tropical varieties undergo significant physiological changes postharvest, including ripening. As climacteric fruits, they experience a sharp increase in respiration regulated by ethylene, which triggers metabolic and biochemical changes, leading to alterations in color, texture, flavor, and aroma (Chan-León et al., 2023). Ethylene influences gene expression associated with softening and flavor development, with enzymes like polygalacturonase and pectin methyl esterase breaking down cell wall components to soften the fruit (Pattyn et al., 2020). However, excessive ethylene exposure can accelerate senescence and decay, making precise management essential during storage and transportation to maintain fruit quality by preventing premature ripening (Establés-Ortiz et al., 2016).

Papaya, a climacteric fruit, is particularly significant in tropical regions like Malaysia due to its nutritional, economic, and health benefits. It is rich in essential vitamins (C, A, E), dietary fiber, and antioxidants, which support immune health, digestion, and reduce chronic disease risk (Pinnamaneni, 2017; Koul et al., 2022). Papayas are also an affordable and easily accessible fruit for low-income populations. Additionally, papayas are a major agricultural product for Malaysia, one of the world's largest papaya producers (Tan et al., 2023). They play a critical role in the local economy by generating income for farmers and contributing to exports. In 2019, Malaysia exported over 19.02 million tonnes of papayas, valued at \$7.44 million (Tan et al., 2023).

Despite their profound nutritional and economic importance, papayas are highly susceptible to postharvest losses due to their high moisture content and thin skin, making them vulnerable to fungal diseases during storage and transportation (Israfi et al., 2022). These fungal diseases significantly impact papaya shelf life, quality, and market value, posing challenges for producers and exporters. Addressing these challenges is crucial for improving food security and ensuring the continued availability of this nutritious fruit for diverse populations.

Traditional pathogen detection methods involve culturing microorganisms on agar plates and using biochemical identification techniques. Although effective, these methods are time-consuming, often requiring days for preliminary identification, and even longer for species confirmation (Law et al., 2015). The process involves multiple steps, such as media preparation, inoculation, and colony counting, and may not always achieve the required sensitivity and specificity (Jayan et al., 2020).

To address these limitations, rapid methods have been developed that offer high sensitivity and specificity for detecting and identifying pathogens in food. These approaches, crucial for the food industry, allow prompt identification of pathogens in both fresh produce and processed foods, even when present in low numbers (Pan et al., 2014). Techniques such as PCR and ELISA provide results within hours, significantly improving pathogen control measures (Law et al., 2015). This shift to more rapid methods has reduced labour, minimised errors, and provided more efficient pathogen detection, enabling better food safety management (Zhang et al., 2022). Evaluating fruit quality involves measuring attributes such as colour, texture, pH, total soluble solids (TSS), and titratable acidity (TA) (Prasad et al., 2018). These parameters change during fruit development and ripening. However, all of these methods, such as PCR, titration, and firmness testing, are often destructive and require professional evaluation (Ali et al., 2023).

In response to these limitations, non-destructive methods have gained attention for the evaluation of fruit quality and early disease detection. These include image-based sensors, optical sensors, and biosensors, which offer rapid and minimally invasive approaches (Ali et al., 2019). For example, image-based sensors assess external characteristics, whereas optical sensors analyse internal qualities using light wavelengths (Khan et al., 2021; Li et al., 2019). Biosensors detect specific molecules or pathogens and provide sensitive and rapid analysis. Techniques such as GC-MS and HPLC also enable non-destructive volatile compound analysis, facilitating early disease detection (Li et al., 2021). Despite their benefits, these methods can be costly and time-consuming, highlighting the need for affordable, efficient alternatives (FDA, 2019).

Among these, the Electronic Nose (EN) has emerged as a promising tool for quality monitoring and early detection of postharvest diseases. EN technology, which detects changes in aroma and volatile metabolites, provides a rapid, reliable method for assessing food quality. The EN simulates human olfaction, using pattern recognition software to identify and classify VOCs emitted by produce, thus acting as a non-destructive marker for quality control (Sanaeifar et al., 2016). Its application has expanded beyond agriculture to sectors such as healthcare, pharmaceuticals, and environmental monitoring, demonstrating its versatility and effectiveness in ensuring product safety and quality (Wilson, 2018; Kiani et al., 2016; Yakubu et al., 2021). EN technology has recently been explored for its ability to detect ripening stages and identify the presence of fungal diseases at an early, asymptomatic stage across various crops. However, its effectiveness in monitoring papaya fruit quality and detecting early stage diseases has not yet been studied. This is particularly important for Malaysia, a major producer and exporter of papayas, highlighting the need for targeted research in this area.

In addition to early detection, researchers are investigating sustainable methods for preventing fungal attacks on fruits. The use of chemical fertilisers and pesticides is increasingly seen as

unsustainable owing to their environmental impact and the rise of microbial resistance. This has led to the development of eco-friendly interventions like edible coatings, which act as protective barriers against pathogens (Blancas-Benitez et al., 2022). Edible coatings and films offer multiple benefits in preserving produce. Derived from natural sources such as chitosan (extracted from shrimp shells) and cellulose (from plants), these coatings are biodegradable and environmentally friendly, decomposing after use, thus minimising environmental impact (Shi et al., 2024). Acting as gas barriers, they create a semi-permeable layer that regulates the exchange of oxygen and carbon dioxide, which is essential for controlling respiration rates in fruits and vegetables and helps delay ripening and spoilage (Blancas-Benitez et al., 2022). Additionally, these coatings serve as moisture barriers that reduce water loss, thereby maintaining the freshness of produce for longer periods (Jafarzadeh et al., 2021).

Furthermore, bionanocomposite films and coatings offer antimicrobial effects through several mechanisms. One common approach is the incorporation of nanoparticles, such as silver or zinc oxide, which disrupt microbial membranes or produce reactive oxygen species (ROS) to kill bacteria and fungi (Li et al., 2024). The addition of natural antimicrobials, such as essential oils or thymol, further strengthens the film by creating an environment that is inhospitable for microbial growth (Bajaj et al., 2023). The structure of bio-nanocomposites also supports the gradual release of these antimicrobial agents, providing sustained, long-term protection against pathogens (Chawla et al., 2021). The general antimicrobial action of these edible coatings, prepared using biopolymers and nanoparticles, is depicted in figure 1.2.

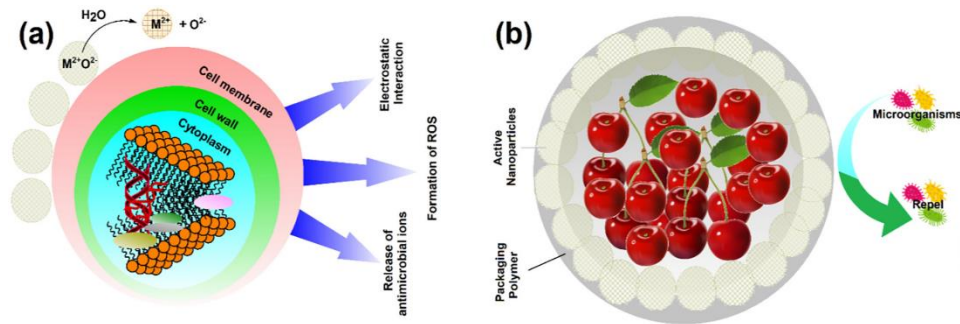


Figure 1.1: Antimicrobial activity and mechanism of bionanocomposite films on fruits (Jafarzadeh et al., 2021).

Zinc oxide nanoparticles (ZnO NPs) have gained considerable attention for their potential to extend the shelf life of fresh produce, partly due to their designation as "Generally Recognized

as Safe" by the U.S. Food and Drug Administration supports their use in food packaging applications (Agarwal et al., 2017). Compared to other nanoparticles, ZnO NPs offer enhanced biocompatibility, making them highly suitable for diverse applications in food preservation. Scientific consensus further underscores the minimal or negligible health risks associated with ZnO NPs, bolstering their appeal for widespread use (Bandeira et al., 2020). Globally, ZnO NPs are ranked as the third most produced metal-containing nanoparticles, following silica and titanium dioxide, a testament to their industrial significance (Kumar et al., 2023). Various synthesis techniques have been developed to address the production costs and enhancing the accessibility and affordability of ZnO NPs for applications, including food preservation (Bandeira et al., 2020).

When fungal infections are detected in fruits such as papaya, implementing treatments, rather than discarding them, is vital to control the spread of infection. Edible coatings offer a versatile solution; however, they must be produced sustainably with minimal environmental impact and low cost to be feasible for farmers in developing countries. While ZnO NPs have shown strong efficacy in previous studies, synthesizing them using eco-friendly methods remains a challenge. Incorporating ZnO NPs into biopolymers like chitosan could offer a synergistic approach to controlling fungal infections in tropical fruits like papaya. However, further research is needed to evaluate their effectiveness specifically on papaya and to explore local, sustainable materials that could be used for developing such treatment solutions.

The existing literature highlights the versatility of EN technology in monitoring various quality parameters of fruits and vegetables, providing a non-destructive approach for detecting postharvest diseases. However, while EN has been applied to a range of fruits like strawberries, apples, and tomatoes, its application to papaya, particularly for detecting ripening stages and early fungal infections, remains largely unexplored. This gap is significant given the importance of papaya in tropical agriculture and its vulnerability to postharvest losses due to fungal diseases.

Additionally, ongoing research has explored eco-friendly methods for disease control, including the use of metal oxide nanoparticles in biopolymer-based edible coatings. Although these coatings show promise in extending the shelf life of produce, most nanoparticles used are not synthesized through green methods, raising environmental and sustainability concerns. While there have been efforts to produce ZnO nanoparticles using eco-friendly approaches like plant extracts, the combination of these nanoparticles with chitosan for papaya protection has not yet been investigated.

This study aims to fill these gaps by focusing on both early disease detection and control in papaya. The objectives of this study are to:

1. Evaluate the efficacy of EN in detecting different ripening stages of papaya during early storage.
2. Investigate EN's potential to identify different postharvest fungal diseases in papaya such as anthracnose, fusarium rot and stem end rot, at early asymptomatic stages.
3. Develop and examine the effectiveness of a chitosan and ZnO NP-based edible coating, synthesized using green methods, in controlling anthracnose disease in papaya.

Chapter 2: Literature Review

Electronic nose as a tool for quality monitoring and early detection of postharvest diseases

2.1 Fundamental principles of EN

2.1.1. Sensory array materials

The fundamental principle of an EN system is to adopt a sensory array setup which can mimic the mammalian nose to stimulate olfactory responses to changes in aroma and odour from volatile metabolites (Suchorab et al., 2019). An inclusive EN system is typically derived from single or multiple sensors that can potentially detect different volatile metabolites emanating from a sample. For example, the EN (PEN 3) used by (Pan et al., 2014) consisted of 10 sensors (S1 to S10) and each sensor was sensitive to specific compounds like aromatic gases (S1), nitrogen oxides (S2), ammonia and aromatic gases (S3), hydrogen (S4), alkenes and aromatic gases (S5), methane (S6), sulfur compounds, alcohols and partially aromatic volatiles (S7), aromatic gases and sulfur organic gases (S8), nitrogen oxides and sulphides (S9), and alkanes (S10). Similarly, different EN models have different combinations of sensors. In most EN setups, sealed vials are employed to hold a certain volume of a liquid or solid sample, and either headspace created with or without incubation is tested. The volatile compounds of the headspace interact with sensors and alter their physical and chemical characteristics, such as electric resistance or optical characteristics, which are converted into electric signals. These signals from each sensor combine to provide multidimensional data that depicts the aroma pattern of the particular sample under examination (Licen et al., 2018; Yakubu et al., 2021). These sensors can detect small changes in volatile metabolites in the sample, thus enabling a sensitive and early detection process (Lou et al., 2018). Besides, various recent works have proved that EN has the potential to detect and discriminate changes in volatile metabolites of different crops' maturity stages, disease identification, quality assessment, shelf-life evaluation, and sensory evaluation thus achieving a real-time monitoring system (Ali et al., 2020; Baietto & Wilson, 2015; Chen et al., 2018).

The detection via EN can identify complex odours which compose of a wide range of gas sensors (Ali et al., 2020; Lioutas et al., 2021). The construction of sensors with high and low specificity can detect the odour and translate the information into a different classification that

creates specific volatile “fingerprinting” for the detection process (Ali et al., 2020). The sensing system via EN sensory array set-up can be established from a single device or combination of the different sensing elements according to the group of volatile metabolites expected from each detection analysis (Licen et al., 2018). The detection process is not just limited to the different types of sensors used for the analysis, but the number of sensors may also contribute to the detection possibilities (Yakubu et al., 2021). Hence, a lot of studies adopted different sensory array setups that typically consist of multiple sensors for better sensing elements. This sensing element feature allows the sensor to chemically react with odour samples and provide real-time detection based on the classification and discrimination of the volatile fingerprint (Shi et al., 2019). In addition, these patterns and fingerprints of known gases can be used to train the pattern recognition system.

Various sensor types have been utilised in Electronic Nose (EN) applications, including Metal Oxide Semiconductors (MOS) (Nunes et al., 2019), Metal Oxide Semiconductor Field-Effect Transistors (MOSFET) (Loutfi et al., 2015), Piezoelectric Crystals (PC) (Pohanka, 2018), quartz crystal microbalances (QCM) (Wang, 2020), Electrochemical Sensors (Xiao et al., 2020), and surface acoustic waves (SAW) (Kus et al., 2021). Among these, MOS sensors offer unique combination of attributes ideal for postharvest applications. MOS sensors operate by detecting changes in the conductance of a metal oxide film when exposed to gases, which allows for accurate detection of volatile organic compounds (VOCs) emitted by fruits or pathogens. MOS sensors offer several advantages over other detection methods: they are cost-effective, cover a wide detection range, and provide a durable and robust solution for gas monitoring. Although MOS sensors require higher operating temperatures (300–500°C), which leads to increased power consumption, their fast response time to quickly capture and analyse VOC profiles is particularly important in postharvest applications, where rapid detection of spoilage or disease is essential (Zheng and Zhang, 2022).

In comparison, while MOSFET sensors provide high reproducibility and QCM sensors offer sensitivity, they lack the speed and cost efficiency required for large-scale agricultural applications (Jae et al., 2024).

MOS sensors also excel in producing fingerprints of volatile emissions, which are critical in identifying the flavour, ripeness, or spoilage stages of crops. This capability makes MOS sensors particularly suited for gas analysis of crop diseases and insect pests (Jae et al., 2024). Their intelligence, accuracy, and fast data output make them an optimal choice over other sensor types for postharvest disease monitoring.

Choosing the type of sensors in an EN system plays a huge role in determining the outcome of the analysis. Generally, the sensor materials give effect based on the chemical compounds detected at the sensor detection site which then reflects pattern signals. These signals are then

subjected to the pattern recognition system or also called post-processing analysis to obtain real-time information and evaluate the efficacy of the EN sensors. The development of such technologies is critical to utilize volatile metabolites profiling to improve crop production and its safety assurance. There are three major steps involved in characterizing the volatile metabolites profiling, namely: (1) odour sampling; (2) disease detection via sensory array analysis, and (3) data acquisition and pattern recognition, as illustrated in Figure 2.1, 2.2.

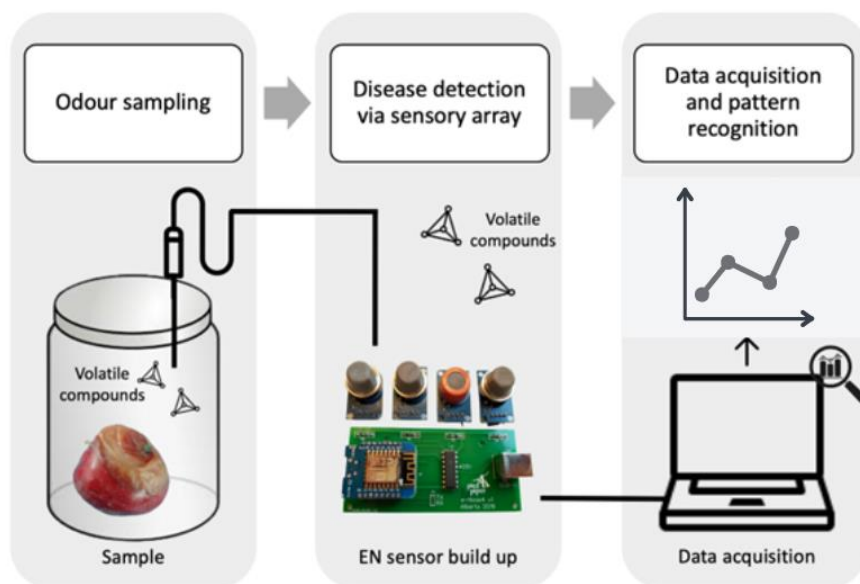


Figure 2.1: Schematic of the working principle of the electronic nose in characterizing the volatile organic compounds released by fruit for early detection and quality monitoring analysis (Graphic created with Microsoft Word Software)

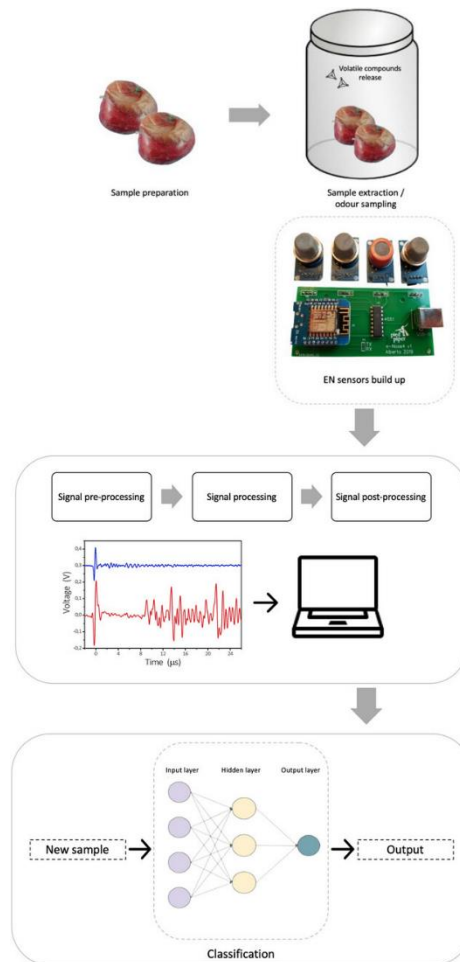


Figure 2.2: Schematic of typical electronic nose sensors signals processing for data acquisition (Graphic created with Microsoft Word Software)

2.1.2 Odour sampling

In an analysis of odourant emanating from a sample, the volatile metabolites were drawn to the sensory array according to the appropriate sampling method. Rapid sampling method with little to zero mechanical damage during analysis is favourable due to the perception and consumer acceptability of the nature of the fresh produce itself (Adedeji et al., 2020). There is a variety of sampling methods conventionally used, which is convenient to the analysis such as static headspace, pre-concentrator, and solid-phase micro-extraction (SPME) method (Dong et al., 2019). The common static headspace method uses a hermetically sealed vial before detection. The sample is then allowed to achieve equilibrium before it is subjected to the sensory array unit for identification of the gaseous compounds (Pascale et al., 2018). Parameters such as the temperature, sample size, and equilibration time need to be evaluated and optimized before use in each analysis. The pre-concentrator or also known as the “purge

and trap” method, uses the stream of inert gas to direct the volatile metabolites onto the detector. Gas flow is supplied to ensure the volatile compounds from the sample can pass through the sensory array set up for identification (Bruno & Harries, 2019). This method seems to be at disadvantage due to the depletion of the volatile metabolites during purging. Other than these two methods, SPME has been widely used in volatile metabolites studies. This method provides a user-friendly technique due to its higher detection rate as compared to the former methods. The principles of SPME lie within the adsorbent layer that can trap volatile compounds onto a specific fiber which are then equilibrated and thermally desorbed to be introduced into the detection system (Qiu et al., 2015). This technique provides a simple and effective extraction method highly recommended for analysis of fresh produce for odourant sampling.

2.1.3 Disease detection and quality characterization

Plant diseases are often split into two categories based on their etiology. Non-infectious diseases are caused by genetic factors, environmental stress, or nutritional deficiencies. This type of disease is not transmitted to other plants. While infectious diseases are caused by pathogens such as fungi, bacteria, or viruses (Singh and Sharma, 2018). Pathogens attack crops at the preharvest or postharvest stage and infect the produce. The infection at a preharvest stage in many cases remains quiescent and does not show any visible symptoms till the time crop is harvested and its resistance toward the pathogen decreases (Tan et al., 2023). The pathogen grows to develop the infection which alters the original state of the harvested crop and modifies its vital functions making it diseased and harmful to human health (Badii et al., 2015). Therefore, the detection of pathogens before the onset of visible symptoms is valuable to execute appropriate management strategies to control the disease or at least prevent the spread of the disease to other produce (Shaikh et al., 2017; Tan et al., 2022). It is well reported that volatile metabolites play substantial roles in plant communication and present promising functionality to improve plant and crop protection (Cui et al., 2018). Volatile metabolites emanating from plant and fresh produce can be directly linked with their real-time physiological health status and may provide bio-information that can act as a volatile biomarker that is useful for rapid and non-invasive disease diagnosis (Loutfi et al., 2015). During the pathogenesis of fresh produce, the generation of different volatile metabolites occurs according to the plant's health status and the biochemical interactions between the plant host and the pathogen (Tait et al., 2014). This interaction may lead to the production of volatile metabolites that give a possible hint of the volatile's relationship with the quality attributes of the crops (Seesaard et al., 2020). Some crucial compounds involved in plant defences are volatile metabolites comprising protective compounds (e.g., terpenoids, essential oils), plant hormones (e.g., ethylene, jasmonates, and methyl-salicylate), insect pheromones, digestive or metabolic by-

products, and compounds derived from cell damage (Cellini et al., 2017). This information, for instance, could be beneficial for disease detection and quality characterization via the EN system.

2.1.4 Data acquisition and pattern recognition

The post-processing phase in EN analysis is essential for finalizing results. EN signals undergo pattern recognition analysis, categorized into supervised or unsupervised, and parametric or non-parametric methods. Unsupervised approaches compare unknown samples, while supervised methods classify based on known sample traits (Yakubu et al., 2021). Pattern recognition utilizes statistical models like Principal Component Analysis (PCA), Linear Discriminant Analysis (LDA), Partial Least Squares (PLS), Functional Discriminant Analysis (FDA), Learning Vector Quantization (LVQ), and Artificial Neural Network (ANN) to interpret EN signals accurately. PCA simplifies multidimensional datasets, though may interpolate features if sensors are nonlinear (Pan et al., 2014). LDA maximizes class-specific data retention but requires data reduction, often via PCA, to enhance accuracy (Zhou et al., 2022). PLS accommodates collinear data, reducing the need for calibration samples (Patel, 2014). Nonlinear methods like ANN are ideal for complex datasets, adapting to fluctuating data trends (Jia et al., 2019). Support Vector Machine (SVM) constructs optimal hyperplanes for classification (Jia et al., 2019). Data preprocessing precedes pattern recognition to filter irrelevant information, ensure data sufficiency, and format data for analysis, employing techniques like baseline processing, normalization, and data compression. Standardizing raw data eliminates environmental disturbances, enhancing classification accuracy (Yakubu et al., 2021).

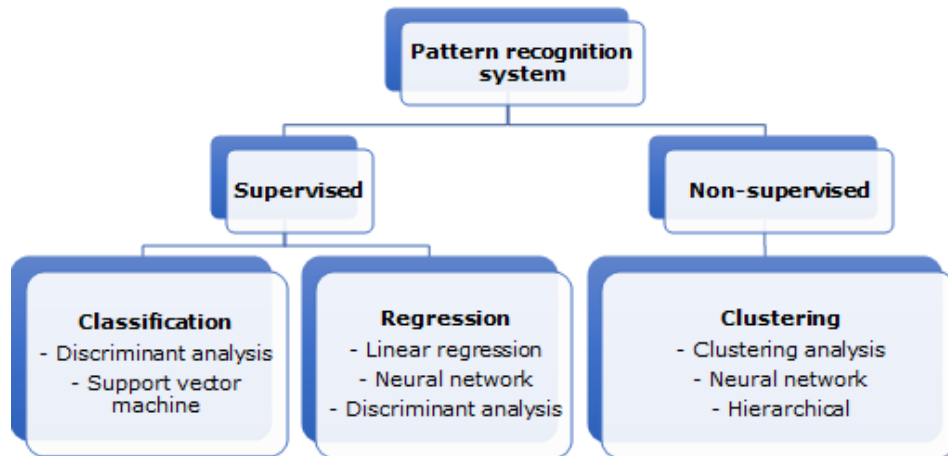


Figure 2.3: Flowchart of pattern recognition systems available for early detection analysis via EN
(Graphic created with Microsoft Word Software)

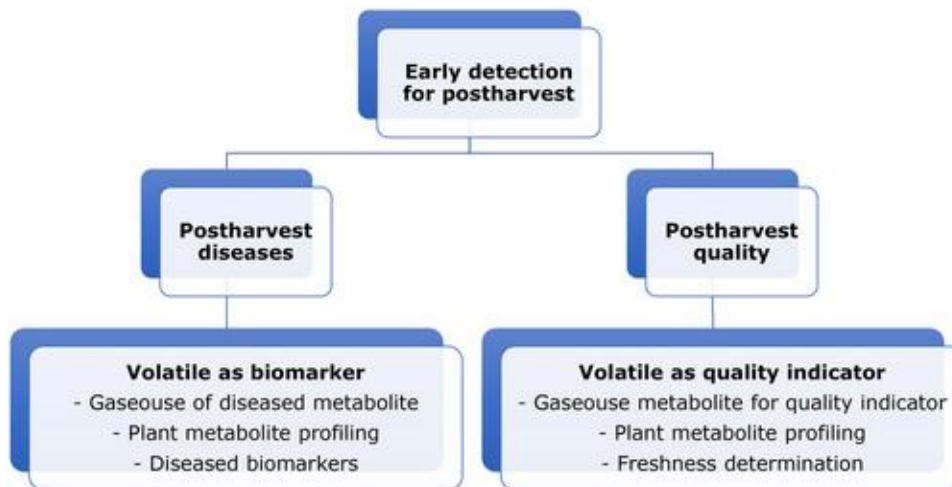


Figure 2.4: Flowchart of early detection tool using electronic nose for postharvest diseases and postharvest quality. (Graphic created with Microsoft Word Software)

2.2 EN for early detection of postharvest diseases

Many diseases occur during the post harvesting period due to latent and senescence infection of pathogens. In which, the disease only progresses and shows symptoms during the transportation process or once it hits the market (Xu et al., 2018). Noteworthy, fruit becomes a host for these pathogens via direct penetration through wound openings or intact cuticles on its surface (Voss et al., 2019). In more serious cases, the pathogen invasion may result in a rapid deterioration rate of fresh produce causing tremendous economic losses. This in turn affects the quality of infected fresh produce such as texture, taste, biochemical compounds, and nutritional contents (Ncama et al., 2018). Therefore, appropriate control measures should be applied to minimize losses due to postharvest diseases enabling more availability of edible food products thus ensuring sustainable food security. However, this is only possible when diseases are detected in advance.

Some volatile metabolites are present as strong aromatic gases, but most of them occur at extremely low concentrations. These volatile metabolites could not be justified by the human olfactory threshold. EN signal responses are often specific for the particular pool of volatile metabolites emanated by the sample. The responses are usually in the form of conductivity (Genva et al., 2019). Volatile metabolites released by plants and fresh produce are often accounted for almost two thirds of the total volatile compounds emanating in the atmosphere. The number of volatile metabolites dependent on the physicochemical factor abides by metabolic changes such as temperature, humidity, and other biological factors (Brilli et al., 2019). Plant secondary metabolites are known to be lipophilic with low boiling points, the high vapor pressure at ambient temperature, and easily vaporized, making them accessible for EN evaluation and identification (Ray et al., 2017). There are possible reasons that fungal colonization could emanate volatile metabolites as part of its metabolism pathway under adverse circumstances (Dukare et al., 2019).

Several recent studies conducted in determining the volatile metabolites emanating from naturally contaminated fresh produce are demonstrated in (Table 2.1). Different odours and volatile metabolites have been identified in different crops and cultivars. Pan et al. (2014) have successfully identified several key characteristic volatile metabolites responsible for decay caused by a fungal infection on strawberries. Three common pathogenic fungi belonging to *Botrytis sp.*, *Penicillium sp.*, and *Rhizopus sp.* were used to inoculate strawberry samples against healthy fruit as control. Commercial EN device (PEN 3) was used as a set-up with 10 MOS sensors coupled with headspace SPME via GC-MS analysis using a polydimethylsiloxane (PDMS), 100 µm SPME fiber. The tests were carried out on days 0, 2, and 4 as the fruits ripened and the disease progressed. Even though EN can analyse the whole chemical odour profile emanating from produce, the exact constitution and quantity of each volatile detected by EN are usually assessed using GC-MS. Non-destructive detection of specific volatile metabolites has been predominantly carried out in the past via GC-MS analysis with the aid of polar stationary phase

columns such as 5-MS and polyethylene glycol (Shi et al., 2019). Despite the higher accuracy of GC-MS detection, EN has recently been investigated for the same application because it is more portable and less expensive than GC-MS. The GC-MS results make it possible to identify certain biomarkers and build an independent EN library for implementation in the field (Wen et al., 2019). The EN used in the study was able to differentiate relative volatile compounds in terms of signal transduction between healthy and infected strawberries. When the PCA was performed, EN response data was able to distinguish between the control and three other infected groups with 96.6% accuracy using a multilayer perceptron neural network. EN could also distinguish volatiles in the samples on different storage days. According to the GC-MS results, compounds such as ethyl hexanoate and hexanoic acid hexyl ester which are usually found in strawberries, were present in lower concentrations in infected strawberries. Styrene and limonene were found only in uninfected strawberries. Octyl acetate, 5-hydroxy methyl furfural, 5-hydroxy maltol, and octanoic acid were present only in strawberries infected with *Botrytis* sp. Methyl cinnamate, benzocyclobutene, γ -dodecalactone, and α -farnesene were present only in strawberries infected with *Penicillium* sp. and *Rhizopus* sp. Consequently, these distinctive volatiles could serve as biomarkers for the presence of the tested fungi. Future research should focus on the early detection of anthracnose disease caused by *Colletotrichum acutatum* which is also one of the major postharvest diseases of strawberries (Feliziani & Romanazzi, 2016).

Table 2.1: Summary of early detection of postharvest related diseases based on volatiles biomarker of different disease infections from various produce using electronic nose sensors.

Sample	Determination	Pathogens	Sensor type	Pattern recognition	Key finding	Limit of detection	References
Strawberry	Detection and discrimination of common fungal pathogens at different storage periods of strawberry	<i>Botrytis sp.</i> , <i>Penicillium sp.</i> , and <i>Rhizopus sp.</i>	10 MOS sensors coupled with GC-MS	PCA and MLP neural network models	96.6% accuracy via multilayer perceptron neural network with discrimination of unique volatile compounds	1 ppm – 100 ppm	Pan et al. (2014)
Peaches	Detection and discrimination of peach spoilage fungi at different storage periods	<i>Botrytis cinerea</i> , <i>Monilinia fructicola</i> , and <i>Rhizopus stolonifer</i>	10 MOS sensors coupled with GC-MS	SNV and PLS-DA models	Determination of unique volatile compounds among control healthy samples (e.g., β -myrcene and α -pinene) and infected samples (e.g., terpenes)	1 ppm - 100 ppm	Liu et al. (2018)
Peanuts	Discrimination of the level of contamination of fungal pathogens on peanuts	<i>Aspergillus sp.</i> (<i>A. flavus</i> , <i>A. parastiticus</i> , and <i>A. ochraceus</i>)	12 MOS sensors (FOX 3000) coupled with NIR spectroscopy	PC- LDA and PLSR models	92.11% accuracy for NIR and 86.84% accuracy via EN	NIR: 0.578 log CFU/g) EN: 0.808 log CFU/g)	Shen et al. (2018)

Table 2.1 continued: Summary of early detection of postharvest related diseases based on volatiles biomarker of different disease infections from various produce using electronic nose sensors.

Sample	Determination	Pathogens	Sensor type	Pattern recognition	Key finding	Limit of detection	References
Apple	Determination of fresh and mouldy apples inoculated with fungal pathogens Classification of spoilage and different degree of decay among apples caused by the fungal pathogen	Penicillium expansum and Aspergillus niger Penicillium expansum	Headspace analysis with commercial EN (PEN 3) 10 MOS coupled with commercial EN (PEN 3)	LDA, BPNN, SVM and RBFNN models PC- LDA and PLSR models	Differentiate fresh and mouldy apples with 72.0% - 96.3% prediction accuracies 100% and 97.22% accuracy via principal component analysis-discriminant analysis	> 100 ppm > 100 ppm	Jia et al. (2019b) Guo et al. (2020)
Citrus	Detection of Citrus Tristeza Virus (CTV) on citrus and differentiate healthy and infected samples (large scale orchard)	CTV Virus	MOS sensors (FOX 3000) coupled with PCR test	Finite-element method (FEM) simulation	95.3 % accuracy via random forest classifier with unique volatile compounds detected	> 0.0999 g/L	Hazarika <i>et al.</i> (2020)

Table 2.1 continued: Summary of early detection of postharvest related diseases based on volatiles biomarker of different disease infections from various produce using electronic nose sensors.

Pomegranate	Discrimination of black-heart fungal disease seriousness	Alternaria sp.	6 MOS EN sensors coupled with headspace GC-MS	PCA, LDA and SVM models	95% - 100% accuracy of healthy and infected samples respectively	1 ppm – 100 ppm	Nouri et al. (2020)
Brown rice	Determination of contamination level of rice	Aspergillus sp.	12 MOS EN sensors (FOX 3000)	PCA, LDA and SVM models	89% accuracy from EN responses with 11 unique volatile compounds	> 100 ppm	Jiarpinijnun et al. (2020)
Garlic	Detection and discrimination of fungal pathogens in garlic	Fusariumoxysporum f. sp. Cepae, Alternariaembellisia (syn. Embellisiaallii), and Botrytis allii	9 MOS sensors	ANOVA, PCA, LDA, SVM, and BPNN	Accuracy on days 0,4,8 SVM- 75%, 92.5%, 92.5% LDA- 90%, 97.5%, 100% BPNN-32%, 92.5%, 97.5%	10-10000 ppm	(Makarichian et al., 2022)

Table notes: **MOS** - Metal Oxide Semiconductors, **GC-MS** - Gas Chromatography-Mass Spectrometry, **NIR**- Near Infrared spectroscopy, **PCA** - Principal Component Analysis, **MLP** - Multilayer Perceptron, **SNV** - Standard Normal Variate, **PLS-DA** - Partial Least Squares Discriminant Analysis, **PC-LDA** - Principal Component-Linear Discriminant Analysis, **LDA** - Linear Discriminant Analysis, **BPNN** - Backpropagation Neural Network, **SVM** - Support Vector Machine, **RBNN** - Radial Basis Function Neural Network, **PLSR** - Partial Least Squares Regression, **CFU/g** - Colony Forming Units per gram, **ANOVA** - Analysis of Variance

Similarly, Liu et al. (2018) also used an EN (PEN 3) sensing device comprising 10 MOS sensors to discriminate and track the growth of common fungi infecting peaches, *Botrytis cinerea* (BO), *Monilinia fructicola* (MO), and *Rhizopus stolonifer* (RH), coupled with HS-SPME GC-MS. Volatile compounds were extracted from healthy and infected peaches using polydimethylsiloxane/divinylbenzene (PDMS/DVB) 65 μm SPME fiber. EN coupled with GC-MS analysis was used to analyse volatile changes and compared with growth data from colony counts of the fungus. The authors reported that terpenes and aromatic compounds are some of the main contributors to the EN analysis. GC-MS was able to further analyse the unique volatiles from all four groups of peaches (control, BO, MO, and RH). This finding is supported by a previous study by Liu et al. (2018), where volatile metabolites, such as terpenes, are species- and strain-specific to some groups of fungi. Thirty-seven volatile compounds were detected in all four groups of peaches mostly from aldehydes, esters, alcohols, lactones, acids, and olefins groups via GC-MS. Among these compounds, hexanal, E-2-hexenal, E-2-nonenal, benzaldehyde, hexyl acetate, alcohols, γ -octalactone, and γ -decalactone were found responsible for the peach-like aroma, and the concentration of hexyl acetate, γ -octalactone, and γ -decalactone significantly decreased during storage in infected peaches. Compounds like furfural, E-2-nonenal, 2-dodecenal, citronellyl acetate, and β -citronellol were identified solely in peaches infected with RH. Heptyl acetate was found only in those infected with BO and MO. The concentrations of hexanal, E-2-hexenal, and linalool in the samples infected with RH were significantly lower ($p < 0.05$) than in samples infected with BO or MO. Moreover, the amount of benzaldehyde, heptyl acetate, ethyl caprylate, and hexadecane in samples infected with BO was significantly greater ($p < 0.05$) than those of peaches infected with MO or RH. As a result, these metabolites or their constituents may be employed as indicators to identify specific fungal species. PLSR was performed on EN sensory array to develop a model showing the correlation between EN and colony-forming units ($R^2 = 0.883\text{--}0.908$, RMSEP = $0.235\text{--}0.435 \log(\text{CFU g}^{-1})$, and RPD = $2.80\text{--}4.16$). The authors also reported that the results showed successful discrimination among healthy and disease-infected samples after 48 h. This research can also further investigate detecting other common postharvest diseases of peaches such as bacterial spot, peach constriction canker, powdery mildew, or peach shot hole to name a few (Luo et al., 2022)

Shen et al. (2018) have derived the feasibility of EN and other tools of analysis in detecting the contamination level of five *Aspergillus* strains on peanuts. Peanut samples were sterilized and artificially infected with fungi and stored for 9 days until they turned moldy. The authors adopted near-infrared spectroscopy (NIR) together with FOX 3000 sensing system as an EN device that was incorporated with 12 MOS sensors to identify different fungal contamination levels. The tests were performed on days 0, 3, 6, and 9. The key volatiles screened by EN were amines, ammonia, alcohols, and ketone groups which differentiated between healthy and

moldy samples. Holistic differences between moldy and healthy samples showed significant signal responses from all 12 conductivity response values. Classification of infection level was assessed based on LDA. In NIR analysis, it was reported that fungal infection would cause a peanut kernel to scatter more light than a healthy one, therefore, the NIR spectra revealed that uninfected peanuts had greater absorbance than the infected ones. Furthermore, only slight spectrum changes between samples infected with various *Aspergillus* strains were found, mostly in the N–H and O–H groups of carbohydrates and proteins, which might be attributed to various metabolites produced by the fungal cells and the breakdown of starch and protein. The study concluded that this may be the result of crushing peanut samples before assessment, which could have a detrimental impact on the fungi's distinctive characteristics or volatile flavor. It was also reported that the analysis achieved correct classification with 86.84% and 92.11% accuracy by EN and NIR spectroscopy, respectively, with only 4.41% misclassification among mouldy peanuts. The score plots of PCA derived from NIR spectroscopy and EN indicated 98.15% and 99.65% difference between the two contamination levels, respectively, which separated the trends among the mouldy and healthy samples. This study provided insightful data related to harmful mycotoxin production and detection based on volatile changes in peanuts (Levasseur-Garcia, 2018). However, no obvious separation among the five *Aspergillus* strains was observed. Although internal changes such as carbohydrate, protein, and fat content were not assessed, the authors correlated the findings with the partial least squares regression (PLSR) model to better predict the contamination level in terms of colony counts. To increase the accuracy and resilience of the model in practical applications, future studies should consider how peanut samples are handled and how they are infected by different fungi under real-world conditions.

In another study, Jia et al. (2019b) utilised EN (PEN3) with 10 different built-in MOS sensors on fresh and mouldy apples infected with pure cultures of *Penicillium expansum* and *Aspergillus niger*. The authors demonstrated prediction accuracies of 96.3% and 90.0% among fresh and mouldy samples (Group A) and 77.7% and 72.0% (Group B), respectively. Group A consisted of pretreated individual apples inoculated with and without different fungi. Group B consisted of a mixture of inoculated apples and healthy apples. The experiment was conducted in a fumed hood chamber to avoid sample interference. Several different pattern recognition systems such as LDA, backpropagation neural network (BPNN), support vector machines (SVM), and radial basis function neural network (RBFNN) were applied to analyse and simplify the analysis. These pattern recognition models were later used to assist in predicting the analysis and assessing the accuracy of the results. The authors also proposed to establish a comparison study between each prediction model based on the different pattern recognition systems applied to the results and concluded that BPNN provided the best performance among all models used (Jia et al., 2018). Among all 10 MOS sensors used in EN sensory array, only a few sensors provided good

responses toward volatile changes which indicated the off-flavour characteristic of mouldy apples. This was addressed by other authors and researchers where the EN sensors, especially MOS, were not sensitive to the changes in volatile metabolites (Song et al., 2020). Nevertheless, the study showed that EN sensors are good at detecting volatile metabolites which reflects the higher prediction accuracy in group A as opposed to group B.

Another study on apple spoilage classification caused by *P. expansum* has been conducted by (Guo et al., 2020) using 10 MOS (PEN 3) combined with a chemometrics test. This recent finding on apple spoilage inferred the same efficiency as a previous study on apples reported by Jia et al. (2019b) with a prediction rate of 87.86% and 10.95% respective to two factors, PC1 and PC2. Hence enabled the classification of healthy and infected samples. The chemometric test allowed the system to predict the spoilage area concerning four different pattern recognition systems such as PCA, LDA, PLSR, and partial least square discriminant analysis (PLS-DA). Among the 10 MOS sensors used, only four sensors were able to generate responses from control and infected samples with a cumulative contribution rate of 99.92%. This contribution rate was then analyzed between two PC groups: spoilage area and degree of corruption with 87.86% and 10.95% in PC1 and PC2, respectively. While the PLS-DA model reached 100% classification based on the degree of corruption alone. As mentioned earlier, the remaining six sensors used in the study were not able to detect the changes in volatile metabolites from the samples. This showed that the build-up of the sensors itself is prone to errors. These problems associated with sensors that were not able to detect volatile changes properly might affect the whole analysis. This will concurrently disrupt the detection quality, hence reducing the efficacy of EN.

Though the two studies mentioned above did not demonstrate key volatiles responsible for the disease infection on apples in general, it does contribute to the practical application in post-processing by applying different pattern recognition analyses to better evaluate the results obtained.

Hazarika et al. (2020) employed two different EN systems typically from Alpha-MOS FOX 3000 EN composed of 12 MOS sensors and a prototype chamber with 9 MOS sensors for *Citrus Tristeza Virus* (CTV) coupled with PCR analysis. EN system showed 95.30% prediction accuracy corresponding to the obtained PCR test. However, the work provided little to no status on CTV infection and no key responsible volatile compounds were addressed. The detection is only limited to common targeted gaseous compounds responsible for maturity stages such as carbon monoxide, methane, butane, and ethanol, disregarding the analysis of the more precise volatile metabolites. Moreover, the sensors used were only able to detect signals in terms of electrical responses (Viejo et al., 2020). Hence, the proposed EN is not applicable as a stand-alone system. A complementary analysis such as GC-MS is required for an in-depth and detailed determination process.

Similarly, quality detection and fungal diseases of pomegranate have been studied by Nouri et al. (2020) considering the use of EN on *Alternaria sp.* The researchers have adopted the MOS sensing system with six biosensors attached for data collection and employed dynamic headspace analysis. The volatiles related to the infection have been narrowed down into alcohols, methane, ammonia, sulfide, and benzene based on the doping sensors. While Jiarpinijnun et al. (2020) conducted a study on fungal infection of Jasmine brown rice via portable EN (FOX 3000) incorporated with 12 MOS sensors. HS-SPME via GC-MS has been used in conjunction with EN. The authors concluded that EN could be used for rapid identification and act as a non-destructive tool for early detection of postharvest disease related to *Aspergillus sp.* during the storage period.

Recently, Makarichian et al. (2022) worked on garlic to detect its common fungal diseases caused by *Fusarium oxysporum* f. sp. Cepae (FU), *Alternaria embellisia* (syn. *Embellisia allii*) (AL), and *Botrytis allii* (BO) using EN consisting of nine MOS sensors. ANOVA, PCA, LDA, SVM, and BPNN were used for data processing. Freshly harvested garlic was tested on days 0, 4, and 8. All the sensors were stimulated at different levels for the different fungal infections; hence, categorizing each infection was successful. All the classification models could identify the differences in aroma from the samples after day 4 of storage. On day 4, PC1 and PC2 explained 48% and 26% of the variance between samples. On day 8, PC1 and PC2 showed 61% and 16% of the variance in the input variables, respectively. The accuracy of the SVM method on days 0, 4, and 8 was 45%, 87.5%, and 92.5%, respectively. LDA classified the samples of each infection treatment on days 0, 4, and 8 with an accuracy of 90%, 97.5%, and 100%, respectively. On day 4 and day 8, the BPNN could classify the samples' aroma based on the type of infection with an accuracy of 92.5% and 97.5%, respectively.

2.3 EN for postharvest quality monitoring

With continuous effort in delivering great quality fresh produce to meet consumers' living standards, general quality requirements, flavour, and sensory taste, a customary evaluation needs to be improved as well. The rules of modern standards have made the use of EN for rapid and feasible identification available for postharvest food quality monitoring (Table 2.2). The quality of fresh produce can be evaluated based on its colour and appearance, firmness and texture, pH, total TSS, ascorbic acid, and TA. All these parameters continually change during the produce's growth from the preharvest to the postharvest stages as they ripen during storage (Baietto & Wilson, 2015). Nevertheless, measuring these quality indices with traditional methods such as titration of pulp and penetrometer to test firmness, is not very accurate and requires destroying the samples. The flavour and aroma characteristics of food are also assessed since they are significant sensory cues for customers. However, it has been very costly

and time consuming to choose and evaluate goods for ripeness at harvest and saleability in commercial fruit markets using professional human graders and panels in the past Chilo et al. (2016). With the advent of EN, a new alternative approach for classifying fruits and other perishable foods using more reliable qualitative and quantitative measures is now available (Baietto & Wilson, 2015). Aroma is a valuable characteristic and indicator that can determine the change in physiochemical features, flavour, freshness, and ripeness stages of postharvest produce. Gases involved in the aroma of fresh produce are generated from their metabolic activities and that can be identified over time during storage. For instance, sensors that are sensitive to organic acids can detect acid degradation, which is a sign of fruit ripening and its relationship to increasing pH. This section reviews how EN has been applied to analyse and predict the different quality indices and ripeness stages by detecting the changes in the volatile profile of the produce.

Table 2.2: Summary of quality monitoring application based on key volatile components detected from different crops using electronic nose sensors.

Sample	Determination	Sensor type	Pattern recognition	Key finding	Limit of detection	References
Mango	Three different mango ripening stages (unripe, ripening, fully ripened)	Commercial EN (zNoseTM)	n/a	Decanal observed as a volatile indicator of mango (cv. Chokanan)	Kovats retention indices	Farhad et al. (2014)
Grapes	Freshness quality of three different types of grapes during cold storage	14 MOS sensors	PCA	95.27% and 91.92% of PC1 (types of grapes) and PC2 (interval period), respectively	Min voltage: 1 V Max voltage: 5 V	Rajin et al. (2015)
Litchi	Freshness quality of litchi at different storage periods	8 MOS sensors	PCA and SNR spectrum models	82.22% of data variance was observed in the PCA analysis and R ² =0.99396 for the SR model evaluation	Min voltage: 0.1 V Max voltage: 1.0 V	Ying et al. (2015)

Table 2.2 continued: Summary of quality monitoring application based on key volatile components detected from different crops using electronic nose sensors.

Wheatgrass	Determination of the sensory traits of hulled and non-hulled Triticum species	Potable (PEN3) EN with 10 MOS sensors coupled with GC-MS	PCA and LSD models	61.8% of total variance for PCA analysis between all genotypes with unique volatile compounds such as 1-penten-3-ol, 1-penten-3-one, E-2-hexenal, and 1-octen-3-ol	n/a	Bianchi et al. (2019)
Bell pepper	Freshness evaluation of fresh-cut bell pepper at different storage periods	Portable EN model with 14 MOS sensors	PCA and hierarchical cluster analysis (HCA)	The cumulative total variance of 98.4% in PCA	Max voltage: 10 V	Chen et al. (2018)
Kiwi	The freshness of kiwi at different storage periods	SAW sensor	PCA model	91.06% of the total variance between PC1 and PC2 analysis	Max voltage: 1.0 V	Wei and Guohua (2015)
Peach	Freshness classification of the different peach growth cycles	13 MOS sensors	PCA and stochastic resonance (SR) models	99.23% and 98.08% accuracy in the validation step and sample test step based on Pearson's	n/a	Voss et al. (2020)

				Chi-square test, respectively		
--	--	--	--	----------------------------------	--	--

Table 2.2 continued: Summary of quality monitoring application based on key volatile components detected from different crops using electronic nose sensors.

Spinach	The freshness of spinach during cold storage	7 MOS sensors	SVM and BPNN models	93.75% accuracy via back-propagation artificial neural network (BPNN) model	n/a	Huang et al. (2019)
Broccoli	Freshness evaluation of fresh-cut broccoli during cold storage	14 MOS sensors coupled with GC-MS analysis	PCA, HCA and canonical discriminant analysis (CDA) models	A cumulative variance of 100% accuracy was obtained	0.02 mmol kg ⁻¹ FW	Chen et al. (2019)
Carrot	Performance evaluation of sensor used in the study at different storage temperatures	QCM sensor	PCA model	44.77% and 38.77% accounted for PC1 and PC2 among samples stored at different temperatures and the presence of terpenoids, respectively	n/a	Gaggiotti et al. (2019)

Table 2.2 continued: Summary of quality monitoring application based on key volatile components detected from different crops using electronic nose sensors.

Berries	Freshness characterization of strawberries in polymer packaging	8 MOS sensors	LDA and SVM models	86.4% and 55.6% accuracy under LDA and SVM models in training and validation processes, respectively	> 10000 ppm	Ghasemi-Varnamkhasti et al. (2019)
	Determination of different ripeness grades of berries (white berry and blackberry)	10 MOS sensors	PCA, LDA and Artificial neural networks (ANN) models	100% and 88.3% of five ripeness grades for blackberry and white berry in ANN analysis respectively. 97% and 93% accounted for PC1 and PC2	n/a	Aghilinategh et al. (2020)
Banana	Ripeness stages of banana (unripe, ripe, and rotten) on	13 gas sensors	BPNN	100% accuracy in classifying the 3 ripeness stages	n/a	Hendrick et al., (2022)

	different storage days					
Pitaya (Dragon fruit)	Physiochemical properties pH, TA, TSS, phenolics content and moisture	6 MOS sensors coupled with NIR-spectroscopy	PCA, LDA, PLS-DA, PLSR	95% accuracy under LDA and >94% under PLS-DA	100-1000ppm	Ferreira et al., (2023)

Table notes: **MOS** - Metal Oxide Semiconductors, **GC-MS** - Gas Chromatography-Mass Spectrometry, **NIR**- Near Infrared spectroscopy, **PCA** - Principal Component Analysis, **MLP** - Multilayer Perceptron, **SNV** - Standard Normal Variate, **PLS-DA** - Partial Least Squares Discriminant Analysis, **PC-LDA** - Principal Component-Linear Discriminant Analysis, **LDA** - Linear Discriminant Analysis, **BPNN** - Backpropagation Neural Network, **SVM** - Support Vector Machine, **RBNN** - Radial Basis Function Neural Network, **PLSR** - Partial Least Squares Regression, **CFU/g** - Colony Forming Units per gram, **ANOVA** - Analysis of Variance

2.3.1 Freshness quality

The freshness quality of fresh-cut green bell pepper (*Capsicum annuum* var. *grossum*) was evaluated by Chen et al. (2018) using an EN sensor composed of 14 MOS and stored at 7°C. The freshness of fresh-cut bell pepper was compared according to the storage periods, aerobic plate count, and malondialdehyde content. Statistical methods such as PCA, PLS, and hierarchical cluster analysis (HCA) were utilized to analyze the data and classify the quality characteristics. The study indicated that the detection of off-flavor compounds including alcohols, ketones and aldehydes, esters and terpenes, sulfides, etc. was increased as the storage period increased. The PCA presented a total variance of 96.22% and 2.26% in PC1 and PC2, associated with different storage periods and the difference in volatile patterns detected, respectively. While the cumulative contribution of both PC1 and PC2 accounted for 98.48%. Whereas, the HCA has successfully differentiated the samples into four different groups with a clear indication of maintained freshness up to day 5 and spoiled at day 7. The authors stated that the EN results obtained were comparable to the GC-MS data which enabled a portable means of detection of volatile changes for quality monitoring purposes.

Chen et al. (2019) conducted another study to monitor the freshness of fresh-cut broccoli with the use of EN coupled with HS-SPME via GC-MS analysis. The authors aimed to investigate the freshness quality determination from volatile compounds and establish a comparison between traditional quality characteristics with EN responses. Statistical analysis such as canonical discriminant analysis (CDA) was used to distinguish between the fresh, medium fresh, and spoiled sample groups. Two CDA groups were obtained which accounted for 91.3% and 8.7% of the variability, respectively. The CDA performed was able to differentiate between all three sample groups with a total of 43 volatile compounds. These compounds were categorized as hydrocarbons, alcohols, esters, ethers, aldehydes, ketones, sulfur, and nitrogen compounds. While the significant accumulation of sulfur compounds (e.g., dimethyl disulfide) was observed as the storage period increased.

Rajin et al. (2015) accessed the quality degradation of grapes based on lab-manufactured EN sensors composed of 14 MOS sensors with one additional sensor responsible to monitor the temperature. The EN sensor developed in the study was used to monitor the quality of freshness of three different kinds of commercially available grapes: green, red, and black grapes, respectively. An air-tight cylindrical glass tube was used to sample the volatile compounds and stored them at 4°C. In 10 days of storage, EN performance was analysed using PCA for quality at different storage periods. Two PCA groups were analysed in the study, the first group of PCA based on the different types of grapes used accounted for 95.27%. The second PCA group tested for different storage periods resulted in 91.92%. Based on these findings, the authors were able to identify a clear distinction between aromatic compounds

associated with three different types of grapes stored for different periods. However, the authors only reported based on combustible gaseous such as methane, propane, butane, hydrogen, carbon monoxide, and hydrogen organic solvents like ethanol. The findings do not assimilate with the true nature of biochemical compounds related to volatile metabolites as a quality indicator. The compounds detected were general and often regarded as compounds that were associated with the respiration of crops (Ventura-Aguilar et al., 2021).

Ying et al. (2015) determined the freshness of litchi using EN composed of 8 MOS sensors with a nonlinear dynamics stochastic resonance (SR) model. The EN sensors were installed in an independent chamber to avoid cross-validation and the volatile compounds were sampled using an air-tight vial sealed with a sealing membrane. The authors also highlighted that the PCA obtained was not reliable hence the SR model was adopted in their study. PC between the two factors obtained show 82.22% of cumulative variance. While the SR model presented high accuracy in evaluating the freshness of litchi with regression coefficients of $R^2 = 0.99396$. Results also show that the EN can continuously detect the responses in terms of voltage, up to day 6 which makes it suitable as a freshness quality monitoring tool. As for the variation of compounds detected in the study, the method could be improved by adopting more sensors in the EN development which is not limited to nitrogen, ammonia, and hydrocarbon compounds. Sensors that could detect aroma compounds should be included.

Wei and Guohua (2015) conducted a study on kiwi based on SAW as an EN sensor for quality determination and consumer's overall acceptance. The authors have incorporated a freshness predictive study for real-time monitoring based on eight SAW sensors attached. Some of the quality indices investigated include weight loss index, moisture loss, colour changes, and a human sensory evaluation by experienced panellists. Hence, a comparison between the EN model and human sensory analyses was included. The freshness quality monitoring based on EN's response toward signals produced by electrical changes was used to characterize the concentration of the volatile compounds. The highest signal produced was analysed at sensor S4 with 0.095 V while the rest of the sensors were only below 0.05 V. The responses are rather weak as compared to any other previous reports. While the PCA results determined the PC1 and PC2 with a total variance of 91.06% between freshness and responses toward complex gaseous. Nevertheless, the authors were able to qualitatively analyse and discriminate samples with different storage times with a high regression coefficient; $R^2 = 0.98093$ and $R^2 = 0.99014$ for both SR and SAW resonance, respectively. It is also highlighted that there were no obvious changes in the first 4 days of human sensory evaluation. The freshness of the kiwi fruit worsened from day 8 onward, which matches the predictive model used.

Another study on peaches was reported by Voss et al. (2020) to monitor its preharvest and postharvest cycles using EN composed of 13 MOS sensors, which were tested in the field. The

authors have developed an EN prototype to classify the growth cycle based on the four growth stages of peaches as a training model (30% of the sample set was used for testing). Pearson's Chi-square test was adopted to analyse the comparison between all four stages. The statistical model used was able to validate the accuracy of the monitoring process with 99.23%. The authors highlighted that the primary volatile compound detected in peaches was solely ethanol. These compounds are mostly responsible for the increase in the ripening stage among the crop profiles, which are related to the respiration rate. Regardless, a quick response with high accuracy was obtained. This study has enabled the development of an EN sensor based on MOS at ambient temperature, and the authors have proven the reliability of EN to be used in the field for easy and low-cost operation for quality monitoring.

Huang et al., 2019 employed EN for volatile profiling to detect the freshness quality of spinach during cold storage at 4°C for 12 days. Seven MOS sensors, which were mainly sensitive to hydrogen sulfide, methane, alcohol, ammonia, and carbon monoxide, were used in this study. A sealed glass beaker was used to sample the volatile compounds of spinach with an incubation period of 1 h at room temperature before EN was introduced. Discriminant models such as a SVM and a backpropagation artificial neural network (BPNN) were used to optimize the pattern recognition system. The authors reported that the BPNN model deliver an 85.42% accuracy classification which was better than the SVM model with 81.25% and 75.00%, respectively, between training and prediction test. The two tests, the training, and prediction tests were used to improve the multisensory performance since a single test was not able to achieve a high accuracy rate. While the sensory score based on physiological metabolism revealed that the freshness of spinach was maintained up to day 3 during storage. However, the correlation between sensor response and physiological qualities was not established by the authors.

Ghasemi-Varnamkhasti et al. (2019) applied the use of EN with eight MOS sensors to characterize the freshness of strawberries from different polymer packaging. Materials such as polyvinyl chloride, polypropylene, and ethylene vinyl alcohol were used to sample the volatile compounds from strawberries and assess their freshness quality. Fruit freshness among all three different packaging materials was analyzed in combination with pattern recognition methods such as PCA, LDA, and SVM. The PCA resulted in 84% accuracy of cumulative variance of the data between two groups, the unpackaged and packaged samples. The LDA and SVM were used to better analyze the performance of PCA. Both LDA and SVM showed high accuracy resulting from sensor response toward unpackaged and packaged samples. Among all eight MOS sensors used, only six performed effectively. Despite that, the EN has prominent features such as long life, high chemical resistance, and low cost.

2.3.2 Ripening quality

The study conducted by Farhad et al. (2014) on mango (*Chokanan cv.*) quality monitoring based on different ripening stages provided an insightful finding on the responsible volatile compounds as a postharvest quality indicator. The research focused on analyzing the concentration of responsible volatiles produced from three different classes of mango namely unripe, ripening, and fully ripened samples using portable EN (zNose™ Model 4200). The EN utilized in this research is an electronic detector, as opposed to other electronic noses that use a myriad of MOS sensors, each of which oversees detecting one or more volatiles. This system is based on gas chromatography and comprises a sensor head, a support chassis, and a system controller. The study only managed to predict unripe and ripening mango stages with highly concentrated compounds. However, the authors described that the data for the fully ripened mango was not accessible due to the climacteric crop profile. Hence, the unripe samples were left for 3 days to assess the trend of volatile compounds during the ripening period. A volatile compound such as decanal was observed in all three classes with decreasing concentration with the increase of maturity stages. While volatile compounds like α -terpinolene were found to be absent in fully ripened mango samples. The trends of volatile compounds were analyzed based on the Kovats retention indices obtained from the portable EN sensor for the determination process. The zNose™ system uses a fast GC method that is as quick as a standard EN and can identify all elements in an odour. It also delivers a complete chemical profile. This study demonstrates that zNose™ can distinguish between the mango ripening stages and has a great deal of promise for application in the field, where picking the right maturity stage for harvest is essential for market satisfaction.

Similarly, Aghilinategh et al. (2020) used GC-MS and EN with 10 MOS sensors that were designed and constructed in the lab to categorize mulberries into five maturity levels (ripe, close to ripeness, intermediate to ripeness, close to unripe, and ripe). The authors effectively categorized the various ripeness classes in berries using the PCA, LDA, and ANN algorithms, with ANN producing the best classification outcomes. The accuracy of ANN's classification between the five ripeness levels was 100% for blackberries and 88.3% for white berries. The 97% and 93% of the variation in the blackberries and white berries, respectively, were defined by PCA analysis. The LDA approach produced the least accurate categorization for white berries. According to the GC-MS findings, C6 aldehydes were mostly present in immature white berries whereas ester and furanone concentrations increased in ripening berries.

Hendrick et al. (2022) developed an EN containing 13 gas sensors that utilized the BPNN approach to distinguish between unripe, mature, and rotten stages of banana ripeness. The purpose of backpropagation is to reduce errors in the ANN's output. This model was able to distinguish between the three stages of banana ripeness with 100% accuracy, and the EN setup additionally displayed the final ripeness stage determination on a website.

2.3.4 Sensory quality

Studies related to the quality evaluation of hulled and non-hulled wheatgrass species, namely *Triticum sp.* were investigated by Bianchi et al. (2019). Authors aimed to differentiate among five *Triticum sp.* and have established a protocol based on taste quality traits and volatile metabolites properties via portable (PEN 3) EN with 10 MOS sensors and HS-SPME analysis via GC-MS using DVB/CAR/PDMS fiber. The study reported that EN sensors were capable of discriminating prevalent volatile compounds of both hulled and non-hulled samples regardless of their genotypes. Some of the compounds reported are alcohols, ketones, and aldehydes. Among the ketones group, the compound 1-penten-3-one was highly reported with over 70% of the total ketones compound identified. Whereas E-2-hexenal from the aldehydes group reported up to 86% and 80% of total aldehydes among the non-hulled and hulled samples, respectively. These compounds also indicate that they were responsible for the green, earthy, and mushroom odours and were supported by other researchers in the agricultural field (Zhang et al., 2020). Apart from accessing the volatile comparison, taste quality-based TSS and TA were analyzed. Samples with higher expressions of 1-octen-3-ol, 1-penten-3-ol, and 1-phenylethanol have resulted in higher TSS content. The detection of volatile compounds is suitable to differentiate between hulled and non-hulled samples but is not able to differentiate the genotypic differences. The PCA applied also confirms the observation regarding genotype differences, which was lower with a total variance of 61.8%.

2.3.5 Other quality parameters

Gaggiotti et al. (2019) assessed the EN performances using QCM biosensors coupled with HS-SPME GC-MS analysis on carrot aroma profiling as a quality indicator. This study did not exactly analyze the ripeness, taste, or how long the freshness of carrots was maintained. The changes in aromatic compounds were monitored for up to 26 days at different storage temperatures (-18, 4, 25, and 40°C). EN equipped with 12 QCM sensors was used in the study using gold nanoparticles (AuNPs) functionalized with hairpin DNA (hpDNA) as a pathogen-specific antibody to the sample. While DVB/CAR/PDMS, 50/30 µm SPME fiber was used in GC-MS to obtain the pool of volatile emanated as a reference to the EN determination. A total of 18 compounds were identified from GC-MS analysis with common compounds such as terpenoids (e.g., α -pinene and γ -terpinolene) and alcohol groups. Whereas the EN responses from the QCM biosensor contribute mostly to the discrimination of the volatiles typically from octanal. In addition to molecular identification using hpDNA for its functionality, the sequence of tetramers (CGGG, TTGG, and CAGC) was reported to be homogenous. This finding later enumerates that the hpDNA-based gas sensors have the same potential as the discrimination of

volatile metabolites via GC-MS analysis. Hence, validate the usability of hpDNA-based gas sensors as part of an early detection tool. The PCA accounted for all carrot samples and volatiles determination stored at different temperatures and the presence of terpenoids among carrot samples showed 44.77% and 38.77% for PC1 and PC2, respectively. The developed EN was successful in tracking changes in the aroma of carrots. However, there is no correlation between data obtained from EN via QCM and GC-MS since the pool of volatiles determined from each method was different. Hence, more relevant work applying the QCM as biosensors needs to be considered in the future.

Quality changes of pitaya were studied by da Silva Ferreira et al. (2023) using a homemade low-cost EN consisting of 8 MOS sensors coupled with NIR spectroscopy. The pitaya samples in storage were analyzed for their physiochemical features: total phenolics content, TSS, TA, pH, and moisture content at two temperatures (15 and 25°C) on days 0, 7, 14, 21, and 25 after harvesting. PCA classified the samples on different storage days with a 66.4% variance. The loadings for the PCA indicated that the EN sensors sensitive to alcohol showed the biggest peaks. Authors reported that these sensors were also selective toward the molecule malic acid and other organic acids due to their OH group. The sensor sensitive to Carbon monoxide showed their levels increasing during storage. Sensors sensitive to methane and propane showed increased responses during the last days of storage when pitayas were getting rotten. The LDA and PLS-DA results showed excellent results with an overall accuracy of 95% and >94%, respectively, in classifying the samples on different storage days even when fruits were kept at different temperatures. The PLSR model was used to analyse the relationship between NIR and EN data with the results of physiochemical features. Only TA and pH were predicted well for EN with R^2 of 0.85 and 0.86, and root mean squared error and prediction (RMSEP) of 0.04 and 0.22, respectively. This is because pitaya contains many organic acids especially malic acid, which starts degrading over the storage days and increases the pH and decreases the TA values. However, TSS, total phenolics and moisture content presented poor correlation. Authors reported that this could be because measurements done on a non-violated fruit were unable to successfully capture enough volatiles by the sensors from the thick peel of pitaya. Albeit the main achievement of this study was developing a portable EN with only \$200 and the price to evaluate each sample with NIR and EN together was less than \$0.10. Future studies should similarly concentrate on creating low-cost EN technologies that will have a better likelihood of adoption by cultivars and useful field usage. In research papers, highlighting the technology's inexpensive installation costs and financial returns can persuade policymakers and businesses to adopt it in developing nations to minimize their food losses.

Combination of green synthesized ZnO NPs with chitosan as edible coatings to control postharvest fungal diseases.

2.4 Green synthesis of ZnO- NPs using plant extract

Zinc oxide nanoparticles (ZnO-NPs) have been successfully produced using a variety of chemical and physical techniques, encompassing sol-gel, hydrothermal, precipitation, co-precipitation, chemical vapor deposition, spray pyrolysis, magnetic sputtering, microwave-assisted methods and solvothermal routes (Al-darwesh et al., 2024). In the realm of physical synthesis, the interaction of nanoscale particles and the formation of substantial, well-defined nanostructures are governed by physical forces. This category includes nanoparticle synthesis through colloidal dispersion techniques, as well as fundamental processes like vapor condensation, amorphous crystallization, and physical fragmentation (Kołodziejczak-Radzimska and Jesionowski, 2014). Although physical approaches often require sophisticated equipment, elevated temperatures, and pressure, chemical methods involve the use of potentially hazardous substances, raising concerns for environmental and occupational safety (Zhou et al., 2023). Moreover, the incorporation of toxic agents in physical and chemical processes may pose risks when applied in medical contexts (Al-darwesh et al., 2024).

Biosynthesis presents an attractive alternative, offering an eco-friendly, simple and economical solution by harnessing microorganisms and plant-based sources for nanoparticle production, particularly relevant for agriculture and biomedical applications (Gadewar et al., 2024). Aligned with the principles of green chemistry, this methodology underscores sustainability and biocompatibility (FDA, 2019). The spectrum of green synthesis includes various biological substrates, such as plants, bacteria, fungi, and algae, enabling the scalable fabrication of ZnO-NPs devoid of additional impurities. Moreover, biomimetic synthesis enhances catalytic activity while minimizing reliance on expensive and hazardous chemicals.

Among biological substrates, plants emerge as prominent candidates for green synthesis, distinguished by their cost-effectiveness, ease of processing, and reduced toxicity compared to microbial sources. Plant extracts, which are easily obtained using solvents such as distilled water or ethanol, harbour a rich repertoire of active compounds, including methylxanthines, phenolic acids, flavonoids, and saponins, which are known for their antioxidant potential. These antioxidants play a pivotal role in bio-reducing or chelating metal ions, facilitating the green synthesis of metallic nanoparticles (Zeghoud et al., 2022). Nonetheless, the intricate composition of plant extracts poses challenges in delineating precise synthesis mechanisms.

2.4.1 A general mechanism of the synthesis of ZnO NPs using plant extract

Step 1: Plant Extract Preparation

- Various plant parts like leaves, fruits, seeds or bark are used.
- These parts are crushed or ground and extracted using water or organic solvents like ethanol.
- The extract is rich in biomolecules like polysaccharides (sugars), proteins, enzymes, and alkaloids. These biomolecules acted as reducing agents. They donate electrons to zinc ions (Zn^{2+}) from a precursor salt (e.g., zinc nitrate or zinc acetate) present in the solution. The reduction reaction converts Zn^{2+} to Zn^0 atoms, which then nucleate and grow into ZnO NPs (Bouttier-Figueroa et al., 2024).

Step 2: Reduction and Nucleation

- The plant extract containing biomolecules is mixed with the zinc precursor solution.
- Depending on the plant extract and reaction conditions (temperature, pH), the reduction process can be rapid or take several hours.
- As the biomolecules donate electrons, Zn^{2+} ions are reduced to Zn^0 atoms.
- These Zn^0 atoms clump together due to van der Waals forces, forming tiny clusters.
- The reduction potential of the biomolecules determines the rate and efficiency of Zn^{2+} reduction. The biomolecules can also act as capping agents, preventing uncontrolled growth and aggregation of ZnO nanoparticles (Gadewar et al., 2024).

Step 3: Growth and Stabilization

- The initial Zn^0 clusters continue to grow by attracting more Zn^0 atoms.
- The biomolecules surrounding these clusters influence their shape and size.
- As the nanoparticles grow, they acquire oxygen atoms from water or the surrounding environment, forming ZnO.
- Notably, plant extracts may serve as substitutes for surfactants and bases, modulating particle growth and precipitation dynamics. Acidic leaf extracts, for instance, may necessitate alkaline agents for zinc oxide/hydroxide precipitation. The functional groups (like hydroxyl or carboxyl groups) present on biomolecules interact with the ZnO surface, stabilizing the nanoparticles and preventing uncontrolled agglomeration. These interactions can also influence the final size, shape, and surface properties of the ZnO nanoparticles (Naseer et al., 2020).

Step 4: Purification and Characterization

- After synthesis, the solution containing ZnO nanoparticles needs purification to remove unreacted precursor salts and biomolecules. Techniques like centrifugation and calcination processes are employed to eliminate volatile constituents, yielding pure ZnO-NPs.
- The purified nanoparticles are then characterized using various analytical methods like X-ray diffraction (XRD) for crystal structure, transmission electron microscopy (TEM) for size and morphology, and UV-visible spectroscopy for optical properties (Aldalbahi et al., 2020).

The extensive array of biological substrates and synthesis conditions, including variations in zinc salt concentration, pH, reaction duration, and temperature, result in nanoparticles exhibiting a diverse range of sizes and morphologies. The most recent studies on preparation of ZnO NPs are summarised in Table 2.3. The entire process of green synthesis is also illustrated in figure 2.5.

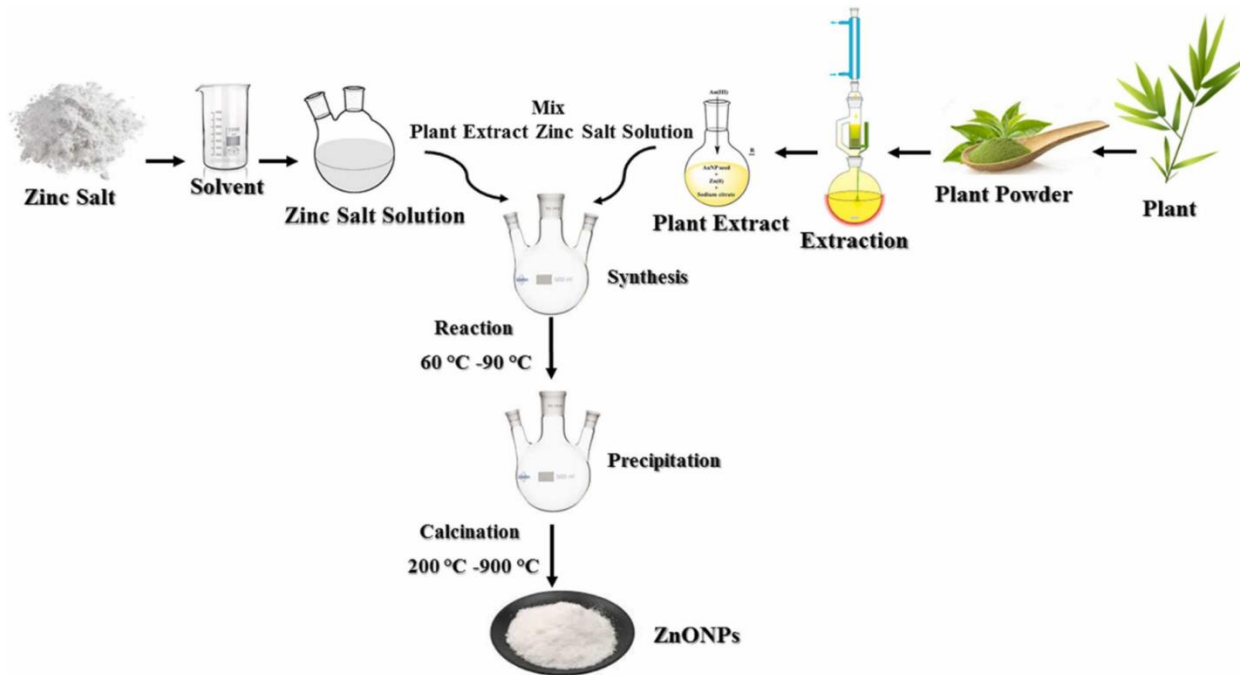


Figure 2.5: Green synthesis of ZnO NPs using plant extract (Zeghoud et al., 2022)

Table 2.3: Recent studies on the preparation procedure of green synthesized ZnO NPs.

Size	Plant material preparation	Precursor preparation	Temperature and pH	Ratio of plant material: precursor	Mixing	Additional chemicals	Final product processing	Reference
80-200nm	Okra seed extract 10g dried seed powder mixed with 150ml Milli-Q water, heated at 90°C for 2.5h	Zinc chloride [ZnCl ₂ .4H ₂ O], 0.1M	Room temperature	3:2	Stir for 3h	0.1M, 20ml Naoh	White precipitate (ppt) Centrifuge at 4000rpm for 10mins. Dried at 60°C in oven, crushed into powder. Calcination- 2.5h at 400 °C	(Fazal and Iftekhar, 2024)
52-98nm	<i>Clerodendrum infortunatum</i> L. 40g of dried leaf powder extracted with soxhlet extraction, 300ml distilled water as solvent	Zinc acetate dihydrate (ZnCH ₃ COO) ₂ .2H ₂ O)	60°C	13g precursor added to 20ml leaf extract and 100ml methanol mixture	Constant stirring	0.5M NaOH 0.1M methanol	Centrifuge at 10000 rpm for 10mins. Ppt washed and dried at 100°C then ground to powder. Calcination at 400 °C for 3 h	(Kumar et al., 2024)

Table 2.3 continued: Recent studies on the preparation procedure of green synthesized ZnO NPs.

43-60nm	<i>Nigella sativa</i> seed 400gm fine powder dissolved in 600 mL of ethanol at 100 °C for 24 h, then filtered.	Zinc nitrate hexahydrate, Zn(NO ₃) ₂ ·6H ₂ O 0.1M	90 °C, pH: 11-12	Leaf extract added dropwise into precursor until pH 11-12.	Stir for 2h		Dark green ppt centrifuged at 5000rpm for 10mins, dried and ground. Annelation at 400 °C for 2 h.	(Fakhar-e-Alam et al., 2024)
5-35 nm	<i>Vitex negundo</i> 5g grounded into a fine paste and dissolved in 100ml Milli-Q water, stirred (660 rpm) under heating at 80 °C for 1 h and filtered.	zinc nitrate hexahydrate, Zn(NO ₃) ₂ ·6H ₂ O 1g powder used	80 °C	1g precursor added to 30ml leaf extract	Constant stirring until colour change and solution turns into a fine paste		A fine paste was obtained, washed and calcined at 350 °C for 2h.	(Venkatesan et al., 2024)

Table 2.3 continued: Recent studies on the preparation procedure of green synthesized ZnO NPs.

30-50nm	<i>Azadirachta indica</i> (Neem) Torn leaves agitated for 4 h with 200 mL of Milli-Q water before being immersed in a water bath at 60 °C for 40 min	Zinc nitrate Zn(NO ₃) 2g powder	60 °C	2g in 40ml extract	Mixture kept in water bath until pasty consistency.		A fine paste obtained that was heated at 400 °C for 2 h.	(Mehmood et al., 2024)
~57nm	Dry waste peels of the onions (<i>Allium cepa</i> L.) blended. 50g blended peel mixed with 100-200ml d H ₂ O	Zinc acetate dihydrate (ZnCH ₃ COO) ₂ ·2H ₂ O) 2 mM	65 °C, 8	1:5	Stirred at 450rpm		Ppt set to stand for 4h and centrifuged at 7000 rpm for 5 min. Ppt washed and dried at 130 °C for 3 h Sample then calcined for 2 h at 500 °C	(Islam et al., 2024)

Table 2.3 continued: Recent studies on the preparation procedure of green synthesized ZnO NPs.

10-30nm	<i>Xanthium indicum</i> dried and grinded to powder 25g powder in 75ml ethanol for extraction with Soxhlet apparatus for 8 h, then filtered	Zinc nitrate hexahydrate $Zn(NO_3)_2 \cdot 6H_2O$ 1 M	80 °C, pH 8	1:25	Stirred for 6h	1 M KOH	Light green ppt washed and kept in a hot air oven at 200 °C for 8 h. Calcination 500 °C for 2h	(Boro et al., 2024)
~20nm	<i>Ipomoea spp.</i> (<i>Convolvulaceae</i>) 10g leaves with 100ml MilliQ water and filtered	Zinc nitrate hexahydrate $Zn(NO_3)_2 \cdot 6H_2O$	80 °C	50ml extract with 5g precursor	Constant stirring until volume reduced to 10ml		Resultant reaction mixture calcined at 300 °C for 2 h	(Nataraj et al., 2024)

Table 2.3 continued: Recent studies on the preparation procedure of green synthesized ZnO NPs.

24 ±0.49 nm	<i>Lantana Camara</i>	Zinc acetate dihydrate $(ZnCH_3COO)_2 \cdot 2H_2O$		Precursor mixed with 50ml leaf extract.	Constant stirring for 2h		Obtained solution centrifuged at 8000	(Sharma et al., 2023)
-------------	-----------------------	---	--	---	--------------------------	--	---------------------------------------	-----------------------

	20g leaves boiled in 200ml Milli-Q water for 2h and filtered						rpm for 20 min and then filtered White ppt calcined 4 h at 300 °C at a heating rate of 5 °C/min	
~34nm	<i>Aquilegia pubiflora</i> dried into powder 30g powder mixed with 200ml water and sonicated for 10 min, maintained in a shaking incubator at 200 rpm and 37°C for 2 days, then filtered.	zinc acetate dihydrate 6g	60°C for 10mins then 25°C	100ml extract with 6g precursor	Constant stirring for 2h		Pellet cetrifuged at 10,000 rpm. oven dried at 80°C Further ground at 500°C for 2h.	(Jan et al., 2021)

In the study by Fazal and Iftekhar, (2024), 0.1 M zinc chloride solution was mixed with okra seed extract and NaOH, resulting in the formation of a white precipitate identified as Zn(OH)₂. The precipitates were separated through sedimentation and decantation, and the resulting sediment was centrifuged to obtain dense zinc hydroxide nanoparticles. In this study, the reaction was done at room temperature instead of heat used to obtain precipitate in most of the studies. After synthesis, the nanoparticles were dried, crushed, and calcined at 400 °C for 2.5 hours to obtain pure ZnO nanoparticles. Kumar et al., (2024) synthesized ZnO NPs by directly mixing 13g of solid zinc acetate dihydrate to *Clerodendrum infortunatum L.* extract which is similar to studies done by Kambale et al., (2024), Venkatesan et al., (2024), Mehmood et al., (2024), Nataraj et al., (2024) and Jan et al., (2021) that also used precursor in solid form and mixed with *Panda oleosa*, *Vitex negundo*, *Azadirachta indica*, and *Aquilegia pubiflora* leaf extracts respectively. Factors like pH can also affect the sizes of nanoparticles. A study by Zhu et al., (2024) synthesised ZnO NPs using *Cinnamomum camphora* leaf extract and it was found that sizes of ZnO NPs synthesized at pH 7, pH 8 and pH 9 were about 13.92, 15.19 and 21.13 nm, respectively. Additionally, it's worth noting that nanoparticles synthesised using the green method are not always confined to sizes below 100 nm. For instance, in a study conducted by Kambale et al. (2024), ZnO NPs with a size of approximately 228.8 ± 3.0 nm. Another study by Thienprasert et al., (2021) also obtained ZnO NPs of size 256 ± 40 nm synthesized using banana peel extract. These nanoparticles in high doses were then shown effective in controlling anthracnose disease symptoms on inoculated orchid leaves.

Researchers conduct trials with varying concentrations of leaf extracts and precursors until the desired nanoparticle size is achieved. The reducing power of bioactive compounds in the leaves determines how effectively they can reduce the precursor compounds, ultimately influencing the size of the resulting nanoparticles. Once the desired nanoparticle sizes are achieved, their suitability for various applications becomes a critical consideration. ZnO NPs find utility across a wide spectrum of fields owing to their unique properties (Zeghoud et al., 2022). In biomedical applications, such as drug delivery and cancer therapy, smaller nanoparticles may offer enhanced cellular uptake and targeting capabilities (Al-darwesh et al., 2024). In the realm of cosmetics and sunscreens, nanoparticles with specific size ranges contribute to improved UV protection and transparency (Chauhan et al., 2022). Furthermore, in environmental remediation, smaller nanoparticles exhibit increased surface area and reactivity, facilitating efficient pollutant degradation (Singh et al., 2022). ZnO NPs also play a pivotal role in electronic devices, where size-controlled nanoparticles are essential for optimizing device performance and functionality (Liu et al., 2021). Thus, tailoring nanoparticle size to suit specific applications underscores the versatility and significance of ZnO NPs in diverse domains.

2.4.2 Antifungal properties of ZnO NPs

ZnO-NPs demonstrate pronounced antifungal efficacy against a spectrum of fungal species, prompting intensive investigation into their underlying mechanisms (Hermida-Montero et al., 2021). Current research elucidates several proposed mechanisms contributing to their antifungal activity. Figure 2.6 illustrates the antifungal mechanism of ZnO NPs.

- **Reactive Oxygen Species (ROS) Generation:** ZnO-NPs initiate the production of ROS, including hydroxyl radicals and singlet oxygen species, which inflict oxidative damage on fungal cellular components, ultimately leading to cellular demise. ROS generation is facilitated through:
 - a. **Direct Interaction:** ZnO-NPs directly interact with fungal cells, eliciting ROS production within the cellular milieu.
 - b. **Photocatalytic Activity:** Upon exposure to light, ZnO-NPs undergo photocatalytic reactions, augmenting ROS generation and thereby enhancing their antifungal potency (Lakshmeesha et al., 2020).
- **Membrane Disruption:** ZnO-NPs exert physical perturbations on fungal cell membranes, resulting in the leakage of vital intracellular contents and subsequent cell death. Membrane disruption occurs via:
 - a. **Direct Interaction:** The nanoscale dimensions and high surface area of ZnO-NPs facilitate adherence to fungal cell membranes, inducing structural damage.
 - b. **Metal Ion Release:** Under specific environmental conditions, ZnO-NPs release zinc ions, which further disrupt membrane integrity, exacerbating cellular vulnerability (Hermida-Montero et al., 2021).
- **Enzyme Inhibition:** ZnO-NPs impede fungal growth and metabolism by interfering with critical enzymatic processes. This inhibition targets:
 - a. **Respiratory Enzymes:** ZnO-NPs obstruct pivotal enzymes involved in energy production pathways, impeding fungal respiration (Huq et al., 2023).
 - b. **Biosynthesis Enzymes:** ZnO-NPs interfere with enzymes responsible for synthesizing essential cellular components, including cell wall constituents, impairing fungal viability (Zheng et al., 2014).

Additionally, ZnO-NPs may exert antifungal effects through:

- **Nutrient Deprivation:** ZnO-NPs may sequester essential nutrients, rendering them inaccessible to fungal cells, thereby impeding growth (Mohd Yusof et al., 2019).
- **Signalling Pathway Interference:** ZnO-NPs have the potential to disrupt fungal signalling cascades, perturb growth regulatory mechanisms, and inhibit fungal proliferation. The photon-induced generation of ROS and the cytotoxic effect resulting from Zn²⁺ release emerged as primary contributors to the antifungal efficacy of ZnO-NPs. These mechanistic

insights underscore the multifaceted antifungal properties of ZnO-NPs, facilitating their potential application in combating fungal infections (Daniel et al., 2023).

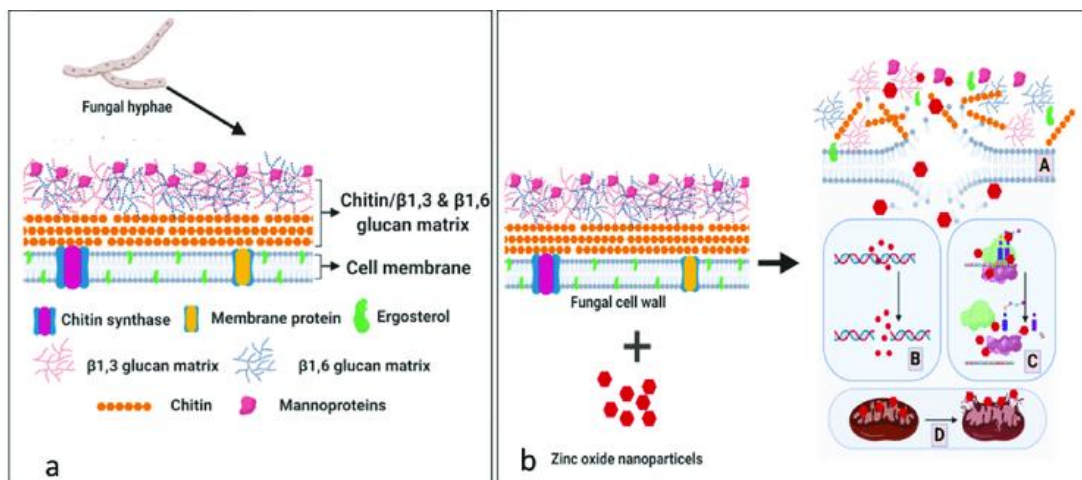


Figure 2.6: Antifungal activity of ZnO NPs. (a) Fungal cell wall; (b) Mechanism of action; (A) Destruction of fungal cell wall; (B) DNA disruption; (C) Inhibition of protein synthesis; (D) Mitochondria disruption (Lakshmeesha et al., 2020).

The antifungal properties of zinc oxide nanoparticles (ZnO NPs) have garnered considerable attention in recent research. Numerous studies have explored whether ZnO NPs synthesized via green methods retain their antifungal efficacy.

For example, Zhu et al. (2024) synthesized ZnO NPs at different pH levels and found that concentrations ranging from 20 to 160 mg/L significantly inhibited the mycelia growth of the fungi *A. alternata* in a dose-dependent manner. Similarly, Elshafie et al. (2023) investigated ZnO NPs prepared using *M. oleifera* extract and observed a notable inhibition of fungal growth against *Alternaria citri*, with reductions ranging from 21.59% to 68.50% at a concentration of 2,000 µg/ml. In the study conducted by Jamdagni et al. (2018), ZnO NPs synthesized were assessed for their antifungal potential against five fungal strains, including *Alternaria alternata* (ITCC 6531), *Aspergillus niger* (ITCC 7122), *Botrytis cinerea* (ITCC 6192), *Fusarium oxysporum* (ITCC 55), and *Penicillium expansum* (ITCC 6755). The results indicated that ZnO nanoparticles prepared using flower extract of *Nyctanthes arbor-tristis* exhibited significant antifungal activity against all tested fungi. Notably, *A. niger* displayed the highest sensitivity with the lowest Minimum Inhibitory Concentration (MIC) value, whereas *B. cinerea* and *P. expansum* exhibited the highest MIC values among the fungal strains tested. Thienprasert et al. (2021) investigated the antifungal properties of ZnO nanoparticles synthesized from banana peels extract against *Colletotrichum sp.* The study's in vitro findings revealed the most potent inhibitory effect on day

7, with a 50% growth inhibition observed at a high concentration of 13,991.6 mg/mL. Similarly, Sivasankarapillai et al. (2022) synthesized ZnO NPs utilizing *Scoparia Dulcis* plant extract and assessed their antifungal efficacy against *Candida albicans* and *Aspergillus niger*. The concentrations ranging from 500 to 50 µg/mL demonstrated significant inhibition of *Aspergillus niger* growth, while only the 500 µg/mL concentration exhibited significant inhibition of *Candida albicans*. These studies collectively demonstrate the robust antifungal efficacy of ZnO NPs synthesized using plant extracts, making them promising candidates for various applications, including the control of postharvest fungal infections. Consequently, there is growing interest in exploring the incorporation of ZnO NPs into edible coatings to enhance the preservation of stored fruits' quality.

2.5 Chitosan as a carrier for metal-oxide nanoparticles to form an edible coating.

Researchers worldwide, particularly in the field of agriculture, are increasingly interested in chitosan (Riseh et al., 2023). Chitosan, a linear polysaccharide comprising glucosamine and N-acetylglucosamine units (as illustrated in Figure 2.7), stands out as the sole cationic pseudonatural polymer (Aranaz et al., 2021). It is derived from the deacetylation of chitin, the second most abundant biopolymer found in nature, primarily sourced from crustacean exoskeletons like those of shrimp and lobster (Ibrahim and Zairy, 2015). Chitosan is recognized for its non-toxic nature, biocompatibility, and biodegradability, making it a renewable, sustainable, and cost-effective material. Moreover, its unique chemical structure affords it appealing physicochemical and biological properties, including bioadhesiveness, the ability to form films on skin and mucous membranes, favorable flow characteristics, and antimicrobial activity (Aranaz et al., 2021).

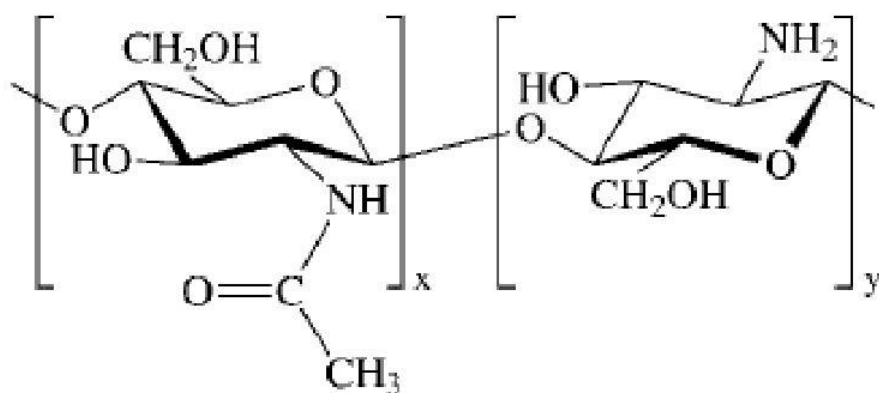


Figure 2.7: Chitosan structure (Ibrahim and Zairy, 2015)

Edible coatings are widely recognized for their ability to slow down the decay and deterioration of fresh fruits. Chitosan has been shown to induce host resistance to pathogens and form a semi-permeable film on the fruit surface, making it a promising natural fungicide in postharvest fruit preservation (Romanazzi et al., 2018). Numerous studies have reported the effectiveness of chitosan coatings in delaying the decay of various fruits, including papayas (Ali et al., 2015), mangoes (Cissé et al., 2015), tomatoes (Sucharitha et al., 2018), dragon fruit (Nguyen et al., 2020) and avocados (Obianom et al., 2019).

Typically, edible films made from proteins or polysaccharides not only help maintain moisture but also extend shelf life. To improve microbial stability, fresh-cut fruits are often dipped in antimicrobial solutions containing essential oils or metal nanoparticles (Chawla et al., 2021). Incorporating antimicrobial agents into edible coatings can enhance their inhibitory effects against spoilage and pathogenic bacteria by maintaining effective concentrations of active compounds on the food surfaces (Riseh et al., 2023). Combining edible coatings with antimicrobial properties or integrating antimicrobial compounds presents a promising alternative to enhance the safety and quality of fresh fruits.

Chitosan has undergone extensive research for its potential use in combination with other antimicrobial agents. Nano-formulations based on chitosan offer enhanced efficacy due to their increased surface area, smaller particle size, improved mobility, and lower toxicity compared to conventionally used pesticide formulations (Frank et al., 2024). Although chitosan exhibits broad-spectrum antimicrobial activity, its effectiveness is limited by its low solubility rate in aqueous media. When combined with metals like copper, chitosan demonstrates promising antibacterial and antifungal properties, as copper has antagonistic effects on fungi and bacteria (Kashyap et al., 2015). Chitosan's free amino group interacts with metal ions to form metal nanoparticles, which exert potent antifungal effects when stabilized by chitosan. Combinations

of chitosan and ZnO NPs demonstrate synergistic effects in inhibiting food-borne pathogens (Mustika and Wardana, 2020).

In the realm of edible coatings, various additives such as antibacterial and antioxidant agents, flavor compounds, and nutrients are commonly incorporated to enhance performance. While organic antibacterial materials may become unstable over time within coatings, inorganic counterparts exhibit greater stability at high temperatures and pressures (Kashyap et al., 2015). Notably, several inorganic oxides, including magnesium oxide (MgO), titanium oxide (TiO₂), and ZnO oxides, have been successfully employed as antibacterial agents in edible coatings (Kumar et al., 2020). Among these, ZnO is deemed safe for human health, given zinc's essential role in numerous metalloenzymes within living organisms (Al-Naamani et al., 2016).

There are several ways to integrate chitosan with nanoparticles. One popular method is coating the nanoparticles by adding a chitosan solution to pre-made nanoparticle compositions. As an alternative, and this is especially possible with polymeric nanoparticles, chitosan can be added during the nanoparticle creation process to coat them (Frank et al., 2020). Figure 2.8 shows both techniques. The positively charged cationic polymer chitosan creates a shell around the nanoparticles when it comes into contact with either formed or forming nanoparticles. The interaction between chitosan's ammonium groups and the negative charges on the surface of the nanoparticles occurs when the environment is acidic. This interaction is known as an interfacial reaction, electrostatic or polyelectrolyte deposition, or a self-organized interaction between chitosan and negatively charged nanoparticles (Arthur et al., 2017). Making a chitosan solution while taking into account the solubility of chitosan is the first stage in creating chitosan-coated nanoparticles. Generally, chitosan is dissolved in an acidic water solution, which usually contains 1% or less of hydrochloric acid, acetic acid, or other buffers, like acetate buffer at pH 3.0 and pH 4.5. Following solubilization, pH can be adjusted. After the chitosan solution is ready, it can be added to premade nanoparticles or used in the previously mentioned nanoparticle synthesis process to include it into nanoparticle formulations.

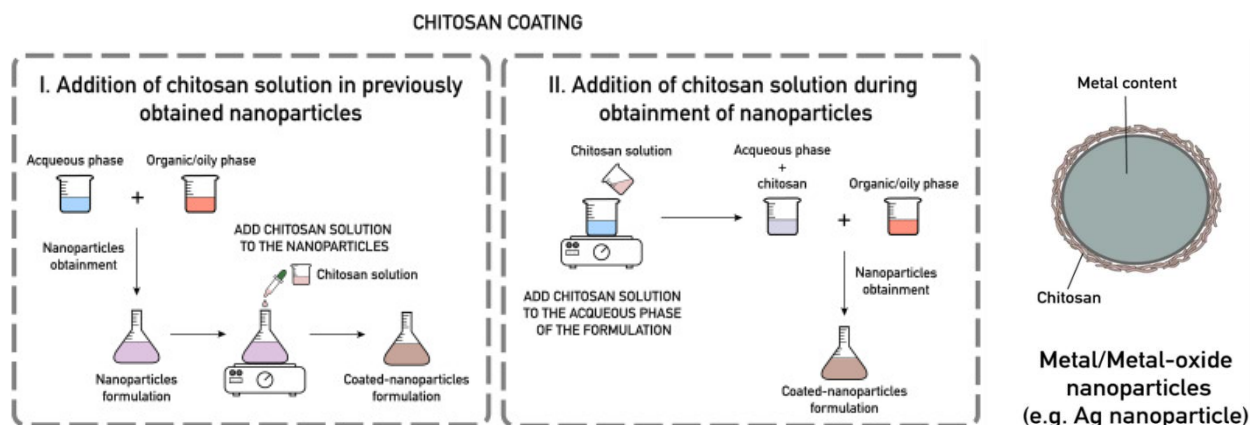


Figure 2.8: Different methods of preparing chitosan–metal nanoparticle solutions and the formation of chitosan shells around the nanoparticles (Frank et al., 2020)

New research is emerging to explore the development of coatings composed of chitosan and ZnO nanoparticles for diverse applications (Table 2.4).

Table 2.4: Recent studies on the application of Chitosan-ZnO NPs coating on fresh produce.

Fruit type	Main coating ingredients	Additional chemicals	ZnO NPs concentrations	Effect	Reference
Cherry tomato	Chitosan, ZnO NPs powder	Acetic acid Glycerin, Tween 80	0.2%, 0.4%, 0.6% (w/v)	Reduced SSC, colour change, bacterial growth after 15 days of storage	(Li et al., 2021)
Strawberry	Chitosan, ZnO NPs solution	Acetic acid	0.15g in 100ml	Lower counts of AMB, molds, yeast. Reduced weight loss, change in firmness and moisture content. Colour, pH, SSC and TA remain same	(García-García et al., 2023)

Wild-simulated Korean ginseng root	Chitosan, ZnO NPs powder	Acetic acid	0.01%, 0.02%, and 0.03% w/v	Reduced mold development and browning	(Kang et al., 2022)
Pistachio	Chitosan nanoparticles (CHNPs), ZnO NPs powder	NaOH, acetic acid tripolyphosphate (TPP)	250 mg L ⁻¹ and 500 mg L ⁻¹	Reduced weight loss, change in firmness, TA, TPC, TFC. Lower microbial decay	(Taghipour et al., 2024)

Table 2.4 continued: Recent studies on the application of Chitosan-ZnO NPs coating on fresh produce.

Banana	Chitosan, Gum Arabic, ZnO NPs powder	NaOH, acetic acid	0.1 %, 0.3 %, 0.5 %, and 1.0 % (w/w)	Reduced ripening by reduced change in colour, weight, TA and firmness	(La et al., 2021)
Avocado	Chitosan, Gum Arabic, ZnO NPs powder	NaOH, acetic acid	0.1 %, 0.3 %, 0.5 %, and 1.0 % (w/w)	Improved appearance and lightness during storage, reduced microbial decay and weight loss. Firmness, SSC retained for 7 days.	(Le et al., 2021)
Passion fruit	Chitosan, glycerol, carnauba	Acetic acid, tween 80	0.05%	Chitosan + resin worked best: reduced	(Junior et al., 2024)

	wax, rosin resin, ZnO NPs powder			weight loss, injuries, microbial growth, change in appearance over 10 days.	
Guava	Chitosan, ZnO NPs gel Sodium alginate	Acetic acid, glycerol	1%v/v _{gel}	Delayed ripening, 20 days without rot signs.	(Arroyo et al., 2020)

Table 2.4 continued: Recent studies on the application of Chitosan-ZnO NPs coating on fresh produce.

Pineapple	Chitosan, Aloe vera gel, ZnO NPs powder	HCL, NaOH, acetic acid	1%	Reduced weight loss, TSS, TA, maturity index. Maintained taste, odour, visual appearance for 15days.	(Basumatary et al., 2021)
Strawberry, red plum	Chitosan, ZnO NPs powder	Acetic acid	5 wt.%	Freshness preserved, improved internal appearance over 8 days, reduced weight loss	(Alamdari et al., 2022)
Fig	Chitosan, ZnO NPs powder	Acetic acid	25, 50, 75, 100, 125, 150, 175, 200ppm	Reduced change in TSS, TA, weight loss, firmness and	(Lakshmi et al., 2018)

				microbial growth.	
--	--	--	--	-------------------	--

Table notes: **SSC** – Soluble solids concentration, **AMB** - Aerobic mesophilic bacteria, **TA** - Titratable Acidity, **TPC** – Total phenolic contents, **TFC** – Total Flavonoids concentration

Li et al., (2021) investigated the effect of chitosan- Nano-ZnO composite films for preservation of cherry tomatoes. All films were fabricated using the solution casting method. A 1% chitosan solution was prepared by dissolving chitosan in a 2% (v/v) glacial acetic acid solution at 30°C. Glycerin (0.25%) and Tween 80 (0.1%) were incorporated into the solution, followed by the addition of various amounts of nano-ZnO (0.2%, 0.4%, 0.6% (w/v)). After thorough stirring and ultrasonic defoaming, composite film solutions with concentrations ranging from 0% to 0.6% nano-ZnO were obtained. Significant findings were observed in various aspects of the quality of the produce. Firstly, the chitosan composite film effectively inhibited respiration and slowed down carbohydrate hydrolysis, leading to a reduction in soluble solids content (SSC) in cherry tomatoes compared to the control group after 15 days of storage. Secondly, the film reduced the colour change of cherry tomatoes by maintaining low O₂ and high CO₂ concentrations, thus preserving their sensory quality. Thirdly, although the film did not significantly delay the appearance of the respiratory peak in cherry tomatoes, it formed a barrier on the fruit surface, inhibiting respiratory intensity and slowing the aging process. Additionally, the chitosan-nano-ZnO composite film significantly reduced the growth of bacteria in cherry tomatoes, exhibiting antimicrobial effectiveness and extending their shelf life.

In another study, chitosan coatings modified with nanostructured ZnO were applied on strawberries to preserve their shelf life. For the coating application, solutions of chitosan and ZnO NPs were prepared separately and then applied to strawberries by submerging them for a brief period. The coatings adhered firmly to the strawberry surface without significant runoff. The strawberries were then stored at 5°C and observed for eight days. Microbiological analysis revealed that coated strawberries exhibited lower counts of aerobic mesophilic bacteria (AMB), molds, and yeasts compared to the control samples. The reduction in microbial growth was particularly evident in the coated strawberries stored at both refrigeration (5 °C) and room temperature (25 °C). Despite the increase in AMB counts in the coated strawberries under refrigeration, they remained within acceptable levels for human consumption. The coatings retarded weight loss and firmness for 8 days due to their barrier properties. Moisture content decreased significantly in control samples, while coatings maintained the moisture, especially under refrigeration. pH, SSC, and TA remained stable in coated strawberries, indicating control over maturity. Colour analysis showed no significant difference in luminosity, but a decrease in redness and increase in browning index in coated strawberries, attributed to moisture loss and enzymatic activity.

In the research conducted by Kang et al. (2022), chitosan-ZnO NPs edible coating was employed to prolong the shelf life of Wild-simulated Korean ginseng root (*Panax ginseng* C.A. Meyer; WsKG). The chitosan-ZnO NPs solution containing varying concentrations of ZnO NPs (0.01%, 0.02%, and 0.03% w/v) were prepared. In the storage test, both coated and non-coated WsKG samples were placed over a K₂SO₄ saturated salt solution to simulate humid conditions. They were stored at temperatures of 5, 10, and 20 °C for 6 weeks. At intervals, samples were taken, homogenized in peptone water, and plated onto Petrifilm™ for microbial enumeration. Coated WsKG initially exhibited a decline in microbial concentration, followed by a gradual increase, with a slower growth rate at lower temperatures. The microbial limit of WsKG was reached faster as storage temperature increased, with non-coated and coated WsKG lasting approximately 3.9 and 6.3 weeks at 5 °C, 1.9 and 4.3 weeks at 10 °C, and 1.3 and 2.0 weeks at 20 °C, respectively. The coating effectively inhibited mould development and browning of WsKG, thereby delaying natural fermentation and deterioration.

In some studies, researchers have explored the effectiveness of chitosan nanoparticles (CHNPs) in preserving food products. Combining CHNPs with ZnO NPs to create a composite could potentially enhance their antimicrobial properties further. This approach is particularly promising as both chitosan and zinc oxide are nano-sized, potentially leading to synergistic effects and increased effectiveness in food preservation.

The study by Taghipur et al., (2024) utilized the ionic gelation method to prepare chitosan nanoparticles (CHNPs), starting with the dissolution of 2.5 g of chitosan in glacial acetic acid solution. After filtration to remove impurities, tripolyphosphate (TPP) solution was added to the chitosan base solution at a specific ratio and stirred for 2 h to form a gel containing CHNPs. The gel was then centrifuged and washed with distilled water to obtain neutral pH CHNPs. Subsequently, a chitosan-Zn nanocomposite was prepared by dissolving 2 g of chitosan in acetic acid solution, followed by the addition of a zinc acetate solution. After ultrasonication and heating in an oil bath, NaOH solution was added to adjust the pH, and the resulting suspension was left to settle for 24 hours to obtain the chitosan-ZnO nanocomposite, which was then centrifuged, washed, and dried. This study assessed the effects of pre-harvest treatments on pistachio trees by directly spraying different concentrations of treatments onto branches and clusters. The treatments included water (control), chitosan (CH) at concentrations of 500 mg L⁻¹ and 1000 mg L⁻¹, CHNPs at concentrations of 250 mg L⁻¹ and 500 mg L⁻¹, and CHNPs-ZnO NPs at concentrations of 250 mg L⁻¹ and 500 mg L⁻¹. These applications were carried out at specific growth stages of the pistachio fruits, followed by post-harvest evaluations. Upon harvesting during the commercial maturity stage, the pistachio fruits underwent sorting based on size, shape, and colour, with damaged fruits being removed. Finally, the pistachios with soft hulls

were packed in transparent polyethylene containers and stored under controlled conditions for further analysis. The study evaluated the efficacy of pre-harvest treatments on pistachio trees, focusing on weight loss (WL), hull firmness, decay index (DI), and biochemical changes in fresh pistachios during storage. Results indicated that WL significantly increased during storage, with control samples exhibiting the highest WL. However, coatings containing CHNPs and CHNPs-ZnO notably reduced WL due to their antimicrobial properties and ability to create a barrier against water evaporation. Furthermore, hull firmness was significantly higher in pistachios treated with composite coatings than in the control and single treatments, indicating the effectiveness of CHNPs-ZnO in maintaining fruit quality. Decay index was also lower in coated pistachios, with CHNPs-ZnO treatments showing the most significant reduction in decay, attributed to the antimicrobial effects of chitosan and ZnO nanoparticles. Moreover, the coatings preserved total phenolic compounds (TPC), total flavonoid compounds (TFC), and total anthocyanin compounds (TAC) during storage, with CHNP-ZnO treatments exhibiting the highest levels of these antioxidants. The coatings also enhanced antioxidant activity, with CHNPs-ZnO treatments showing the highest free radical inhibition.

In the study by (La et al., 2021) ZnO NPs were synthesized through a hydrothermal method involving the dissolution of zinc acetate dihydrate and Hexamethylenetetramine in water, adjusting pH to 8, heating the solution in an autoclave at 150°C for 24 hours, filtering the precipitates, washing and drying them, and finally calcining the powder at 400°C in N₂ to obtain ZnO NPs. These nanoparticles were then integrated into chitosan/gum arabic (CH/GA) edible coatings for bananas, prepared by dissolving GA in water, dissolving CH in water with CH₃COOH, adjusting pH, and mixing solutions with varying ZnO contents. It then investigated the preservation efficacy of edible CH/GA/ZnO coatings on bananas over a storage period of 17 days at 35°C and 54% relative humidity. Without coatings, bananas rapidly ripened and rotted within the timeframe. The application of CH/GA coatings delayed ripening and maintained the colour of the banana at the yellow stage. Incorporating ZnO nanoparticles further enhanced preservation, visibly reducing the ripening process. This improvement was evidenced by a delayed change in peel colour and reduced weight loss, from approximately 25% in uncoated bananas to 15% with 0.5% ZnO. Additionally, the coatings preserved acidity levels, with a T value of 0.3% observed with 0.5% ZnO, compared to 0.225% in uncoated bananas. The coatings also mitigated sugar generation, slowing the increase in reducing sugar content. Furthermore, they enhanced fruit firmness, maintaining it at approximately 42 N with 1% ZnO compared to less than 10 N in uncoated bananas. Overall, the CH/GA/ZnO coatings demonstrated superior preservation compared to reported edible coatings, especially under ambient conditions, showcasing their potential for extending banana shelf life.

Similar to the previous study on bananas, another research also focused on the preservation of avocados using CH/GA coatings with the addition of ZnO NPs (Le et al., 2021). Application of the edible coating significantly improved avocado appearance and lightness during storage at room temperature, with coated avocados retaining up to 56% of their brightness compared to uncoated ones. Internal appearance remained fresh in coated avocados, while uncoated ones showed signs of decay after 7 days. Weight loss, an indicator of moisture loss and respiration process, was effectively minimized with coating application, particularly with 0.3% ZnO content. Coated avocados also exhibited better firmness retention, with the 0.3% ZnO formulation performing best over 7 days. Furthermore, the coating preserved reducing sugar content, with coated avocados maintaining freshness for a longer period compared to uncoated ones.

Some studies have also explored the addition of multiple biopolymers or antimicrobial agents, as well as other types of agents, to coating mixtures in order to augment the treatment's effectiveness.

In the study by Junior et al. (2023), edible coatings comprising chitosan, glycerol, carnauba wax or rosin resin, and ZnO NPs were developed and applied to passion fruit. These coatings aimed to enhance fruit quality and extend shelf life. Physical-chemical characterization during storage highlighted several important findings. pH values remained within typical ranges but increased over time, except for resin-treated fruit, possibly due to ripening and organic acid consumption. Although acidity decreased during storage, resin-coated fruits maintained higher acidity levels. TSS decreased, impacting the sugar-acid balance, while vitamin C content decreased in all samples. Weight loss was observed in all treatments, with carnauba wax-coated fruits experiencing the highest loss. However, the coatings effectively reduced transpiration and preserved fruit firmness, especially in resin-coated fruits. Colour analysis indicated brighter fruits with reduced greenness and increased yellowness in coated samples. Coatings also minimized wrinkling and dark spots, particularly in resin-coated fruits. Higher resin concentrations further improved weight loss, firmness retention, and visual appearance, indicating their efficacy in preserving fruit quality during storage. Incorporating resin alongside chitosan and ZnO NPs can further enhance the effectiveness of edible coatings, suggesting a promising avenue for improving post-harvest preservation and extending the shelf life of passion fruit.

Another study incorporated alginate with chitosan and ZnO NPs for coating using the casting method. Sodium alginate and chitosan were solubilized separately, then glycerol was added followed by ZnO NPs. The resulting filmogenic solutions were reserved for application on guavas, suggesting a potential method for enhancing fruit preservation (Arroyo et al., 2020). Different combinations of sodium alginate and chitosan concentrations were tested. Coatings with 100% chitosan, 90% chitosan - 10% alginate, and 90% alginate - 10% chitosan demonstrated the most effective delay in fruit ripening, extending the shelf life to 20 days

without signs of rot. However, coatings with higher alginate content showed higher weight loss, indicating poor barrier properties. The coatings also affected texture and colour preservation, with chitosan-based coatings showing better results. Additionally, coatings with chitosan and nanoZnO maintained lower SSC content and higher acidity, indicating a slower ripening process. Finally, the antibacterial properties of nanoZnO helped prevent external injuries, highlighting its potential for fruit preservation.

The study by Basumataray et al., (2021) utilized chitosan, ZnO NPs, and aloe vera gel (AVG) for postharvest treatment of pineapple fruits. Chitosan solution mixed with acetic acid was prepared and divided into five beakers. Aloe vera gel (AVG) was added to two pairs of beakers in different concentrations (25% and 50%). ZnO NPs were then incorporated into the AVG-containing formulations. This process resulted in five formulations: chitosan alone, chitosan with 25% AVG, chitosan with 50% AVG, chitosan with 25% AVG and 1% ZnO NPs, and chitosan with 50% AVG and 1% ZnO NPs. The coatings effectively reduced weight loss during storage, with CH/AVG-50/ZnO-1 formulation reduced the weight loss by 5.2% compared to uncoated fruits. Additionally, TSS loss was minimized in coated fruits, especially with CH/AVG-50/ZnO-1, which decreased TSS loss by 2.97%. Coatings slowed down the reduction in TA and maturity index, indicating delayed ripening. Decay index was significantly lower in coated fruits, particularly with CH/AVG-50/ZnO-1 formulation. Sensory analysis revealed that coated fruits maintained sweetness, taste, odour, and visual appearance better than uncoated fruits, with CH/AVG-50/ZnO-1 showing the highest overall acceptance. Visual observation confirmed that coated fruits maintained colour, freshness, and internal tissue integrity better than uncoated fruits throughout the 15-day storage period.

In a study by Alamadari et al., (2022), ZnO NPs were synthesized using extract from wild *M. pulegium* leaves. Chitosan solution was mixed with these green-synthesized ZnO NPs and a plasticizer to create a dough, which was subsequently dried to produce transparent and flexible ZnO/Chitosan nanocomposite films. The composite films, incorporating ZnO/CH, demonstrated significant efficacy as packaging materials for strawberries and red plums, preserving their freshness and appearance. Specifically, strawberries coated with ZnO/CH exhibited a substantially improved internal appearance compared to uncoated ones after eight days of storage, while red plums wrapped in ZnO/CH remained fresh and visually appealing even after ten days, unlike those packaged in conventional plastic films. Moreover, the application of ZnO/CH films effectively minimized the weight loss of red plums during storage, with the weight reduction reduced by over 25% compared to uncoated samples.

Similarly, a study by Lakshmi et al., (2018), chitosan and ZnO NPs were employed for coating figs, starting with the biosynthesis of ZnO NPs using spinach leaves and zinc nitrate hexahydrate as a precursor. ZnO NPs at various concentrations [T1 (25), T2 (50), T3 (75), T4 (100), T5 (125),

T6 (150), T7 (175) and T8 (200) ppm] were then added to the chitosan solution. The resulting coating solution underwent ultrasonication for 30 minutes. Fresh fig fruits were immersed in 100 ml of the prepared solution for coating. Initially, the total TSS ranged from 12.90 to 11.94 °Brix after the first day of treatment, showing an increase with storage time and a decrease with higher nanoparticle concentrations. The maximum TSS after six days was 14.43 °Brix in control and 12.23 °Brix in treatment T8. pH levels decreased with increasing nanoparticle concentrations, ranging from 4.79 to 5.56 after six days, with the lowest pH in treatment T8. Colour values exhibited a decrease in L* and b* values and an increase in a* values over storage time. Coated fig fruits experienced lower weight loss, ranging from 19.01% in treatment T8 to 27.22% in the control after six days. Firmness decreased with storage time but increased with higher nanoparticle concentrations, with treatment T8 recording the highest firmness after six days. Microbial counts were lower in coated fig fruits compared to uncoated fruits, with treatment T8 recording the lowest count after six days. The antimicrobial property of coated ZnO NPs and potential enhancement by chitosan contributed to the observed microbial reduction.

Some research studies have explored the possibility of incorporating antimicrobial agents into food packaging materials rather than solely applying coatings directly to the food. This approach is motivated by the potential for food packaging to not only maintain freshness but also inhibit or delay microbiological decay in food products. Antimicrobial packaging materials involve the integration of antimicrobial substances into the packaging system to mitigate the risk of contamination by pathogens. A study aimed to explore how the shelf life and quality of okra (*Abelmoschus esculentus*) were affected by using low-density polyethylene (LDPE) packaging films coated with chitosan and chitosan-ZnO nanocomposites. LDPE films were treated with plasma to provide a hydrophilic surface, enhancing the attachment of chitosan to the PE surface. This treatment removes organic contaminants and promotes surface oxidation and hydroxylation, thereby increasing surface wettability. After plasma treatment, the chitosan-ZnO nanocomposite solution was sprayed onto the PE surface and allowed to dry at room temperature. The quality test results indicated a slight increase in acidity over the twelve-day storage period, but no significant changes in the pH values were observed. TSS remained relatively unaffected, likely due to the indirect coating of chitosan on the packaging films, unlike direct coating on the food itself. Moisture loss was minimal, attributed to LDPE's barrier properties against water vapour loss and its ability to reduce the vegetable respiration rate. Similarly, the weight loss in okra samples was lower owing to reduced transpiration rates inside the packaging films. Overall, the coatings on LDPE packaging did not significantly influence the chemical and physical properties of okra, suggesting that indirect chitosan coating on plastic films may not have the same impact as direct coating on fruits and vegetables.

This review identifies a critical gap in postharvest disease control, particularly concerning the use of green-synthesised ZnO NPs combined with chitosan as edible coatings for tropical fruits. Although numerous studies have used both chemically and commercially synthesised ZnO NPs for various applications, including biomedical delivery and food preservation, their integration with biopolymers remains limited. Although there has been substantial research on the synthesis of ZnO NPs through eco-friendly methods using various plant extracts, these studies often focus on general applications and do not explore their potential in postharvest contexts.

Chitosan is increasingly used in the food industry owing to its biodegradability, antimicrobial properties, and compatibility with edible coatings. However, research on integrating chitosan with green-synthesised nanoparticles such as ZnO NPs, specifically for postharvest applications is needed. The integration of chitosan and ZnO NPs could offer a dual-action solution by harnessing the antimicrobial efficacy of ZnO along with the biocompatibility and film-forming properties of chitosan. Despite the promising potential of this combination, particularly for tropical fruits, only a few studies have investigated its efficacy in controlling pathogen attacks.

Further research is needed to explore their efficacy across a broader range of tropical fruits, many of which are highly perishable and susceptible to fungal diseases. This includes conducting evaluations on fruits such as mangoes, pineapples, and papayas, which are widely cultivated but often lack sustainable and effective postharvest treatments.

2.6 Papaya as the crop for this study

Papayas (*Carica papaya*) were selected as the model crop for this study because of their nutritional, economic, and agricultural significance, particularly in tropical regions such as Malaysia (Koul et al., 2022). Rich in essential vitamins, such as C, A, and E, dietary fibre, and powerful antioxidants, papayas offer numerous health benefits by supporting the immune system, improving digestion, and reducing the risk of chronic diseases (Pinnamaneni, 2017). In addition to being a critical income source for local farmers, papaya exports contribute significantly to Malaysia's economy, especially as the demand for tropical fruits grows globally (Tan et al., 2023). In 2019 alone, the export value of papayas reached \$7.44 million, with over 19.02 million tonnes of papayas shipped. However, between 2017 and 2019, export value and volume declined by 18.8% and 25.3%, respectively, underlining the impact of postharvest losses and highlighting the need for improved preservation practices (Tan et al., 2023).

Papayas are highly susceptible to postharvest losses, particularly from fungal infections such as anthracnose, which rapidly deteriorates fruit quality during storage and transportation. Due to their high moisture content and thin skin, papayas are especially vulnerable to fungal pathogens, leading to significant economic losses for both producers and exporters (Tan et al., 2022). Anthracnose, caused by *Colletotrichum gloeosporioides*, is a prominent postharvest disease that manifests as dark lesions on the fruit surfaces. These lesions expand and deepen, sometimes producing pinkish spore masses under humid conditions and significantly reducing fruit quality and shelf life. The disease can spread from infected to healthy fruits during handling and storage (Zakaria, 2021). Other common fungal issues include Fusarium rot, which begins as surface wounds and leads to water-soaked, discoloured areas that progress to internal decay (Zakaria, 2023), and stem end rot caused by *Lasiodiplodia theobromae*, which form dark, mushy lesions near the fruit stem that spread into the pulp (Rodrigues et al., 2021). Improper handling and inadequate storage conditions exacerbate these issues, reducing both shelf life and market value, ultimately impacting the livelihoods of farmers dependent on this crop (Rodrigues et al., 2021).

Papayas are also a staple fruit for low-income populations, providing an affordable source of essential nutrients and adding dietary versatility to the option of consuming them at various ripeness stages (Okon et al., 2017). However, the high rate of postharvest losses threatens food security, limiting access to this nutritious fruit, especially in vulnerable populations. Furthermore, for Malaysia to boost its export value, particularly in high-demand regions such as Europe, it is crucial to meet stringent international quality standards. Export prerequisites, especially in European markets, require fruits to be clean, fresh, firm, and free from pests and storage-related abnormalities, necessitating improved postharvest management practices (Tan et al., 2023).

Given these factors, this study addresses the urgent need for effective postharvest disease management strategies for papayas by exploring two innovative techniques: using EN technology for early disease and ripeness detection and eco-friendly chitosan-based coatings combined with ZnO NPs as a disease control strategy. There has been no research on the application of EN technology for detecting ripeness and the onset of fungal diseases in papayas. Moreover, there is no existing research that has specifically examined the use of green-synthesised ZnO NPs and chitosan coatings for papaya to control anthracnose disease. This study sought to fill these gaps by focusing on papayas, aiming to reduce postharvest losses, extend shelf life, and ensure the continued availability of this valuable fruit to all socioeconomic groups, ultimately contributing to Malaysia's economic, agricultural, and food security goals.

Chapter 3: Electronic Nose to accurately monitor ripening stages of papaya during post-harvest storage.

3.1 Introduction

This experiment explored EN application in discerning papaya ripening stages (days 1, 3, and 5 post-harvest) through odour profile changes. Even after harvesting, the fruits continue to ripen, albeit at a slower rate. Monitoring ripeness allows farmers and handlers to adjust storage conditions, such as temperature, humidity, and gas composition (e.g. controlled atmosphere storage) to slow down or accelerate the ripening process. This practice also reduces postharvest losses by promptly identifying and removing fruits with undesirable ripeness levels or those showing signs of decay. For farmers who export their produce, meeting specific ripeness standards is often necessary. Monitoring ripeness helps farmers comply with these standards, ensures that their fruit meets the quality expectations of international markets, and improves brand reputation.

In this study, Case-Based Reasoning (CBR) was employed as a pattern recognition approach for EN sensor data, which is a problem-solving methodology that leverages past experiences and knowledge to solve new problems. CBR comprises of four cyclical steps: retrieval, reuse, revision, and retention. In the retrieval step, the system searches a database of past cases to identify a similar case that can serve as the starting point for solving the current problem. During the reuse step, the system adapted the solution from the retrieved case to address the current problem. In the revised step, the system modified the adapted solution as needed to fit the current problem more closely. Finally, in the retain step, the system stores the current problem and solution as a new case in the database for future use.

Compared with other pattern recognition techniques, such as PCA, PLS-DA, or SVM, CBR has several advantages, including flexibility, interpretability, and adaptability. This contributes to an additional layer of novelty in this research. CBR can handle noisy or incomplete data, learn incrementally from new cases, and provide explanations for decisions based on retrieved cases. In addition, CBR can be easily customised to fit specific domains or applications by selecting different similarity measures, case representations, or adaptation methods.

GC-MS was also used to examine the variations in volatile compounds emitted during papaya ripening. This is because although the chemical volatile profile as a whole can be analysed and evaluated by EN, the exact composition and content of compound characteristics detected by EN are still usually analysed and compared by GC-MS.

Although EN and GC-MS have been utilised together in previous studies on other produce, this is the first instance of their combined application in papaya. The application of EN technology in monitoring papayas is important and novel because it addresses specific challenges and opportunities associated with this unique fruit. It expands the knowledge base regarding EN's versatility in different agricultural contexts, potentially improving papaya quality, sustainability, and marketability while contributing to the broader field of sensor-based quality assessment in agriculture.

3.2 Methodology

3.2.1 Sample preparation

Papaya samples obtained for this experiment were freshly of '*Sekaki*' cultivar purchased from a local fruit distributor, Chai Organic Fruit & Vege Farming at Kajang, Selangor, Malaysia. All the samples were unripe, at the maturity stage 1, characterized by green peel colour with no yellow coloration (Ruslan and Roslan, 2016). The samples had similar weights of 1 kg, with no mechanical damage or injuries observed in the orchard.

3.2.2 Volatile profiling of papaya ripening using EN

A portable EN system (E-Anfun Model P1.0) was rented from Synbion Sdn Bhd, Gambang, Pahang, Malaysia. The portable EN was built using metal oxide semi-conductive (MOS) sensors consisting of four different chemical sensor arrays (Sr1, Sr2, Sr3, and Sr4), each capable of detecting specific groups of volatile compounds, such as alcohols, alkanes, carbon monoxide, and hydrogen (Table 3.1). Ten papaya samples were first incubated by placing them inside 5-litre glass beakers sealed airtight with cling wrap for 1 h equilibration. This allows the headspace volatiles to reach a steady phase and obtain high sensor responses. Once the EN displayed the sign "Neutralized", a cut was made on the cling wrap on top of the beaker to insert the EN nozzle into the beaker, and the EN was run to collect odour data of the headspace for 50 s. The EN chamber draws in the odour through the pump situated in its upper section, while the sensor array collects readings of odour profile from the papaya sample that has accumulated within the beaker. The sensor outputs a resistance signal, which generally results in a change in electrical resistance directly proportional to the concentration of the target gas (Figure 3.1). Prior to the analysis, an empty glass beaker was tested to ensure that it was free from any environmental volatiles, thus facilitating proper standardisation of the container. After collecting readings from each sample, EN was allowed to run freely for 10 min to remove any odour interference from the previous samples.

Table 3.1: Gas sensor array of the EN system

Sensor name	Compounds detected	Typical detection ranges
Sr1	Carbon monoxide	10-2000 ppm
Sr2	Alcohols	0.04mg/L-4mg/L
Sr3	Alkanes	10-1000 ppm
Sr4	Flammable gases	300-10000ppm

Table notes: Sr – Sensor

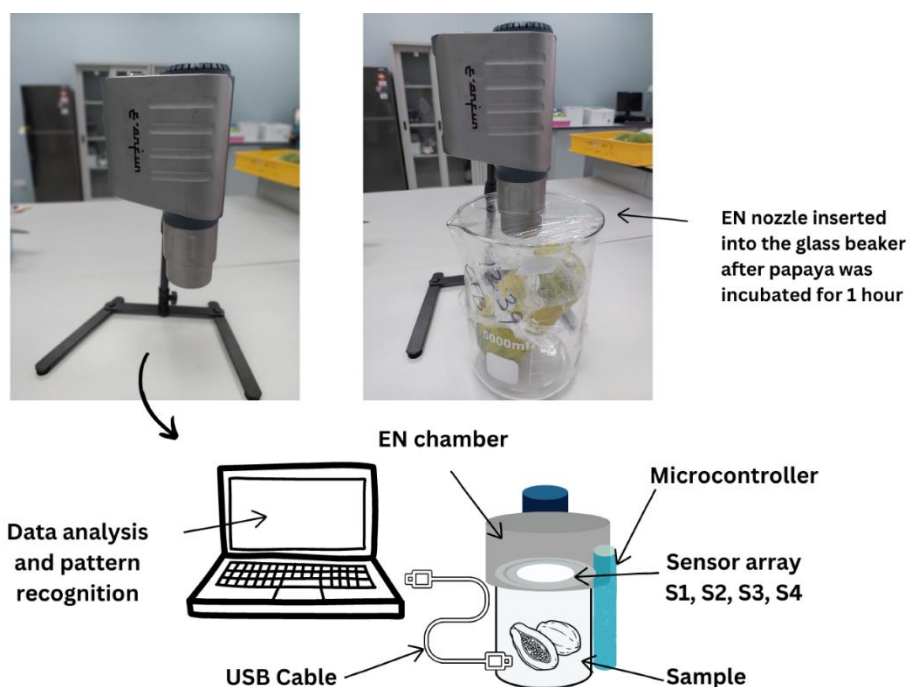


Figure 3.1: Electronic nose principle and experimental setup. Graphics were designed using Canva software.

Changes in aroma often precede visible colour alterations during ripening. EN can detect subtle shifts in volatile compounds, such as the initiation of ethylene release, enabling farmers to anticipate the ripening of papayas even before the skin turns yellow. This proactive approach helps to prevent over-ripening, ensuring that papayas reach consumers or the market at the desired level of maturity. Hence, in this experiment, EN was used to measure the odour profiles of 10 samples on days 1, 3, and 5 of the harvest. The selected days represented distinct phases of papaya ripening. Day 1 signifies that the fruit is still unripe, and day 3 marks a transitional period as the fruit undergoes changes toward ripeness. Day 5, although papaya typically attains

a fully yellow colour at this point, remains integral to the experiment. The aim is to provide a comprehensive understanding of the complete volatile profile, which is essential for building an extensive EN library. This approach ensured that the experiment covered the entire ripening spectrum, from unripe to fully ripe. While the application of an Electronic Nose (EN) is more crucial and practical during the very early stages of maturity, there are instances where papayas may not have fully transitioned to a yellow colouration by day 5. However, even in such cases, biomarkers indicating ripening can still be detected. Therefore, the inclusion of day 5 in the experiment is essential to capture this valuable information, showcasing the effectiveness of EN in detecting ripening markers, especially when visual cues alone, such as colour changes, may not provide accurate insights.

3.2.3 Volatile profiling of papaya ripening using GC-MS

The volatile profiles of the papaya samples were analysed using gas chromatography-mass spectrometry (GC-MS) to provide further insights into the chemical composition of the samples. The samples were prepared by placing two healthy papaya samples in a 5-liter glass beaker with a septum attached to the lid for gas sampling. Prior to GC-MS analysis, the samples were incubated for 2 h at room temperature to induce ripening process of the fruit. A magnetic stirrer was added to the beaker to ensure thorough equilibration of volatile compounds before analysis. For the extraction of volatiles, a solid-phase microextraction syringe (Supelco, Bellefonte, PA, USA) was manually injected into the container, and a fibre (50/30 μm divinylbenzene/carboxen/poly-dimethylsiloxane, 24 ga needle size, 1 cm fibre length) was exposed for 30 min to capture the volatile compounds. The fiber was then introduced into the injector of the GC-MS for analysis. GC-MS (Clarus™ SQ 8 GC-MS system, Perkin Elmer, USA) analysis was performed with some modifications based on the protocol described by Li et al. (2019). A fused silica capillary column (30 m length, 0.25 mm i.d., 0.25 μm film thickness) (HP-5MS, Agilent) was used for separation of the volatile compounds. The temperature settings for the column were as follows: an initial temperature of 40 °C for 3 min, with a helium flow rate of 1 ml/min. The temperature was then increased to 150 °C and held for 30 min for analysis. For MS analysis, an ion source temperature of 250 °C and an electron energy of 70 eV were used. The temperature of the interface zone was maintained at 250 °C and the scan range was set from 40 to 600 Da to capture a wide range of volatile compounds. The samples were analysed by GC-MS on days 1, 3, and 5, with one injection performed for each biological sample to ensure the accuracy and reproducibility of the results.

3.2.4 Analysis of physicochemical properties of papaya during ripening

Over a period of five days, the evolving trends in the physicochemical properties of papaya samples were examined, starting from the day of purchase. Ten samples were used to test the quality indices on each day of analysis.

Weight:

The weights of the same fruits were recorded on each day of the experiment using a digital balance (EK-600H, Japan). Measurements were made in grams, and any notable variations were analysed using statistical analysis.

Firmness:

An Instron Universal Testing Machine (Model 5540, USA) was used to assess the firmness of the fruit in compression mode each day. The fruits were tested using a probe with a diameter of 50 mm, speed of 50 mm/min, and load capacity of 100 N. To ensure accuracy, five technical replicates were conducted per sample by inserting the probe on five sides of the fruit. The compression force was calculated in Newtons (N) and recorded at the highest peak of the chart.

pH and titratable acidity (TA):

To determine the pH of the papaya fruit, 20 g of pulp from each sample was blended with 250 ml of water in an electric kitchen blender. The resulting papaya juice (30 ml) was then centrifuged (Eppendorf 5810R Centrifuge, Germany) at 2000 rpm to separate the coarse fibres, allowing them to settle at the bottom of the centrifuge tube. Subsequently, the upper supernatant of the juice was filtered using Whatman filter paper. The pH of the filtered juice was then measured 5 times using a digital pH meter. After measuring the pH, the filtered juice was used to determine TA using a titration method. For the TA measurement, 2 ml of the filtered juice was diluted with distilled water to achieve a total volume of 25 ml. Next, three drops of 0.2 % phenolphthalein were added as an indicator, and the solution was titrated with 0.5 N NaOH until a pink colour appeared, indicating the titration endpoint. Five replicates were conducted per sample, and an average was obtained. The results are reported as the percentage of citric acid per 100 g of fresh weight.

Soluble solids content (SSC):

The SSC of papaya fruit was determined by extracting papaya juice and measuring the concentration of soluble solids in the pulp using a Palette Digital Refractometer (Model: PR-32 α Atago Co., Ltd. Japan). The SSC was calculated 5 times on each sample and presented as %.

Colour change:

The change in peel surface colour of the papaya fruit was determined using a colorimeter (MiniScan XE Plus Spectro colorimeter, USA), with six readings taken on opposite sides of the equatorial region. A colorimeter measures the colour of an object by quantifying the amount of light reflected from its surface. Colour was expressed in terms of L*, a*, and b* values, where

L* represents lightness, a* represents redness/greenness, and b* represents yellowness/blueness.

3.3 Data analysis

3.3.1 Data analysis and pattern recognition of EN sensor readings

The data collected from the four EN sensors produced resistance values, which were sent to a computer for data storage and interpretation. For each treatment, 1000 readings were obtained from each sensor (Table 5). Hence, all the raw data collected were normalised, and the features of each sample were extracted using the method described by Daud et al. (2017). When comparing several variables or datasets, it can be helpful to guarantee that all values are on the same scale by using normalised values. Data normalisation helps to prevent bias and guarantees that each variable receives the same weight in the analysis.

Table 3.2: In the table above, 1000 data measurements were collected from 5 repeated experiments for every sample. Sr1, Sr2, Sr3 and Sr4 indicate sensor 1, sensor 2, sensor 3 and sensor 4 respectively. DM represents the data measurement of papaya samples.

Data measurements	Sr1	Sr2	Sr3	Sr4
1	DM ₁₁	DM ₁₂	DM ₁₃	DM ₁₄
2	DM ₂₁	DM ₂₂	DM ₂₃	DM ₂₄
3	DM ₃₁	DM ₃₂	DM ₃₃	DM ₃₄
.
.
.
1000	DM ₁₀₀₁	DM ₁₀₀₂	DM ₁₀₀₃	DM ₁₀₀₄

Table notes: **Sr** - Sensor

3.3.2 EN data preprocessing

Equation (1) was used to normalise the raw data collected earlier. To obtain normalised values, each row of raw data was divided by the highest value in its own row. This rescales the values to a smaller range, between 0 and 1. A normalised value of 0 represents the minimum value and a value of 1 represents the maximum value. Normalised values are useful for extracting odour profiles.

$$R' = R / R_{\max}$$

Equation1 (*R means raw data*)

Prior to data classification, feature extraction was performed using normalised values. Normalised values were clustered into sample groups based on the day they were collected. Two cases were obtained from each group by calculating the mean of 10 normalised values. These cases were tabulated and stored as "previous experiences" or "cases stored" in the memory of the system for the classification process.

3.3.3 Intelligent classification with Case Based Reasoning method (CBR)

In CBR, similarity percentages are used to determine how closely a new case or problem matches existing cases in the case library. The similarity measure calculates a percentage value that represents the degree of similarity between a new case and each other in the library.

In the CBR retrieval cycle, a single case was selected from a collection of 30 stored cases to assess the similarity percentage between the two cases. The remaining 29 cases were retained as stored cases. The similarity percentage was calculated using Eq. (2) to determine the resemblance level. When the similarity percentage between the two cases is high, it signifies that the distance separating them is minimal, indicating that they are likely to belong to the same group.

Equation 2:

$$\text{Similarity}(T, S) = \frac{\sum_{i=1}^n f(T_i, S_i) \times w_i}{\sum_{i=1}^n w_i}$$

where T and S denote the target case and source case, respectively, n represents the number of attributions for the papaya sample, where i signifies the individual attribution for each case, f denotes the formulation of the similarity function, and w represents the weight assigned to each attribution.

In this study, EN sensor readings collected from different samples on different days were compared to determine the similarity percentage. A percentage similarity of over 99 % shows that the two samples are significantly similar to each other. Values below 99 or 98 % showed a significant weak difference. These similarity percentages indicate how accurately EN could distinguish the samples measured each day.

3.3.4 Determination of VOCs composition during papaya ripening with GC-MS readings

For GC-MS analysis, two samples were tested on three alternate days of papaya storage: days 1, 3, and 5. Although a minimum of three replicates are typically employed in many studies to generate a statistically significant result, GC-MS is a highly sensitive and accurate analytical tool that provides robust molecular identification and quantification of VOCs. The superior accuracy of GC-MS ensures that two replicates are sufficient to capture the necessary data. The focus of this research was to investigate whether the EN can distinguish the differences in the overall volatile profile of different samples. Since the ten replicates used for EN offer comprehensive coverage and statistical rigor, the GC-MS's two replicates are complementary, providing the necessary depth of molecular characterization. The raw GC-MS data were processed using OpenChrom, a widely used software for chromatographic data analysis, before deconvolution using an Automated Mass Spectral Deconvolution and Identification System (AMDIS), which is a powerful tool for peak identification in complex chromatograms. The identities of the detected peaks were analysed using NIST 11 and the MS Search Program (Version 2.0), which are commonly used reference libraries for the mass spectral identification of compounds. This ensured accurate identification of the volatile compounds present in the papaya samples. To gain further insights into the overall trends and patterns of volatile compounds, Principal Component Analysis (PCA) was performed using OpenChrom. PCA is a multivariate statistical technique that can reduce the dimensionality of the data and provide a visual representation of the relationships between samples based on their chemical profiles. The results from the GC-MS analysis were used as inputs for PCA, and the output was presented as a 2D score plot showing the distribution of samples along the first and second principal components (PC1 vs. PC2). This allowed for the clustering of data from each sample group and identification of any distinct patterns or trends in the volatile profiles. Furthermore, the detected volatile compounds were analysed for potential metabolic pathways based on previously reported literature.

3.3.5 Statistical analysis of physiochemical test results during papaya ripening

The data for physiochemical tests are presented as the mean of 10 replicates with (\pm) standard deviation (SD). Statistical analysis was performed using ANOVA, and mean values were

compared using the least significant difference test at a significance level of $p < 0.05$, using the IBM SPSS software program version 28. Spearman’s correlation analysis was conducted to investigate the potential correlation between EN responses and changes in papaya quality indices. The significance of the correlations was determined using Tukey’s test at a significance level of $p \leq 0.05$.

3.4 Results and discussion

3.4.1 Change in VOCs profile during papaya ripening detected with EN.

The four sensor readings from the samples measured on days 1, 3, and 5 were normalised to rescale the values to a smaller range between 0 and 1. A normalised value of 0 represents the minimum value and a value of 1 represents the maximum value. The average of all the raw data after normalisation is tabulated in Table 3.3. The highest sensor reading for all samples was obtained for sensor Sr1, whereas Sr4 showed the lowest sensor reading for all papaya samples. Figure 3.2 shows the pattern of all sensor readings after normalisation for each day.

Table 3.3: Average of all raw data from 4 sensors after normalisation collected on days 1, 3 and 5 (D1, D3, D5). The highest sensor reading for all samples is at Sr1, hence the values are 1 after normalization.

Sensors/ day	Sr1	Sr2	Sr3	Sr4
D1	1	0.89156	0.71102	0.53834
D3	1	0.49768	0.58241	0.42386
D5	1	0.48096	0.59745	0.41091

Table notes: Sr – Sensor, D1, D3, D5- day1, day3, day5

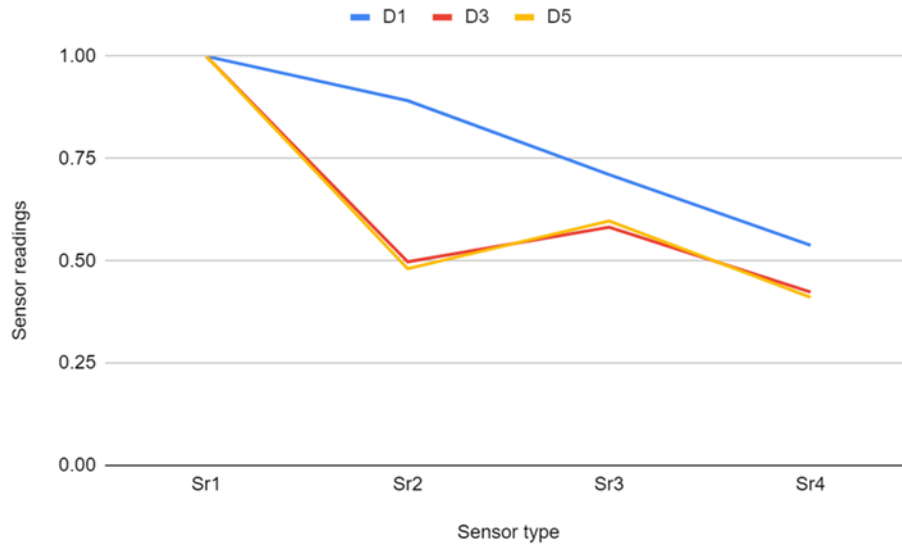


Figure 3.2: Graph of normalized data after averaging all the raw sensor values (Sr1, Sr2, Sr3, Sr4) measured on days 1, 2 and 3 (D1, D3, D5).

3.4.2 Distinguishing the different ripening stages of papaya using CBR classification.



The EN sensor readings were first compared with those of the samples tested on the same day. The CBR results obtained from the EN analysis showed that the similarity percentage between all samples was 97.17 % on day 1, 98.45 % on day 2 and 98.45 % on day 3 (Table 3.4). These percentages are close to 99 %, indicating a significant level of similarity between the biological replicates. This suggests that EN can accurately identify samples as biological replicates and maturity stages. When the samples were compared on different days (Table 3.5), the average similarity percentage between day 1 and 3 samples was 84.25 %, which is well below 98 %. This significant difference in similarity percentage suggests that EN can accurately distinguish between different samples on days 1 and 3. The similarity percentage between the samples on days 1 and 5 was 82.81 %, which was also a significant difference, indicating that EN has the potential to detect changes in the volatile compounds of papayas between days 1 and 3 and between days 1 and 5.

However, the similarity percentage between the samples on days 3 and 5 was 94.19 %, which was not as low as expected based on the results between days 1 and 3 and between days 1 and 5, although the papaya samples were both considered to be at different maturity stages of 3 and 5. This finding suggests that the volatile compounds on day 3 did not undergo substantial changes till the 5th day of storage. The similarity in volatile compound profiles between days 3 and 5 suggests that the fruit had reached a certain stage of ripening by day 3, and the

subsequent two days of storage did not significantly alter the composition of these volatile compounds. Nevertheless, the percentage similarity of 94.19 % between these two days was lower than that of 99 %, indicating a weak but significant difference. Therefore, the EN technology can accurately identify samples at different maturity stages.

Overall, these results suggest that EN is a useful tool for monitoring and evaluating the quality of papaya samples at different maturity stages. EN can accurately identify biological replicates of papaya samples and detect changes in volatile compounds at different maturity stages. The GC-MS results further confirmed the specific volatile compounds responsible for the significant differences between each day of measurement. The results from the physiochemical tests can confirm whether the changes in quality parameters (pH, TA, colour, etc.) correlate with EN signal responses.

Table 3.4: Similarity percentages between samples measured on the same day. A percentage similarity of over 99 % shows that the two samples are significantly similar to each other. Values below 99 or 98 % showed a significant weak difference.

Days of EN measurement	Average similarity percentages between the samples on the same day	Pictures of 2 samples from each day.
Day 1	97.17 %	
Day 3	98.45 %	


Day 5	98.45 %	
-------	---------	--

Table 3.5: Similarity percentages of samples compared on different days. A percentage similarity of over 99 % shows that the two samples are significantly similar to each other. Values below 99 or 98 % showed a significant weak difference.

Days of EN measurement	Average similarity percentage between different days
Day 1 and 3	84.25 %
Day 1 and 5	82.81 %
Day 3 and 5	94.19 %

3.4.3 Identifying potential volatile biomarkers at different stages of papaya ripening using GC-MS

EN analysis showed that papaya samples have significant differences in their odour profiles on days 1, 3, and 5 using the CBR classification method. GC-MS analysis was conducted to further investigate the specific volatiles responsible for the changes during papaya ripening. Based on the results of principal component analysis (PCA) as depicted in Figure 3.3, each papaya fruit sample collected on different days of incubation exhibited distinctive groupings based on dot colour. The first two components of the score plot accounted for 70 % and 17 % of the total variance, respectively. Notably, all samples showed significant proximity within their respective groups, but there was clear differentiation between the groups. The score plot revealed a noticeable separation of the samples into three major groups. Specifically, the day 5 sample exhibited significant differentiation from the day 1 and day 3 samples along the PC1 axis, indicating a substantial difference in volatile composition between these time points. When compared along the PC2 axis, distinct separation was observed among all samples without any clustering, suggesting significant differences in both the composition and concentration of volatiles during the fruit ripening process. In summary, PCA confirmed significant differences in

the volatile profiles of papaya samples, both in terms of composition and concentration, during the fruit ripening process. The score plot provided visual evidence of clear separation between different time points, indicating changes in volatile composition over time.

In this study, the selection of potential biomarkers for different days was based on the identification of VOCs that were uniquely present on specific days, as identified through the GC-MS analysis. The GC-MS results provided a detailed chemical profile of the VOCs emitted by the samples on each day, allowing us to observe which compounds were exclusive to certain time points. Some VOCs were only detected on a particular day, suggesting that they could be linked to a unique stage in the sample's ripening or senescence process.

Based on the findings presented in Table 3.6, 32 volatile compounds were detected and identified through volatile profiling of the papaya samples. These volatile compounds belong to various chemical classes including alkanes, alcohols, ketones, carboxylic acids, and esters. Among them, vinyl butyrate, 1,5-Hexadien-3-ol, 1-Hexanol, 1-Pentanol, 4-methyl-, Butane, 2,2,3-trimethyl and Heptane and 3,3-dimethyl were identified as the potential biomarkers for the day 1 samples. For day 3 samples, acetone and tridecane were identified as potential biomarkers for papaya fruit ripening, as these two compounds began to appear on day 3, thereby indicating the onset of ripening. In the case of day 5 samples, ethylene oxide, cyclobutanol, oxalic acid, butyl propyl ester, oxalic acid, isobutyl hexyl ester, and 3-Buten-2-ol, Decane, 4-methyl-, 4-Penten-2-one, Acetyl valeryl, 2-Pentanol, propanoate, Octane, 2,4,6-trimethyl-, Heptane, 4,4-dimethyl-Hexane, 3,3-dimethyl and Undecane, 3,8-dimethyl- were identified as potential biomarkers of fully ripe fruit. Among these, 3-Buten-2-ol was reported for the first time in papaya, whereas cyclobutanol was previously detected in papaya fruit treated with 1-MCP (Sundaram and Prabhakaran, 2017). Additionally, volatile esters have been synthesised in ripe fruits, including papaya. Oxalic acid, butyl propyl ester, and isobutyl hexyl ester have been detected in other fresh and processed products, namely ripe starfruit and pork jerky, respectively (Zhao et al., 2016; Ramadan et al., 2020). In addition to the branch chain volatiles previously reported in ripe papayas, this study identified a higher percentage of butane, 2,2-dimethyl-, decane, 2,4-dimethyl-, heptane, 4,4-dimethyl-, hexane, 3,3-dimethyl-, and undecane, 3,8-dimethyl- on day 5. The concentrations of hexadecane, 2-undecen-4-ol, 1-butanol, 2-methyl-, and propanoate were found to decrease from day 1 to day 3 in papaya samples and were not detected on day 5. Butanol has been identified previously in the initial stages of papaya ripening, and its presence diminished over time; it was not detected on day 5 (Fabi and do Prado, 2019; Kushwaha et al., 2021). This suggests that these compounds may be involved in the early stages of papaya ripening, but their concentrations decrease as the fruit ripens further. However, the specific role of these biomarkers in papaya ripening remains unknown and warrants further investigation using genomic and proteomic analyses.

Papaya is known for its wide variability in volatile profiles, which can vary significantly among different varieties. This study adds to the existing body of knowledge by identifying and characterising volatile compounds in papaya during ripening, some of which have been previously reported, while others are novel findings. For instance, ester compounds were identified in this study, including some that have been reported in previous research, and compounds such as linalool, which has been frequently reported in papaya ripening in previous studies, were not detected in our findings (Fabi and do Prado, 2019).

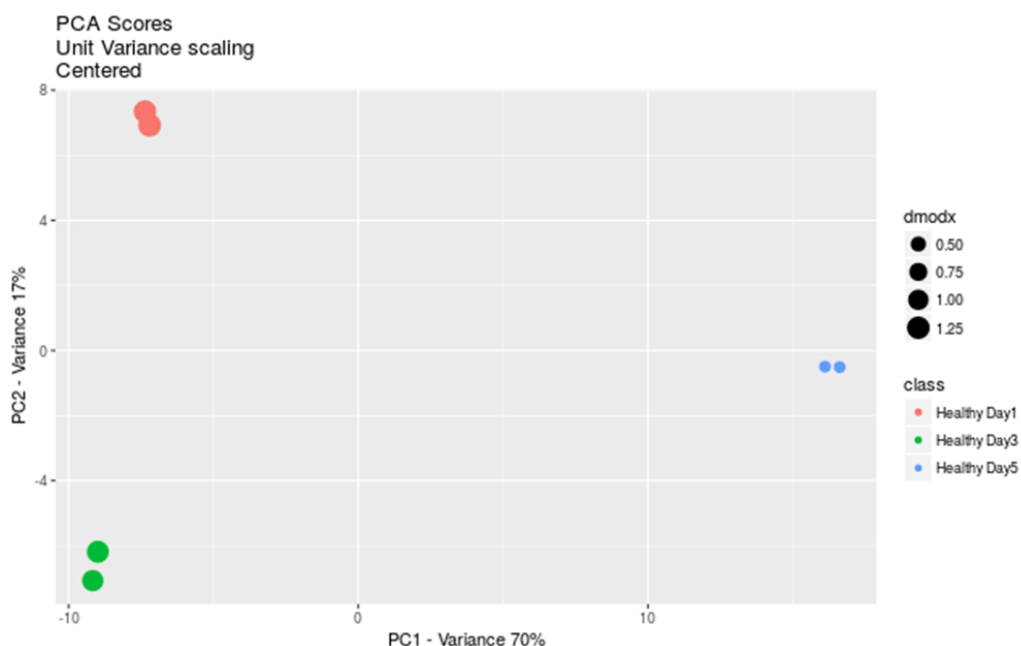


Figure 3.3: Loading plot of the first two principal components of PCA for healthy papaya fruit after 5 days of incubation. The numbers indicate the number of replicates. PC1 and PC2 accounted for 70 and 17 % of the variance, respectively.

Table 3.6. The overall potential biomarkers of healthy papaya fruit after five days of incubation were determined by GC-MS analysis.

Compound	Odour Description	Retention Time	Area Percentage (%)			References
			Day 1	Day 3	Day 5	
Ethylene oxide	Ether	1.03	-	-	0.086	-

Cyclobutanol	Unknown	1.05	-	-	0.079	(25),(20)
Vinyl butyrate	Unknown	1.76	0.590	-	-	-
Acetone	Fruity	1.82	-	0.007	0.012	-

Table 3.6 continued. The overall potential biomarkers of healthy papaya fruit after five days of incubation were determined by GC-MS analysis.

Allyl propionate	Sweet, Fruity	1.87	1.559	0.004	-	-
1,5-Hexadien-3-ol	Unknown	1.94	1.642	-	-	(26)
2-Pentanone	Unknown	2.00	2.973	0.014	-	-
1-Hexanol	Sweet, fruity	2.09	0.244	-	-	(27),(28)
1-Pentanol, 4-methyl-	Nutty	2.16	0.491	-	-	(29),(30),(31)
Oxalic acid, butyl propyl ester	Unknown	10.04	-	-	0.355	(22)
Oxalic acid, isobutyl hexyl ester	Unknown	10.24	-	-	0.136	(21)
3-Buten-2-ol	Unknown	10.25	-	-	0.044	-
Decane, 4-methyl-	Pungent, Acidic	10.37	-	-	0.082	-
4-Penten-2-one	Unknown	11.56	-	-	0.047	-
Acetyl valeryl	Buttery	11.6	-	-	0.136	(32)
Undecane	Faint	14.29	0.392	0.437	-	(33)
Undecane, 4,7- dimethyl-	Unknown	16.05	0.220	0.063	0.001	-
2-Pentanol, propanoate	Unknown	17.29	-	-	0.235	-
Octane, 2,4,6- trimethyl-	Unknown	18.44	-	-	0.122	-
Octane, 4,5-dimethyl-	Unknown	18.70	0.029	0.017	0.001	-
Butane, 2,2-dimethyl-	Gasoline	19.80	-	0.001	0.054	(33),(34)

Table 3.6 continued. The overall potential biomarkers of healthy papaya fruit after five days of incubation were determined by GC-MS analysis.

Decane, 2,4-dimethyl-	Unknown	19.81	0.010	0.020	0.045	(35)
-----------------------	---------	-------	-------	-------	-------	------

Butane, 2,2,3-trimethyl-	Unknown	19.83	0.083	-	-	-
Heptane, 3,3-dimethyl-	Unknown	20.26	0.033	-	-	-
Heptane, 4,4-dimethyl-	Unknown	21.23	-	-	0.039	-
Hexane, 3,3-dimethyl-	Unknown	21.24	-	-	0.034	-
1-Butanol, 2-methyl-, propanoate	Fruity	21.67	0.051	0.006	-	(27)
3-Ethyl-3-methylheptane	Unknown	21.68	0.037	0.014	-	-
Tridecane	Slight gasoline	22.42	-	0.201	0.012	(36)
Hexadecane	Slight gasoline	22.45	0.022	0.005	0.001	(36)
2-Undecen-4-ol	Unknown	22.46	0.139	0.007	-	(37)
Undecane, 3,8-dimethyl-	Unknown	26.11	-	-	0.594	-

3.4.4 Changes in physicochemical properties during papaya ripening and their correlation with EN readings.

The mean values of papaya quality indices during the 5 d of storage are presented in table 3.7. The mean weight of the papaya samples does not show any significant ($p \leq 0.05$) changes throughout the storage period. Typically, weight loss in fresh fruit and vegetables during storage is primarily attributed to the peel, which is influenced by the vapor pressure gradient between the fruit tissue and the surrounding atmosphere. (Parven et al, 2020). This can result in flesh softening, fruit ripening, and senescence through metabolic reactions such as ethylene production. Transpiration, or the loss of water through the peel, can also result in the removal of other soluble substances. Additionally, weight loss may occur due to respiration, with a carbon atom lost from the fruit as CO₂ during each metabolic cycle (Zhang et al, 2023). However, after the fruit is harvested from the tree, metabolic processes slow down, and in this experiment where papaya samples were stored for only 5 d, no significant changes in weight² were observed. The peel colour of papaya underwent continuous changes from green to yellow during the storage of the fruit. The L* (lightness) values showed a significant ($p \leq 0.05$) increase from 41.2 on day 1 to 63.4 on day 5. The a* and b* values also changed significantly ($p \leq 0.05$)

from -6.95 to 7.69 and 35 to 50.5, respectively, over the course of 5 d, indicating a shift towards a less green colour and a more yellow hue.

In general, changes in the peel colour of papaya fruit occur during the ripening and senescence processes, which may be attributed to chlorophyll degradation or qualitative and quantitative alterations of the green pigment into another pigment (Kasampalis et al, 2020). This colour change is often accompanied by a softer and sweeter pulp, as the ratio of sugars to starch increases and characteristic aroma develops (Parven et al., 2020). This was also observed in the firmness test, where the firmness of papayas declined significantly ($p \leq 0.05$) during storage, decreasing from 147.73N to 13.84N in 5 d. According to the findings, there was a significant increase ($p \leq 0.05$) in TSS from 0.82 % to 1.66 % within 5 days. This increase in TSS is attributed to the hydrolysis of starch into soluble sugars, such as glucose, sucrose, and fructose, as most of the TSS content in fruit comprises sugars. The pH increased significantly ($p \leq 0.05$) for the first two days and then decreased on day 3, and again started increasing until day 5. The overall increase in pH was due to a decrease in hydrogen ions provided by organic acids during ripening. TA values increased significantly ($p \leq 0.05$) from 0.00225 on day 1 to 0.00625 on day 5. Previous research has reported that TA of papaya keeps increasing until the fruit turns 75 % yellow mainly because of the citric acid content (Barragán-Iglesias et al, 2018). The physiochemical tests conducted on the fruit provided evidence supporting its ripening process, which was observed up until day 5. These findings validate the results obtained from the analysis using the EN and GC-MS.

Table 3.7: Mean values (with standard deviations) of quality indices for papaya samples during 5 days of storage. Different letters for the same parameter indicate significant differences between storage days according to ANOVA ($p < 0.05$).

Days	Mean weight	Mean TA	mean TSS	Mean pH	Mean Firmness	Mean L*	Mean a*	Mean b*
Day 1	1.576 ± 0.050	0.00225 ^a ± 0.000	0.82 ^a ± 0.447	6.056 ^a ± 0.005	147.73 ^a ± 8.340	41.2 ^a ± 2.268	-6.95 ^a ± 10.919	35.002 ^a ± 10.723
Day 2	1.576 ± 0.050	0.0039 ^b ± 0.000	1.24 ^b ± 0.055	6.04 ^b ± 0.007	69.83 ^a ± 8.250	47.516 ^b ± 3.372	-6.666 ^a ± 2.514	30.572 ^{ab} ± 5.703
Day 3	1.574 ± 0.048	0.00445 ^b ± 0.001	1.44 ^c ± 0.055	5.908 ^c ± 0.008	57.85 ^b ± 9.293	55.698 ^c ± 3.858	-1.038 ^{ab} ± 3.737	45.358 ^{bc} ± 7.586
Day 4	1.574 ± 0.048	0.00585 ^b ± 0.000	1.56 ^d ± 0.055	5.938 ^d ± 0.008	14.62 ^c ± 4.550	59.65 ^{cd} ± 0.856	6.686 ^b ± 1.027	48.52 ^c ± 3.296
Day 5	1.572 ± 0.046	0.00625 ^c ± 0.000	1.66 ^d ± 0.090	6.248 ^e ± 0.008	13.84 ^d ± 3.102	63.436 ^d ± 2.662	7.686 ^b ± 1.004	50.496 ^c ± 2.449

Table notes: **TA** - Titratable Acidity, **TSS** - Total Soluble Solids, **L*** - Lightness (a component of the CIELAB color space) **a*** - Red/Green chromaticity (positive a* values indicate red, and negative values indicate green) **b*** - Yellow/Blue chromaticity (positive b* values indicate yellow, and negative values indicate blue)

To elucidate the relationship between papaya quality parameters and EN sensor array responses, a Spearman correlation test was performed. Table 3.8 displays the relationship between quality indices and the sensor array. After normalisation, sensor Sr1 readings remained constant, hence no correlation information for Sr1 is available. Most of the quality indices and the other sensors (Sr2, Sr3, and Sr4) show a significant correlation. This suggests that the EN sensor responses are influenced by the shelf life of papaya.

The correlation coefficient, which ranges from -1 to +1, quantifies the degree and direction of the linear relationship between the variables. A correlation coefficient of -1 indicates a perfect negative correlation, a correlation value of +1 indicates a perfect positive correlation, and a correlation coefficient of 0 indicates no correlation.

In Table 3.8, the significance level of the correlations is also presented as a 2-tailed significance. A more substantial correlation between variables was indicated by a lower significance value. Asterisks indicate correlation pairings with significance below 5 %, and double asterisks indicate correlation pairs with significance below 1 % (showing a highly significant relationship between the variables).

Significant correlations were found between the signals of the sensors (Sr1, Sr2, and Sr3) used in the EN system and the quality indices of papaya. Sr2 sensor showed a high correlation with weight ($R^2= 0.845$, $p<0.05$), TA ($R^2= -0.943$, $p<0.01$) and a^* ($R^2= -0.943$, $p<0.01$). Sr3 sensor showed a high correlation with TSS ($R^2=-0.883$, $p< 0.05$) and L^* ($R^2= -0.943$, $p<0.01$). Sr4 sensor showed a high correlation with TA ($R^2=-0.886$, $p< 0.05$), TSS ($R^2=-0.971$, $p<0.01$), L^* ($R^2=-1.000$, $p<0.01$) and a^* ($R^2=-0.886$, $p< 0.05$). This implies that the sensors provide more features for the prediction of papaya quality indices.

These results are significant because the physiological properties of the fruit are closely related to the chemical processes that take place during the shelf-life period, despite the fact that it may seem unexpected that quality indices such as colour, pH, TA, and TSS can be predicted by the responses of sensors to organic volatiles emitted by the fruit. In other words, EN monitors volatiles instead of directly measuring quality indicators, which are closely related to fruit colour, pH, TA, and TSS.

Table 3.8: Spearman correlation between EN sensors and quality indices of papaya.

	Weight	TA	TSS	pH	L*	a*	b*	Sr1	Sr2	Sr3	Sr4
Weight	1.000	-0.845*	-0.696	-0.169	-0.676	-0.845*	0.169	ND	0.845*	0.676	0.676
TA	-0.845*	1.000	0.912*	0.371	0.886*	1.000**	0.086	ND	-0.943**	-0.771	-0.886*
TSS	-0.696	0.912*	1.000	0.5	0.971**	0.912*	0.059	ND	-0.765	-0.883*	-0.971**
pH	-0.169	0.371	0.5	1.000	0.486	0.371	0.6	ND	-0.086	-0.257	-0.486
L*	-0.676	0.886*	0.971**	0.486	1.000	0.886*	0.2	ND	-0.771	-0.943**	-1.000**
a*	-0.845*	1.000**	0.912*	0.371	0.886*	1.000	0.086	ND	-0.943**	-0.771	-0.886*
b*	0.169	0.086	0.059	0.6	0.2	0.086	1.000	ND	-0.029	-0.029	-0.2
Sr1	ND	ND	ND	ND	ND	ND	ND	1.000	ND	ND	ND
Sr2	0.845*	-0.943**	-0.765	-0.086	-0.771	-0.943**	-0.029	ND	1.000	0.714	0.771
Sr3	0.676	-0.771	-0.883*	-0.257	-0.943**	-0.771	-0.029	ND	0.714	1.000	0.943**
Sr4	0.676	-0.886*	-0.971**	-0.486	-1.000**	-0.886*	-0.2	ND	0.771	0.943**	1.000

Table notes: **TA** - Titratable Acidity, **TSS** - Total Soluble Solids, **L*** - Lightness (a component of the CIELAB color space) **a*** - Red/Green chromaticity (positive a* values indicate red, and negative values indicate green) **b*** - Yellow/Blue chromaticity (positive b* values indicate yellow, and negative values indicate blue), **Sr** - Sensor

*Correlation is significant at the 0.05 level (2-tailed).

**Correlation is significant at the 0.01 level (2-tailed).

3.5 Chapter conclusion

Overall, the results of this study indicate that EN has great potential for practical use in determining papaya ripening trends. The classification based on CBR was successful in distinguishing between different storage periods of papaya, revealing 84.25% similarity between papayas stored on day 1 and 3, 82.81% between days 1 and 5, and 94.19% between days 3 and 5, all below 98%, indicating very significant differences. This proves that EN can distinguish between papayas on different storage days of ripening. The EN signal responses correlated well with the results of the GC-MS analysis and physiochemical tests. Through GC-MS analysis, specific volatile compounds were identified as potential biomarkers for the different stages of papaya ripening. The potential biomarkers for day 1 of papaya ripening included vinyl butyrate, 1,5-Hexadien-3-ol, 1-Hexanol, 1-Pentanol, 4-methyl-, Butane, 2,2,3-trimethyl and heptane and 3,3-dimethyl. Acetone and tridecane were nominated as potential biomarkers for day 3, whereas ethylene oxide, cyclobutanol, oxalic acid, butyl propyl ester, oxalic acid, isobutyl hexyl ester, and 3-Buten-2-ol, decane, 4-methyl-, 4-Penten-2-one, Acetyl valeryl, 2-Pentanol, propanoate, octane, 2,4,6-trimethyl-, heptane, 4,4-dimethyl, hexane, 3,3-dimethyl, and undecane, 3,8-dimethyl- were nominated for day 5.

Chapter 4: Early detection and classification of major post-harvest fungal diseases in papaya fruit using Electronic Nose

4.1 Introduction

This study aimed to explore the effectiveness of EN technology in detecting and distinguishing three postharvest fungal infections in papaya during the early storage stages. Additionally, the volatile compounds present in both infected and healthy fruits were analysed using GC-MS to identify any differences.

Although both EN and GC-MS have been utilised together in previous studies on other produce, this is the first instance of their combined application in papaya. Papayas were individually inoculated with three major postharvest disease-causing fungi, *Colletotrichum gloeosporioides*, *Fusarium solani*, and *Lasiodiplodia theobromae*, including a group that was inoculated with all three fungi to assess the changes in volatile compounds. This experimental design is particularly relevant in practical settings where more than one fungus can simultaneously affect the same fruit. This aspect of the research adds a distinct contribution to the literature on postharvest diseases in papayas.

4.2 Methodology

4.2.1 Sample preparation

All the papayas used in this research were freshly harvested papaya samples of 'Sekaki' cultivar purchased from a local fruit distributor, Chai Organic Fruit & Vege Farming at Kajang, Selangor, Malaysia. All the samples were unripe, at the maturity stage 1, characterized by green peel colour with no yellow coloration (Ruslan and Roslan, 2016). The samples had similar weights of 1 kg, with no mechanical damage or injuries visually inspected in the orchard.

4.2.2 Inoculation

Pure cultures of *Colletotrichum gloeosporioides*, *Fusarium solani*, and *Lasiodiplodia theobromae* were grown on potato dextrose agar (PDA) and stored for seven days prior to all experiments at 24°C and 85% relative humidity. Before inoculation, all papaya samples were washed with 70% ethanol and 0.5% Clorox and rinsed with distilled water for 10 min. The samples were air-dried in paper towels. Four inoculation treatments were performed in a sterile environment. The agar plug method was used for inoculation. Each papaya sample was individually inoculated by placing three mycelial agar plugs excised from the margins of the respective fungal colonies. To

insert agar plugs of fungal colonies, three holes of 3 mm depth were cut aseptically with a sterile cork borer onto the surface of the papayas before inoculation. The three holes covered the entire surface of the fruit adequately and ensured more accurate measurements of the lesion area while maintaining a controlled and manageable experimental setup. E-nose and GC-MS measurements were conducted simultaneously on days 1, 3, and 5.

Papaya samples were divided into five groups, and each group contained 10 samples.

- 1: Control group of healthy papayas (H) with no inoculation of fungus
- 2: *Colletotrichum gloeosporioides* (CG) inoculated in papayas
- 3: *Fusarium solani* (FS) inoculated in papayas
- 4: *Lasiodiplodia theobromae* (BC) inoculated in papayas
- 5: All three fungi inoculated in papayas (CFB)

4.2.3 Volatile profiling of inoculated papaya samples with EN and GC-MS

Papaya samples inoculated with different fungi were first incubated and set up with EN and GC-MS equipment, similar to the method described in section 3.2.1 and 3.2.2.

4.3 Data analysis

4.3.1 Data analysis and pattern recognition of EN sensor readings and the determination of VOCs composition using GC-MS

The EN sensor data and GC-MS were analysed using the protocol described in section 3.3.

4.3.2 Disease incidence and disease severity

The disease incidence and severity percentages for the control group and the four inoculation treatments are shown in a graph. Disease incidence is represented as the percentage of fruits displaying disease symptoms out of the total number of fruits in each treatment. To assess fungal growth and disease progression, disease severity was visually assessed on a scale of 1 to 5 (0=0% of fruit surface rotten; 1=1–20%; 2=21–50%). It was then computed using the following formula: $[(0 \times N_0 + 1 \times N_1 + 2 \times N_2) \times 100 / (2 \times N)]$, where N is the amount of measured fruit and N₀, N₁, and N₂ are the respective numbers of fruits for each grade scale corresponding to the severity of the disease.

4.4 Results and discussion

4.4.1 Distinguishing volatile odour from different papaya fungal infections with EN

The four sensor readings taken from all samples measured on days 1, 3, and 5 were normalised to rescale the values to a smaller range between 0 and 1. A normalised value of 0 represents the minimum value and a value of 1 represents the maximum value. The average of all the raw data after normalisation is presented in (Table 4.1). The highest sensor reading for all samples was at sensor Sr1, whereas Sr4 showed the lowest sensor reading for all papaya samples.

Table 4.1: Average of all raw data from the four sensors after normalisation from the control group (H), fruit infected with CG, FS, BC, and CFB collected on days 1, 3, and 5 (D1, D3, and D5). Sr1, Sr2, Sr3, and Sr4 denote sensors 1, 2, 3, and 4, respectively. The highest sensor reading for all samples was obtained at Sr1; hence, the values were 1 after normalisation.

	Sr1	Sr2	Sr3	Sr4
H_D1	1	0.89156	0.71102	0.53834
H_D3	1	0.49768	0.58241	0.42386
H_D5	1	0.48096	0.59745	0.41091
CG_D1	1	0.59415	0.64968	0.46623
CG_D3	1	0.46413	0.59191	0.40585
CG_D5	1	0.42958	0.61442	0.31533
FS_D1	1	0.67039	0.70807	0.54673
FS_D3	1	0.48664	0.58129	0.40343
FS_D5	1	0.41873	0.62839	0.31104
BC_D1	1	0.71992	0.74201	0.58238
BC_D3	1	0.47916	0.6214	0.51135
BC_D5	1	0.53397	0.90367	0.65154
CFB_D1	1	0.60674	0.64708	0.4813
CFB_D3	1	0.51004	0.61643	0.43571
CFB_D5	1	0.42296	0.69998	0.37899

Table notes: **H**- Healthy, **CG** - *Colletotrichum gloeosporioides*, **FS** - *Fusarium solani*, **BC** - *Botrytis cinerea*, **CFB** - Combination of Fungal Blends, **Sr**- Sensor

4.4.2 EN to detect the disease progression in papayas during 5 days of storage.

EN sensor readings for each inoculation treatment were compared on different days to investigate whether EN could detect changes in the volatile profile as the disease progressed in papayas. When the similarity percentages between the EN readings of papaya samples inoculated with CG were analysed on day 1, these samples exhibited a similarity of 94.36% compared with day 3, indicating that there was a discernible change in the volatile profile within this time frame. Similarly, the similarity between days 1 and 5 was 91.58%, while the similarity between days 3 and 5 increased to 96.08%. The percentage similarities for papaya samples inoculated with BC, FS, and CFB were below 99% (Table 4.2) when comparing different days. This suggests that EN could successfully distinguish changes in the volatile profile as the disease progressed during the 5-day storage period. Overall, these findings demonstrate that EN can effectively identify and track the alterations in the volatile profile as the disease advances in papayas over the course of 5 days. This analysis is pivotal because early symptom detection enables growers to take timely action, either by treating the affected fruits or segregating them from the rest of the batch.

Table 4.2: Similarity of each treatment group (CG, FS, BC, and CFB) between different storage days. The average values of replicates from each group were compared. A percentage similarity of over 99% shows that the two samples are significantly similar to each other. Values below 99 or 98% showed a significant weak difference.

	Average similarity% of CG	Average similarity% of FS	Average similarity% of BC	Average similarity% of CFB
Days 1 and 3	94.36%	88.68%	88.59%	96.83%
Days 1 and 5	91.58%	86.31%	90.66%	91.70%
Days 3 and 5	96.08%	95.10%	88.71%	93.96%

Table notes: **CG** - *Colletotrichum gloeosporioides*, **FS** - *Fusarium solani*, **BC** - *Botrytis cinerea*, **CFB** - Combination of Fungal Blends

4.4.3 EN to distinguish between papayas infected with different fungi.

The objective of this section is to investigate whether EN could discern volatile differences in papayas inoculated with different fungi, thus enabling the identification of specific diseases. The results obtained from the EN sensor readings, presented in Table 4.3, revealed that the percentage similarities between the readings for each treatment were consistently below 99% on days 1, 3, and 5. On day 1, fruits infected with CG showed 94.27% similarity with fruits infected with FS, 91.70% similarity with fruits infected with BC, and 98.91% similarity with fruits infected with CFB. This shows that even on the first day, EN can identify the changes in fruit

samples as they are infected with different fungi. On day 3, the percentage similarity between CG and BC was 96.74%, that between FS and BC was 96.33%, and that between CFB and all other infections were between 96-97.43%. However, the percentage similarity between FS and CG was 98 % on day 3 which is less than 99%, but still shows that papayas infected with FS and CG could have a very similar volatile composition on day 3. On day 5, papaya fruits infected with BC showed a similarity of 83.86% with FS, 83.40% with CG, and 86.99% with CFB. This shows that EN can significantly differentiate fruits infected with BC as it is observed, BC shows significantly different volatile composition. Further details on the specific volatile compounds that caused changes in the percentage similarity of fruits were confirmed by GC-MS analysis.

Table 4.3: Percentage similarity between papaya samples inoculated with different fungi (CG, FS, BC, and CFB) on days 1, 3, and 5. The average values of replicates from each group were compared. A percentage similarity of over 99% shows that the two samples are significantly similar to each other. Values below 99 or 98% showed a significant weak difference.

Day 1	CG	FS	BC	CFB
CG	-	94.27%	91.70%	98.81%
FS	94.27%	-	97.43%	94.82%
BC	91.70%	97.43%	-	92.25%
CFB	98.81%	94.82%	92.25%	-
Day 3	CG	FS	BC	CFB
CG	-	98.07%	96.74%	96.43%
FS	98.07%	-	96.33%	96.97%
BC	96.74%	96.33%	-	97.43%
CFB	96.43%	96.97%	97.43%	-
Day 5	CG	FS	BC	CFB
CG	-	98.57%	83.40%	95.79%
FS	98.57%	-	83.86%	96.88%
BC	83.40%	83.86%	-	86.99%
CFB	95.79%	96.88%	86.99%	-

Table notes: **CG** - *Colletotrichum gloeosporioides*, **FS** - *Fusarium solani*, **BC** - *Botrytis cinerea*, **CFB** - Combination of Fungal Blends

4.4.4 EN to distinguish between infected and healthy papayas during 5 days of storage.

The EN sensor readings for all four treatment samples were compared with those of the healthy control samples each day using the CBR classification method, as shown in Table 4.4. On day 1, the papayas inoculated with CG exhibited a similarity percentage of 88.79% compared with the healthy control samples. Similarly, papayas inoculated with FS showed a similarity percentage of 94.31%, those inoculated with BC showed 95.20%, and those inoculated with all three fungi

showed 89.33% similarity when compared to the healthy control samples. Similarly, on days 3 and 5, all papayas inoculated with fungi showed a percentage similarity below 99%, indicating that EN can identify the differences between healthy and unhealthy fruits. The objective of this comparison was to determine whether EN could effectively differentiate between infected and healthy papayas when stored together, reflecting real-life post-harvest storage conditions. As the infection continued to spread and unique volatile compounds were released, the percentage similarity between infected and control samples increased. By day 5, papayas inoculated with CG exhibited a similarity percentage of 96.34%, FS showed 95.33%, BC showed 85.84%, and those inoculated with all three fungi demonstrated 95.31% similarity compared to the healthy control samples. Visual representations of disease progression are provided in Table 4.7, revealing that by day 4, all infected papayas displayed symptoms of infection.

Table 4.4: Percentage similarity between each treatment sample (CG, FS, BC, and CFB) and healthy control samples on days 1, 3, and 5 (D1, D3, and D5). The average values of replicates from each group were compared. A percentage similarity of over 99% shows that the two samples are significantly similar to each other. Values below 99 or 98% showed a significant weak difference.

	H_D1		H_D3		H_D5
CG_D1	88.79%	CG_D3	97.65%	CG_D5	96.34
FS_D1	94.31%	FS_D3	98.94%	FS_D5	95.33%
BC_D1	95.20%	BC_D3	97.12%	BC_D5	85.84%
CFB_D1	89.33%	CFB_D3	98.01%	CFB_D5	95.31%

Table notes: **H**- Healthy, **CG** - *Colletotrichum gloeosporioides*, **FS** - *Fusarium solani*, **BC** - *Botrytis cinerea*, **CFB** - Combination of Fungal Blends, **Sr**- Sensor

4.4.5 Disease incidence and disease severity percentage

During storage, papaya fruit decay was observed in both treated and control groups. In the first two days, no disease symptoms appeared on any of the fruits. The symptoms of all fungal inoculations began to appear on day three. On day 3, 65% of papayas inoculated with CG showed symptoms. Similarly, 52.5%, 72%, and 80% of papayas inoculated with FS, BC, and CFB, respectively, started showing symptoms on a disease severity grade scale of 1 (Tables 4.5 and 4.6). Based on the results (figure 4.1 and 4.2), after day 3, the disease incidence and severity both started increasing; hence, it is expected that EN would distinguish the changes in the volatile profile from day 3 of papaya storage.

Table 4.5: Disease incidence % measured for the healthy control group (H) and all four fungal inoculation treatments (CG, FS, BC, and CFB).

Days	Disease incidence (%)				
	H	CG	FS	BC	CFB
Day 1	0	0	0	0	0
Day 2	0	0	0	0	0
Day 3	0	65	52.5	72	80
Day 4	0	100	90	100	100
Day 5	5	100	100	100	100

Table notes: **H**- Healthy, **CG** - *Colletotrichum gloeosporioides*, **FS** - *Fusarium solani*, **BC** - *Botrytis cinerea*, **CFB** - Combination of Fungal Blends

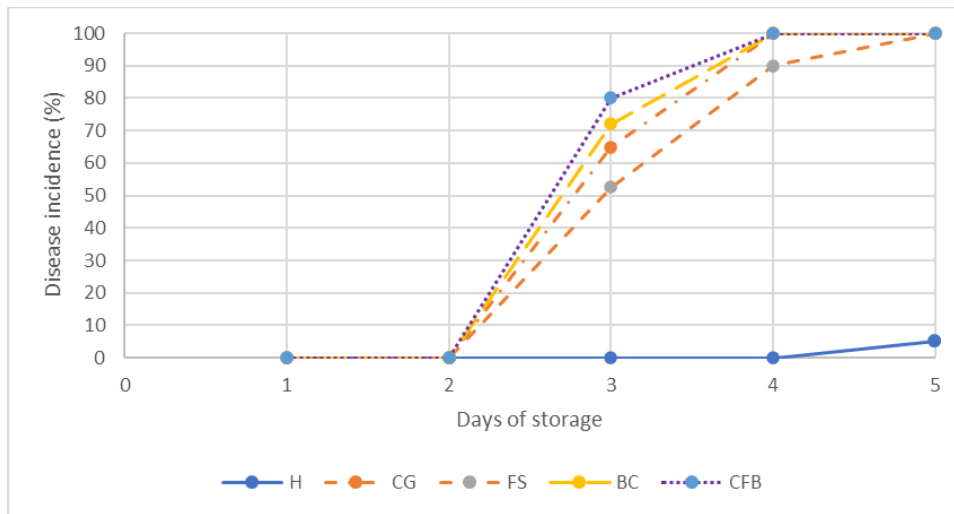


Figure 4.1: Percentage of papaya samples showing disease symptoms for the control group (H) and each of the four inoculation treatments (CG, GF, BC, and CFB) after 5 days of storage.

Table 4.6: Disease severity % measured for the healthy control group (H), and all four different fungal inoculation treatments (CG, FS, BC, and CFB) after 5 days of storage.

	Disease severity (%)				
	H	CG	FS	BC	CFB
Day 1	0	0	0	0	0
Day 2	0	0	0	0	0
Day 3	0	32.5	26.25	36	40
Day 4	0	87.5	45	97.5	93.75
Day 5	2.5	95	81.25	100	100

Table notes: **H**- Healthy, **CG** - *Colletotrichum gloeosporioides*, **FS** - *Fusarium solani*, **BC** - *Botrytis cinerea*, **CFB** - Combination of Fungal Blends

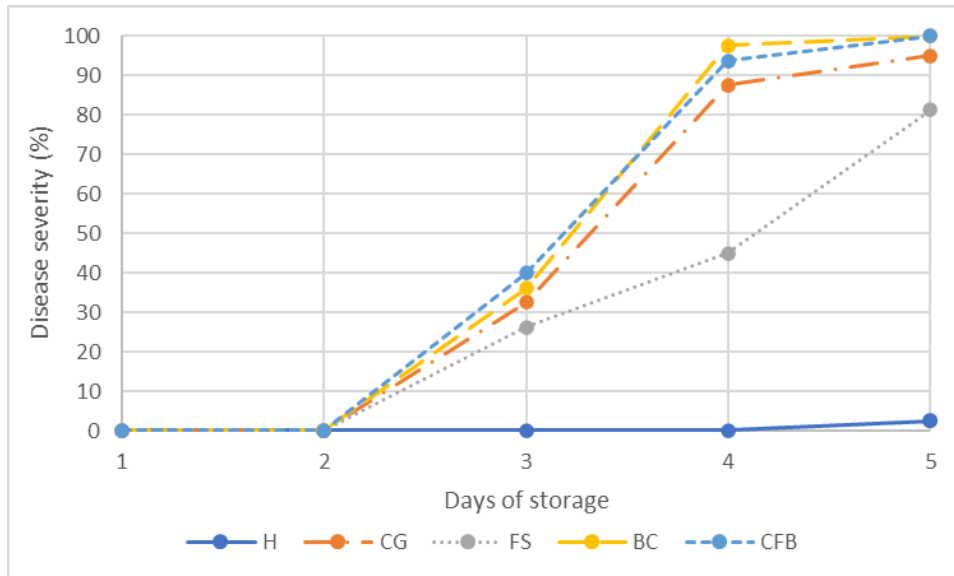


Figure 4.2: Percentage of disease severity calculated for the control group (H) and each of the four inoculation treatments (CG, GF, BC, and CFB) after 5 days of storage.

Table 4.7: Pictures of disease progression in papaya samples inoculated with different fungi (CG, FS, BC, and CFB) and stored for 5 days.

Day /sample	CG	FS	BC	CFB
1				
2				

Table 4.7 continued: Pictures of disease progression in papaya samples inoculated with different fungi (CG, FS, BC, and CFB) and stored for 5 days.

3				
4				
5				

Table notes: **H**- Healthy, **CG** - *Colletotrichum gloeosporioides*, **FS** - *Fusarium solani*, **BC** - *Botrytis cinerea*, **CFB** - Combination of Fungal Blends

4.4.6 GC-MS analysis of papaya fruit inoculated with CG over 5 days of storage.

Based on the PCA score board presented in Figure 4.6, each fruit sample was sorted into different groups based on the dot colour. The first two components of the score plot accounted for 75.0% and 9.0% of the variance. Most of the samples showed close relationships within the groups but distinct differences between the groups. Furthermore, the score plot shows a clear separation of the samples into three major groups. However, certain sample groups exhibit a close relationship, as shown in Figure 3.

The first group included samples from days 1 and 2 (yellow), indicating that the fungus had not commenced infection. The second group included day 3 and day 4 samples (blue), in which the fruit had started ripening, and the infection process had begun. The final group consisted of only five samples (red), in which the severity of infection was significant. In general, group 3 showed significant differences along PC1 when compared with groups 1 and 2, indicating a significant difference in the volatile composition between each sample group. When compared

with PC2, a strong separation was observed between the Group 1 and Group 2 samples, highlighting the difference between the healthy and diseased samples. This suggests that the volatile composition of papaya fruit can differentiate fruits with various health statuses.

Furthermore, the grouping indicated that the volatile profiles on days 1, 3, and 5 were sufficient to differentiate potential biomarkers for the early detection of anthracnose disease (see Table 4.8). As shown in Table 4.8, the potential biomarkers for day 1 consisted of alkanes, which created a gasoline-like to odourless aroma. These include undecane, 5,7-dimethyl-, heptane, 4,4-dimethyl-, undecane, 3,7-dimethyl-, undecane, 4,4-dimethyl-, undecane, and 3,9-dimethyl-. The sweet aroma produced by the day 3 sample is contributed by oxalic acid and butyl propyl ester, which have also been reported in the volatile profile of starfruit (Ramadan et al., 2020), and ethanol and isopropyl alcohol have also become biomarkers for the diseased fruit on day 3, suggesting the ability of the fungus to ferment via secreted enzymes such as amylases (Gong et al., 2022). On day 5, ethanol, formamide, acetoin, isopropyl alcohol, 2-methyl-1-propanol, and isobutyl acetate were identified as potential biomarkers because they created a pungent odour. Acetoin, 2-methyl-1-propanol, and isobutyl acetate have been reported as end products of fermentation by various microbes, suggesting that *Colletotrichum gloeosporioides* undergoes fermentation during infection (Gong et al., 2022; da Silva Vale et al., 2022).

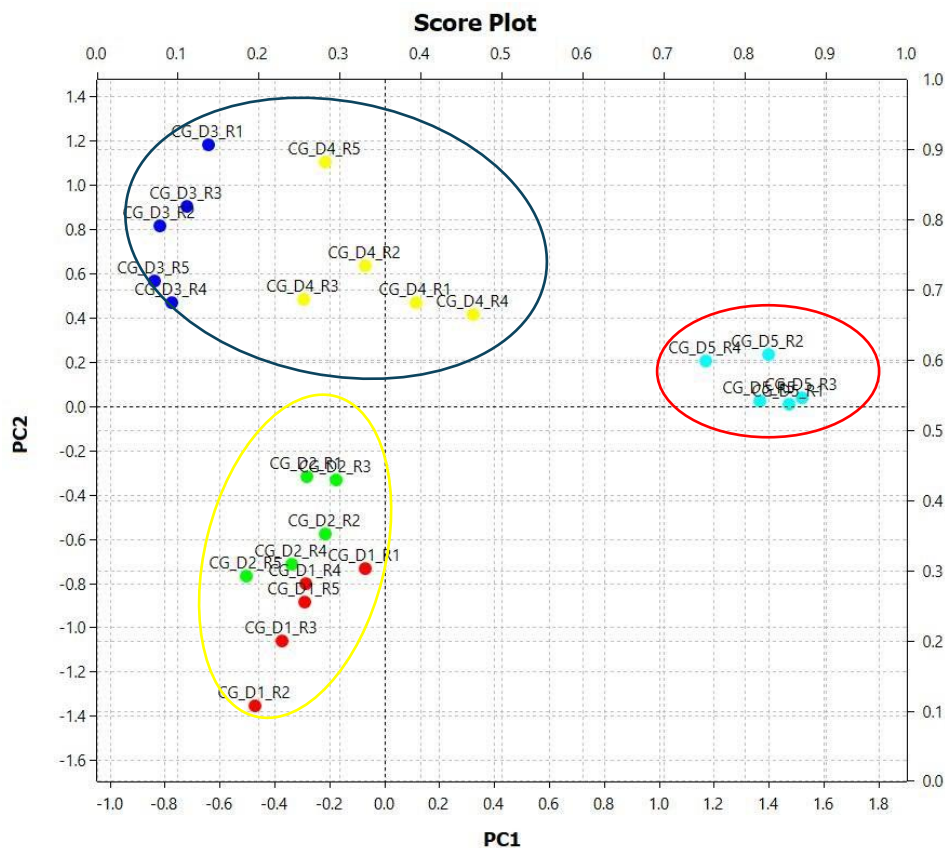


Figure 4.3: Loading plot of the first two principal components of PCA for papaya fruit samples

infected by *Colletotrichum gloeosporioides* (CG) over 5 days (D1–D5) of incubation. The numbers following the label “R” indicate the number of replicates. PC1 and PC2 accounted for 20.8% and 39% of variance, respectively. The coloured circle highlights the grouping based on similarity in the volatile profile, where yellow indicates group 1, blue indicates group 2, and red indicates group 3.

Table 4.8. Potential biomarkers for papaya (cv. Sekaki) fruit infected with CG after 5 d of incubation, based on GC-MS analysis. The number under the area percentage indicates the day of incubation.

Compound	Retention Time	Area Percentage (%)		
		1	3	5
Ethanol	1.02		1.660	1.140
Formamide	1.03			0.277
Acetoin	1.04			0.162
Isopropyl Alcohol	1.05		0.201	0.033
1-Propanol, 2-methyl-	1.42			0.131
Isobutyl acetate	1.53			0.137

Table 4.8 continued. Potential biomarkers for papaya (cv. Sekaki) fruit infected with CG after 5 d of incubation, based on GC-MS analysis. The number under the area percentage indicates the day of incubation.

Acetonitrile	2.50			0.097
Undecane, 5,7-dimethyl-	11.49	0.125	0.549	
Heptane, 4,4-dimethyl-	12.67	0.069		
Undecane, 3,7-dimethyl-	14.31	0.312		
Oxalic acid, butyl propyl ester	17.25		0.027	
Undecane, 4,4-dimethyl-	22.01	0.093		
Undecane, 3,9-dimethyl-	22.44	0.229		

4.4.7 GC-MS analysis of papaya fruit inoculated with BC over 5 days of storage.

Based on the PCA score board presented in figure 4.4, each fruit sample was sorted into different groups based on dot colour. The first two components of the score plot accounted for 60% and 73% of the variance, respectively. All samples showed a close relationship within their respective groups; however, there were distinct differences between the other groups. Furthermore, the score plot shows a clear separation of the samples into four major groups.

However, there was a close relationship between certain sample groups, as shown in Figure 4.4.

The first group included samples from days 1 and 2 (yellow), indicating that the fruit remained healthy with no infection. The second group involved day 3 samples (blue), which showed the infection process, as it had a distinct relationship with group 1. Groups 3 and 4 involved day 4 (highlighted in green) and day 5 (red) samples, respectively, where the severity of the infection was significant. Along PC1 and PC2, all groups showed clear differences from each other based on grouping, indicating significant differences in the volatile composition between each sample group. This suggests that papaya fruit can differentiate between fruits of various health statuses. Therefore, volatile profiling on days 1, 3, and 5 was sufficient to identify potential biomarkers for the early detection of stem-end rot disease (Table 4.9).

As shown in Table 4.9, the potential biomarkers for day 1 consisted of alkanes such as Undecane, Undecane, 4,7-dimethyl-, and undecane, 2-methyl-, which created a slight gasoline-like to odourless aroma. On day 3, various fermentative volatiles were selected as biomarkers, including lactic acid, Isopropyl Alcohol, acetoin, formamide, 1-Heptanol, and DL-2,3-Butanediol. Previous studies have suggested that this indicates the potential of *L. theobromae* to cause fermentation of the fruit because of its secretion of various cell wall-degrading enzymes (Felix et al., 2018). Ethylene oxide is considered a biomarker for day 3 samples and as mentioned previously its role is well established in controlling ethylene biosynthesis and indicating that the fruit might trigger plant defence mechanisms by converting ethylene to ethylene oxide through enzymatic reactions. On day 5, ethanol, 1,4-Butanediol, and 1-Pentanol were considered as biomarkers. ethanol and 1,4-Butanediol have been reported as fermentation, 1-Pentanol be in previous studies as the main biomarkers for mango fruit infected with BC (Forte et al., 2016). This validates 1-Pentanol as the main biomarker for BC-infected fruit.

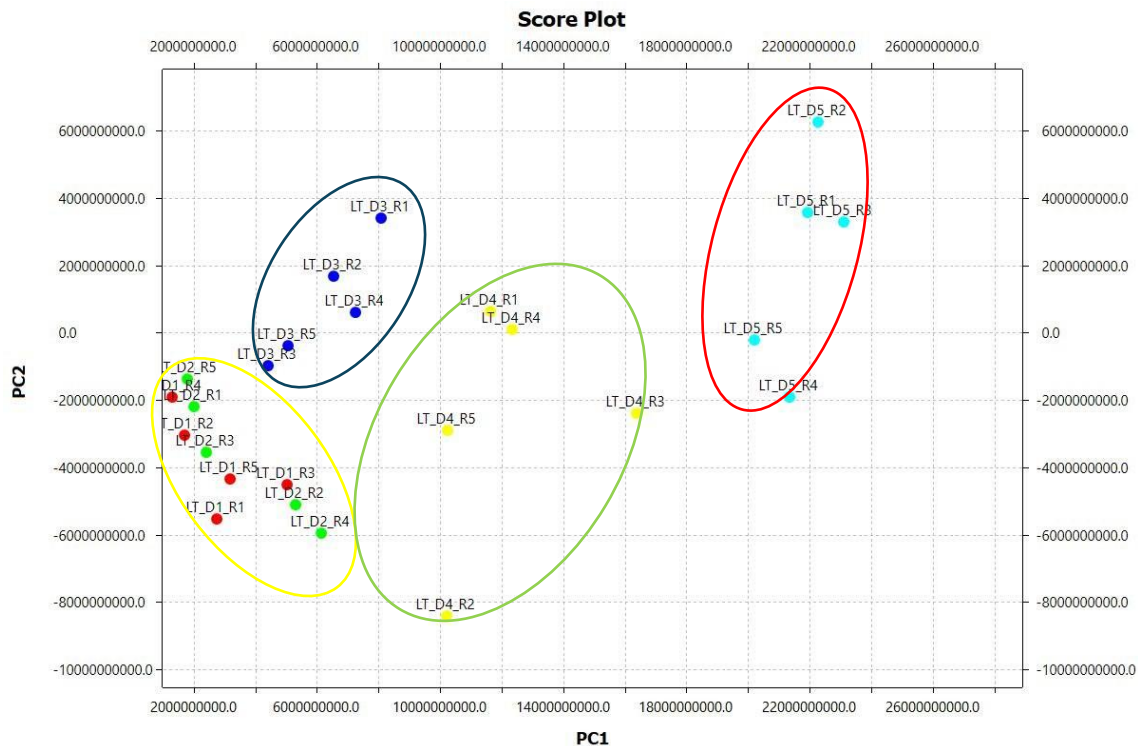


Figure 4.4: Loading plot of the first two principal components of PCA for papaya fruit samples infected with *Lasiodiplodia theobromae* (BC) over 5 days (D1–D5) of incubation. The numbers following the label “R” indicate the number of replicates. PC1 and PC2 accounted for 60 and 73% of the variance, respectively.

Table 4.9. Potential biomarkers for papaya (cv. Sekaki) fruit infected with *Lasiodiplodia theobromae* after 5 days of incubation, based on GC-MS analysis. The number under the area percentage indicates the day of incubation.

Compound	Retention Time	Area Percentage (%)		
		1	3	5
Ethanol	1.45			0.090
L-Lactic acid	1.52		0.046	0.188
Ethylene oxide	1.59		0.056	
Isopropyl Alcohol	1.60		0.046	0.065
Acetoin	3.09		0.043	0.088
Formamide	3.14		0.002	0.046

Table 4.9 continued. Potential biomarkers for papaya (cv. Sekaki) fruit infected with *Lasiodiplodia theobromae* after 5 days of incubation, based on GC-MS analysis. The number under the area percentage indicates the day of incubation.

1-Heptanol	3.67		0.295	0.030
------------	------	--	-------	-------

1,4-Butanediol	3.72			0.084
1-Pentanol	3.75			0.012
DL-2,3-Butanediol	12.16		0.036	0.032
Undecane	16.06	0.218	0.050	
Undecane, 4,7-dimethyl-	21.45	0.037		
Undecane, 2-methyl-	22.44	0.215		

4.4.8 GC-MS analysis of papaya fruit inoculated with FS over 5 days of storage.

Based on the PCA score board presented in figure 4.5, each fruit sample was sorted into different groups based on dot colour. The first two components of the score plot accounted for 30.8% and 49.3% of the variance, respectively. Some of the samples showed a close relationship within their respective groups, but there were distinct differences between the other groups, particularly in the day 5 sample. Furthermore, the score plot shows a clear separation of the samples into three major groups. However, there is a close relationship between certain sample groups, as indicated in the figure.

Overall, the first group included the day 1 and day 2 samples (yellow), indicating that the fruits were healthy and unripe. The second group involved day 3 and 4 samples (blue), suggesting that the fungus had initiated the infection process, as evidenced by its distinct relationship with Group 1. The final group, Group 3, consisted of only day 5 samples (red), in which the severity of the infection was significant. Along PC1, Group 1 showed a clear difference from the other groups based on grouping. When analysed along PC2, Group 3 exhibited distinct differences from Groups 1 and 2. This indicates that papaya fruit can differentiate between fruits at various health statuses, and the volatile profiling of days 1, 3, and 5 is sufficient to differentiate potential biomarkers for the early detection of *Fusarium* rot disease (see Table 4.10).

As shown in Table 4.10, the potential biomarkers for day 1 include alkanes such as dodecane, dodecane, 4,6-dimethyl, undecane, undecane, 5,7-dimethyl-, and hexadecane, which contribute to a slight gasoline-like to odourless aroma. Notably, the presence of methylpent-4-enylamine also significantly contributed to the unripe fruit, based on previous studies (Sundaram and Prabhakaran, 2017). On day 3, oxalic acid, butyl propyl ester, hexane, 2,4,4-trimethyl- and DL-2,3-Butanediol. Although oxalic acid and butyl propyl ester have been reported to affect the volatile profile of starfruit and DL-2,3-Butanediol is a common fermentative product, the roles of hexane and 2,4,4-trimethyl- in causing diseases remain uncertain, and further investigation is needed. The presence of DL-2,3-Butanediol also suggested the ability of *Fusarium solani* to induce fermentation which has been reported in previous studies (Azabou et al., 2016; Anasontzis and Christakopoulos, 2014).) On day 5, the

potential biomarkers included ethanol, formic acid, acetoin, ethyl butanoate, 1-hexanol, butyl butanoate, and isopropyl alcohol. Although ethanol and acetoin have been identified as fermentation products, the presence of 1-hexanol, ethyl butanoate, and butyl butanoate confirmed that the fruit had fully ripened.

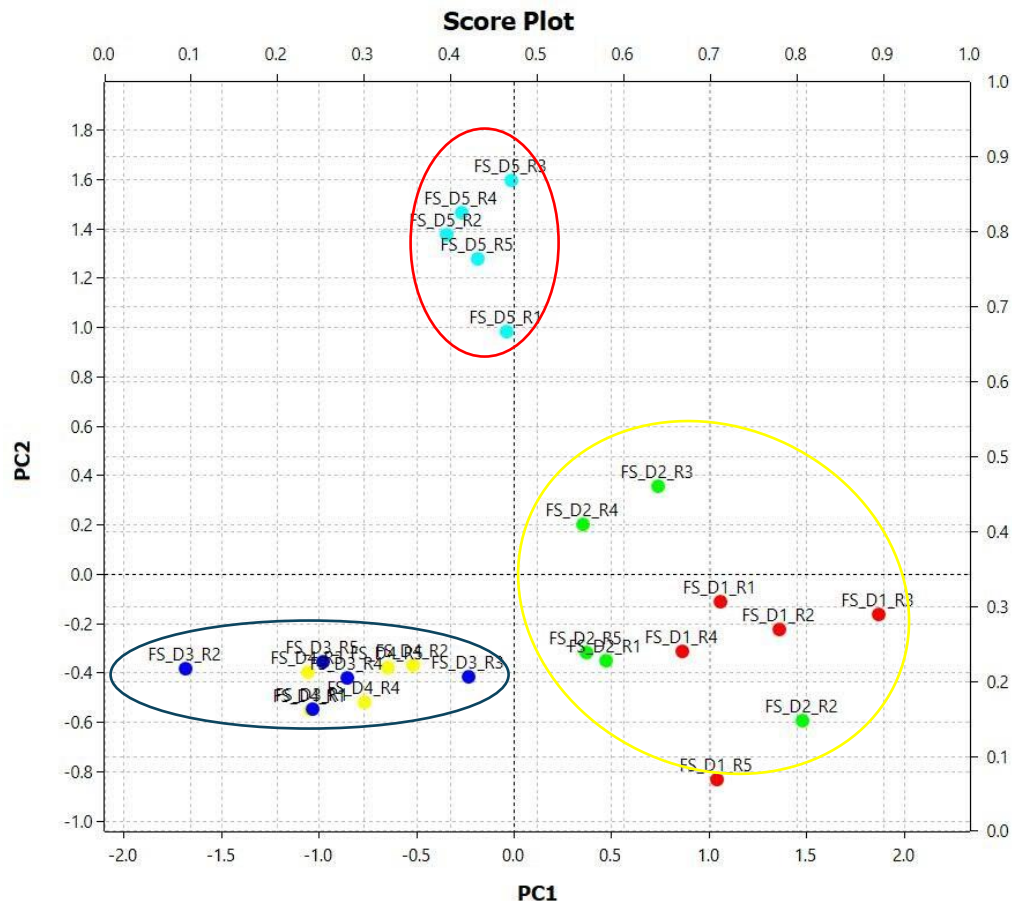


Figure 4.5: Loading plot of the first two principal components of PCA for papaya fruit samples infected with *Fusarium solani* (FS) over 5 days (D1–D5) of incubation. The numbers following the label “R” indicate the number of replicates. PC1 and PC2 accounted for 30.8% and 49.3% of variance, respectively.

Table 4.10. Potential biomarkers for papaya (cv. Sekaki) fruit infected with *Fusarium solani* after 5 days of incubation, based on GC-MS analysis. The number under the area percentage indicates the day of incubation.

Compound	Retention Time	Area Percentage (%)		
		1	3	5
Ethanol	1.02			0.894
Formic acid	1.10			0.102

Methylpent-4-enylamine	1.93	0.009		
Acetoin	2.03			0.227
Ethyl butanoate	3.32			0.950
1-Hexanol	5.30			0.243
Butyl butanoate	9.47			0.184
Isopropyl Alcohol	9.60			0.478
Oxalic acid, butyl propyl ester	10.76		0.007	
Dodecane	14.29	1.055	0.453	
Dodecane, 4,6-dimethyl-	16.03	0.460	0.239	
Undecane	16.04	0.481	0.239	
Undecane, 5,7-dimethyl-	21.24	0.065		
Hexane, 2,4,4-trimethyl-	21.68		0.197	
DL-2,3-Butanediol	21.69		0.012	0.048
Hexadecane	22.44	0.706	0.333	

4.4.9 GC-MS analysis of papaya fruit inoculated with CFB over 5 days of storage.

Based on the PCA score board shown in Figure 4.6, each fruit sample was categorised into different groups based on the colour of the dots. The first two components of the score plot accounted for 21% and 77.5% of the variance, respectively. Most of the samples exhibited closely related patterns within their respective groups but displayed distinct differences compared to the other groups. Additionally, the score plot clearly demonstrated the notable separation of the samples into three major groups.

The first group, represented by red dots, comprised day 1 samples, indicating fruit in healthy and unripe conditions. The second group, indicated by yellow dots, consisted of day 3 samples, suggesting that fungal infection was initiated during the fruit ripening process, as evidenced by its distinct relationship with group 1. The final group, denoted by blue dots, exclusively included day five samples, indicating a significant level of infection severity as the fruit had fully ripened. Along the PC1 and PC2 axes, all groups exhibited significant differences when compared to the other groups, highlighting the ability of the fruit to differentiate and monitor its health status from healthy to diseased.

Furthermore, the volatile profiling of day 1, 3, and 5 samples proved to be sufficient for differentiating potential biomarkers for early detection of postharvest diseases, as observed in the PCA analysis of each individual disease (Figure 4.3-4.5). These findings were consistent with the grouping observed over the 5-day incubation period. As shown in Table 4.11, the potential biomarkers for the day 1 samples contributed to the overall aroma transitioning from odourless to a slight gasoline-like scent, including alkanes such as octane, 3,3-dimethyl-, undecane, and undecane, 4,7-dimethyl-. Undecane has previously been reported in the volatile profile of

Colletotrichum gloeosporioides, whereas undecane and 3,3-dimethylundecane have been associated with *Fusarium solani* on days 1 and 3, respectively.

On day 3 of incubation, acetoin, (S)-isopropyl lactate, and formamide contributed to the overall aroma characterised by a sweet but fermented scent, indicating the invasion of the fruit by fungi through fermentation caused by all fungi after day 3 of incubation. Previous studies have highlighted the involvement of volatile compounds in fungal infections (Félix et al. 2018; da Silva Vale et al. 2022). By day 5, the overall aroma exhibited fermented and pungent characteristics attributed to various alcohols, carboxylic acids, and acetates, including 4-Penten-2-ol, Isopropyl Alcohol, (S)-(+)-1,2-Propanediol, oxalic acid, lactic acid, acetone, ethyl acetate, 1-Butanol, 3-methyl-, 2,3-Butanediol, 1-Hexanol, and 1-Heptanol.

Some of these volatile compounds were detected in all three individual fungi, whereas others were specific to a particular fungus. For instance, lactic acid, isopropyl alcohol, acetoin, formamide, 1-Heptanol, and DL-2,3-Butanediol were detected in the volatile profiles of *L. theobromae*, and 1-Heptanol is considered a potential biomarker for this fungus. Acetoin and 1-Hexanol were identified in the combination diseases, with 1-Hexanol showing potential as a specific biomarker for *Fusarium solani* compared to other volatile profiles. Furthermore, formamide, acetoin, and isopropyl alcohol were detected in fruits infected with CG; however, their presence was also observed in the volatile profiles of fruits infected with BC and FS. The absence of certain volatiles specific to CG, such as 2-methyl-1-Propanol and Isobutyl acetate, indicated that the intensity of volatiles produced by other fungi surpassed that produced by CG during the infection process, likely due to differences in disease severity.

Overall, the utilisation of GC-MS allows researchers to differentiate the volatiles produced by various fungi, suggesting potential biomarkers, and establishing it as a powerful tool for the development of innovative and rapid detection technologies.

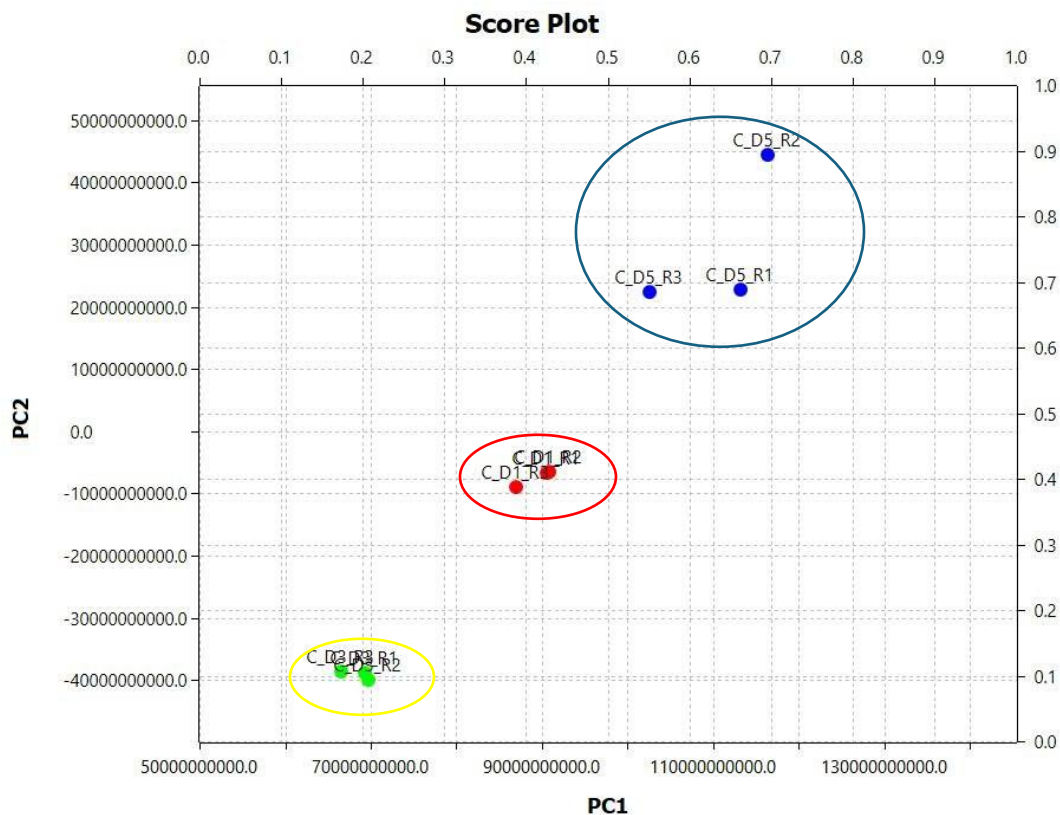


Figure 4.6: Loading plot of the first two principal components of PCA for papaya fruit samples infected with combination diseases over 5 days (D1–D5) of incubation. The numbers following the label “R” indicate the number of replicates. PC1 and PC2 accounted for 21.0% and 77.5% of variance, respectively.

Table 4.11. Potential biomarkers for papaya (cv. Sekaki) fruit infected with a combination of diseases after 5 days of incubation, based on GC-MS analysis. The number under the area percentage indicates the day of incubation.

Compound	Retention Time	Area Percentage (%)		
		1	3	5
4-Penten-2-ol	1.35			1.245
Isopropyl Alcohol	1.38			0.029
(S)-(+)-1,2-Propanediol	1.39			0.435
Oxalic acid	1.41			0.042
L-Lactic acid	1.42			0.548
Acetone	1.50			0.043
Ethyl Acetate	1.90			0.089

2-Pentanone	1.95	0.027		
1-Pentene, 4-methyl-	2.00	0.288		
Acetoin	3.01		0.250	0.083
(S)-Isopropyl lactate	3.04		0.194	0.020
Formamide	3.06		0.007	0.004
1-Butanol, 3-methyl-	3.42			0.625
2,3-Butanediol	4.51			0.151
1-Hexanol	7.15			0.184
1-Heptanol	8.35			0.057
Octane, 3,3-dimethyl-	14.30	0.117		
Undecane	16.04	0.485	0.211	
Undecane, 4,7-dimethyl-	16.04	0.082	0.211	

4.4.10 Relationship between EN sensor responses and GC-MS results.

The unique profiles of volatile compounds and their relative contents between healthy and infected papaya fruits, identified through GC-MS, played a pivotal role in discerning the presence and specific types of infections, allowing for rapid and accurate identification of fungal pathogens using EN. GC-MS analysis revealed that on day 1, all papaya samples predominantly contained alkanes, which imparted odourless aroma. However, from day 3 onwards, the contribution of esters and alcohols became more significant in discriminating between decay and fungal infection types in papaya.

When fungi attach to the fruit surface, the rupture of the host surface and hydrolysis of fruit cell walls trigger a cascade of processes, including defence and attack mechanisms in both the fungi and the fruit. This led to the release of enzymes and volatile compounds. Among these compounds, oxalic acid is released by *Lasiodiplodia theobromae* and *Colletotrichum gloeosporioides* to induce oxidative stress and damage fruit tissue. Thus, in this study, oxalic acid was identified as a biomarker on day 3, which differentiated infected fruits from healthy fruits. GC-MS also revealed that each fungus released its own unique volatile compounds that were detected by EN sensors. For example, 1-Hexanol was only detected in fruits infected with *Fusarium solani*, 1-Heptanol in fruit infected with *Lasiodiplodia theobromae*, and isobutyl acetate was detected in fruits infected with *Colletotrichum gloeosporioides*. The EN sensors used in this study were sensitive to aromatic, alkane, and alcohol compounds, confirming their appropriateness for analysis. The selected sensors effectively captured the variations in the volatile compounds emitted from the four treatment groups. Thus, both E-nose and GC-MS data provide compelling evidence that pathogenic fungal infections significantly alter the volatile compound profiles.

4.5 Chapter conclusion

Overall, the results of this experiment demonstrate the immense potential of EN as a highly promising technology that effectively discriminates decay in papayas in the early storage phase and successfully distinguishes between the three prevalent fungal infection types using the CBR classification method. The EN was proved capable of distinguishing between healthy and infected papayas, with significant differences in the volatile profiles from day 1 onward. For example, CG-infected fruits had an 88.79% similarity with healthy samples, while BC-infected papayas had a 95.20% similarity. By day 5, the differences became even more pronounced, particularly for BC-infected fruits, which showed an 85.84% similarity to healthy ones. The EN also successfully tracked disease progression in papayas, with noticeable changes in the volatile profile detected as early as day 3, particularly in samples inoculated with CG, which showed a 94.36% similarity between days 1 and 3. The device also differentiated between papayas infected with different fungi, such as CG and FS, which had a 94.27% similarity on day 1. By day 5, papayas infected with BC were clearly distinct, with only 83-87% similarity compared to other infections. These results highlighted the EN's potential for early detection and improved postharvest disease management of papaya.

Chapter 5: Application of chitosan combined with green synthesized ZnO NPs as edible coating to control anthracnose disease in papaya during postharvest storage

5.1 Introduction

In the ongoing pursuit of sustainable and effective postharvest disease management, researchers have increasingly focused on eco-friendly alternatives to conventional chemical treatments. Among these, the use of edible coatings and bio-nanocomposites has gained significant attention for their ability to extend the shelf life of fruits while reducing microbial contamination. More research is needed to investigate the application of chitosan-based coatings integrated with green-synthesized zinc oxide nanoparticles (ZnO NPs), as a novel approach to controlling fungal diseases in papaya, offering a promising strategy for maintaining fruit quality and reducing postharvest losses. Hence, this study focused on evaluating the effectiveness of eco-friendly edible coatings made using chitosan combined with green-synthesised ZnO nanoparticles to manage anthracnose disease in papayas, with the aim of reducing losses and improving shelf life while maintaining environmental sustainability.

5.2 Materials and methodology

5.2.1 Materials

All the papayas used in this research were freshly harvested papaya samples of '*Sekaki*' cultivar purchased from a local fruit distributor, Chai Organic Fruit & Vege Farming at Kajang, Selangor, Malaysia. All the samples were unripe, at the maturity stage 1, characterized by green peel colour with no yellow coloration (Ruslan and Roslan, 2016). The samples had similar weights of 1 kg, with no mechanical damage or injuries visually inspected in the orchard.

Chemicals: Zinc acetate dihydrate $Zn(CH_3COO)_2$ (Chemiz UK, 99.5%), Sodium Hydroxide NaOH (Fisher Chemical™, 99.81%), Acetic acid, glacial (EMSURE®, 100%), Chitosan, Medium molecular weight (Sigma-Aldrich)

5.2.2 Pandan (*Pandanus amaryllifolius*) leaves as the leaf extract

This study utilised fresh pandan leaves sourced from a local farmers' market in Semenyih, Selangor, Malaysia. Many Southeast Asian nations, including Thailand, Malaysia, Laos, Indonesia, India, Singapore, New Guinea, Taiwan, the Philippines, and Vietnam, regularly cultivate pandan leaf. They are frequently used in cooking for flavour improvement, food colouring, and aromatic infusion (Gopinath et al., 2023). Therefore, they are inexpensive and easily available in local markets. The flavour characteristics of these leaves is greatly enhanced by the abundance of 2-acetyl-1-pyrroline, a basmati aroma component. Moreover, pandan leaves contain bioactive substances with functional properties such as rutin, kaempferol, naringin, epicatechin, ferulic acid, gallic acid, and catechin. These substances have anti-carcinogenic, free radical-scavenging, and antioxidant properties, among other health benefits (Gopinath et al., 2023).

5.2.3 Preparation of leaf extract

To ensure a sterile environment, all glassware was sterilised by autoclaving before the experiment. Fresh *Pandanus amaryllifolius* leaves were thoroughly washed with tap water to remove dust or foreign particles. Subsequently, the leaves were finely chopped and subjected to oven drying at 60°C overnight, followed by grinding into a fine powder (Naiel et al., 2022). A total of 100 g of dried leaves was then boiled in 800 ml of deionised (DI) water at 60°C for 60 min using a water bath apparatus, resulting in the extraction of a dark brown solution. After cooling to room temperature, the extract was filtered through Whatman filter paper No.1 and stored in a refrigerator for further use (Md Akhir et al., 2020).

5.2.4 Preparation of ZnO NPs

The synthesis of ZnO NPs was optimised by refining the existing methods, as outlined in Chapter 2 and Table 3, with a focus on simplicity, efficiency, and quality. The method aimed to streamline processes, reduce chemical usage, and minimise the analysis time to obtain nanoparticles suitable for application to fruits. This involves iterative testing to determine the optimal synthesis method. Initially, a 0.05M Zinc acetate dihydrate solution was prepared as the precursor. The synthesis involved mixing the leaf extract and precursor in a 2:1 ratio, with 200 ml of the leaf extract combined with 100 ml of the precursor under continuous stirring at 500rpm. 2M NaOH was then added dropwise to adjust the pH to 9. The mixture was then heated at 60°C for 2 h in a water bath, leading to the formation of a bio-reduced salt, visible as a brown precipitate at the bottom of the flask. After 24 hours of aging at room temperature, the precipitated ZnO NPs were collected, washed five times with Milli-Q water via centrifugation at 10000 rpm for 10 minutes. Finally, the precipitate was dried at 120°C for 1 h in

an oven and dispersed in various tubes of deionised water depending on the desired concentrations of ZnO NPs for subsequent analysis (Al-darwesh et al., 2024).

5.2.5 Characterization of nanoparticles

FESEM imaging coupled with EDX analysis was conducted to verify the presence of the synthesised ZnO NPs and to determine their elemental composition. For this purpose, a drop of the suspension was deposited onto carbon tape attached to a stub using a Pasteur pipette and subsequently allowed to dry. The dried samples were then subjected to high-resolution observations and recordings. The size, polydispersity index (PDI), and surface charge (zeta potential) of ZnO NPs were evaluated using a Malvern Zetasizer Ultra instrument (Nano-ZS, USA). To achieve this, 10 mg of ZnO NPs powder was dispersed in 10 mL of Milli-Q water, followed by sonication for 20 min at 80 kHz and 100% power. Subsequently, 1 mL of the suspension was analysed (Harikrishnan et al., 2023).

5.2.6 In vitro antifungal assay of ZnO NPs against *Colletotrichum gloeosporioides*

To evaluate the in vitro antifungal effectiveness of ZnO nanoparticles against *Colletotrichum gloeosporioides*, the causative agent of anthracnose, ZnO nanoparticle suspensions were incorporated into PDA medium to achieve final concentrations of 0.5g/L, 1.2g/L, and 2.0g/L. Following solidification of the PDA, mycelial plugs (6 mm in diameter) from 7-day-old *Colletotrichum gloeosporioides* cultures were simultaneously inoculated onto the centre of each Petri plate. The plates were then incubated at 25°C for 7 days, after which the diameter of the mycelial colony was measured, and the area of the fungal growth was calculated (Mosquera-Sánchez et al., 2020). This experimental procedure was conducted with ten replicates for each concentration.

5.2.7 Preparation of chitosan-ZnO NPs coating treatments

The chitosan solution was prepared by dissolving 10 g of medium-molecular-weight chitosan in 1 L of 1% acetic acid, followed by continuous stirring for 72 h to ensure complete dissolution. The pH of the chitosan solution was maintained at 5.6 by the gradual addition of 2M NaOH. This process was repeated to yield four jars, each containing 1 L chitosan solution. ZnO NPs solutions of three different concentrations were prepared by dispersing ZnO nanoparticle powder in 1L of deionized water and autoclaved. Subsequently, the solutions were sonicated for 20 min at a frequency of 80kHz and power of 100%. To determine the volume required to fully coat a medium-sized papaya (1 kg), the coating solution was tested, requiring a volume of 2 L. Consequently, all components of the coating were added based on the final volume.

Four treatment solutions of 2L were prepared in 2.5L glass beakers, each containing a final concentration of 0.5% Chitosan. Three of the treatment solutions, including varying concentrations of ZnO NPs (0.5 g/L, 1.5 g/L, and 2.5 g/L). The fourth group contained only 0.5% chitosan (Figure 5.1). The chitosan concentration was maintained at a low and constant value to highlight the notable antifungal effect of ZnO NPs against *Colletotrichum gloeosporioides*. Previous research has already demonstrated the efficacy of higher concentrations of chitosan coatings in managing anthracnose disease in papayas (Ali et al., 2015).

5.2.8 Preparation of spore suspensions

Pure cultures of *Colletotrichum gloeosporioides* were sub-cultured and cultivated on PDA medium and maintained at 24°C and 85% relative humidity. To prepare the pathogen inoculum, 10mL of sterilized distilled water was poured over a 1-week-old *C. gloeosporioides* culture. Gentle scraping with a sterile glass rod dislodged the conidia from the surface and the resulting conidial suspension was filtered through a double layer of sterilised muslin cloth to eliminate mycelial fragments. Following filtration, the suspension was centrifuged for 5 minutes at 4000rpm. The conidial concentration was then adjusted to 10^4 conidia mL⁻¹ using a hemacytometer.

5.2.9 In vivo antifungal assay of chitosan-ZnO NPs coating against *Colletotrichum gloeosporioides*

For the in vivo assessment of the antifungal properties of the chitosan-ZnO NPs coating, papaya fruits were thoroughly washed with a 0.01% sodium hypochlorite solution for 3 min, rinsed with distilled water, and air-dried at ambient temperature (26 ± 2 °C). After drying, the fruits were immersed in a conidial suspension of *C. gloeosporioides* containing 10^4 conidia mL⁻¹ for 1 minute. Subsequently, the treated fruits were air-dried for an additional hour before being dipped into chitosan-ZnO NPs solution for 1 min and left to dry for 2 h. Each treatment group comprised of 15 papayas. The treated fruits were stored in plastic containers covered with plastic cling wrap at room temperature (Figure 5.1).

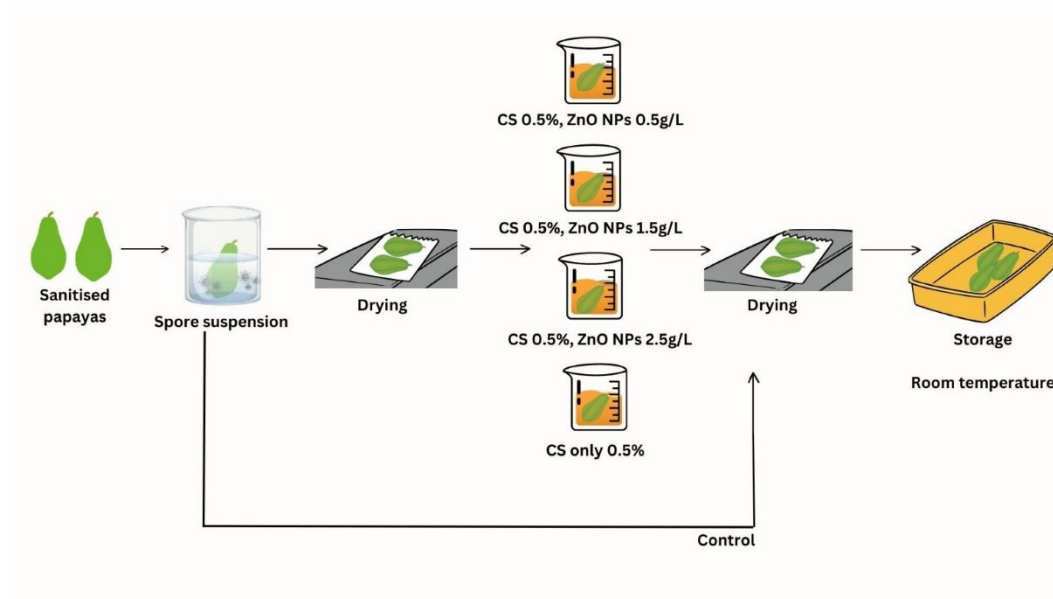


Figure 5.1: Illustration of application of Chitosan (CS)-ZnO NPs coatings on papaya for in vivo antifungal assay. Graphic created using Canva software.

5.2.10 Evaluation of disease Incidence and severity

Throughout the 12-day storage period, disease incidence and severity were assessed daily. Disease incidence was represented as the percentage of fruits displaying anthracnose symptoms out of the total number of fruits in each treatment, whereas disease severity was visually evaluated on a scale of 1–5 (1=0% of fruit surface rotten, 2=1–25%, 3=26–50%, 4=51–75%, and 5=76–100%).

5.3 Statistical analysis

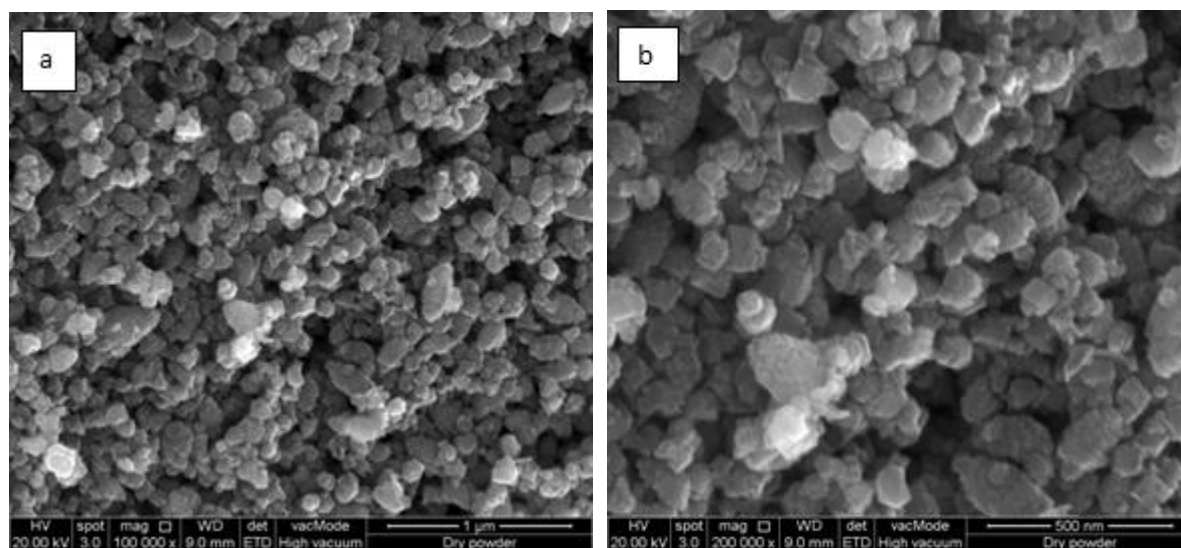
Statistical analysis was conducted using SPSS statistics software (version 28.0), employing Student t-tests and one-way analysis of variance (ANOVA), followed by Tukey's honestly significant difference (HSD) post hoc test. A significance level of $p \leq 0.05$ was adopted to determine statistical significance.

5.4 Results and discussion

5.4.1. Characteristics of nanoparticles

SEM was utilised for morphological analysis of the ZnO NPs synthesised using the green method. The particles exhibited a spherical shape and were slightly agglomerated, as shown in Figure 5.2. This tendency for agglomeration in aqueous solutions has been well-documented in the literature (Lavinia et al., 2019). EDX analysis confirmed the formation of ZnO NPs, with oxygen constituting 53.65% of the atomic weight and 22.07% of its weight, whereas zinc accounted for 46.35% of the atomic weight and 77.93% of its weight. Additionally, minor constituents in the ZnO NPs were attributed to the presence of leaf extract, as illustrated in Figure 5.3.

The average size of the ZnO NPs was determined using a zetasizer, yielding a size of 239.7 nm and PDI of 0.161. A size distribution graph is shown in Figure 5.4. Zeta potential, indicative of colloidal stability, was measured in Milli-Q water, revealing a value of -17.9 mV, classifying the suspension as strongly anionic (Figure 5.5). This negative zeta potential underscores the dispersion capability of the greenly synthesised ZnO NPs. The presence of extract compounds binding to the NPs accounts for this negative surface charge, enhancing the stability of the ZnO NPs and mitigating particle aggregation, which is consistent with findings from previous studies (Faisal et al., 2021).



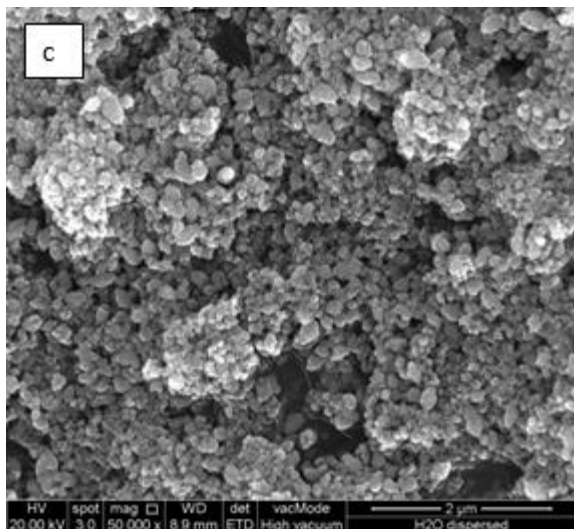


Figure 5.2: SEM photographs of ZnO NPs of (a) dry powder at x10000 magnification (b) dry powder at x20000 magnification (c) powder dispersed in water at x50000 magnification.

Element	Weight%	Atomic%
O K	22.07	53.65
Zn K	77.93	46.35
Totals	100.00	

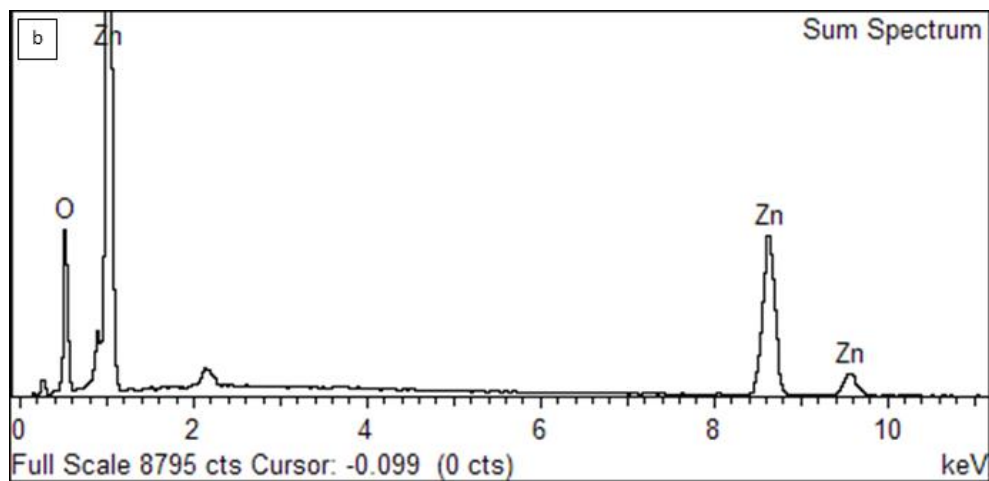


Figure 5.3: EDX spectrograph of green synthesized ZnO NPs

	Size (d.n...	% Number:	St Dev (d.n...
Z-Average (d.nm): 239.7	Peak 1: 191.5	100.0	82.63
Pdl: 0.161	Peak 2: 0.000	0.0	0.000
Intercept: 0.938	Peak 3: 0.000	0.0	0.000

Result quality Good

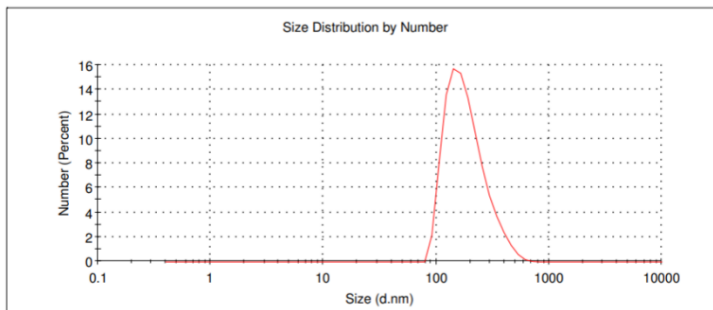


Figure 5.4: Average size, PDI, and size distribution graph of the green-synthesised ZnO NPs obtained from Zetasizer.

Results

	Mean (mV)	Area (%)	St Dev (mV)
Zeta Potential (mV): -17.9	Peak 1: -17.9	100.0	3.97
Zeta Deviation (mV): 3.97	Peak 2: 0.00	0.0	0.00
Conductivity (mS/cm): 0.0678	Peak 3: 0.00	0.0	0.00

Result quality Good

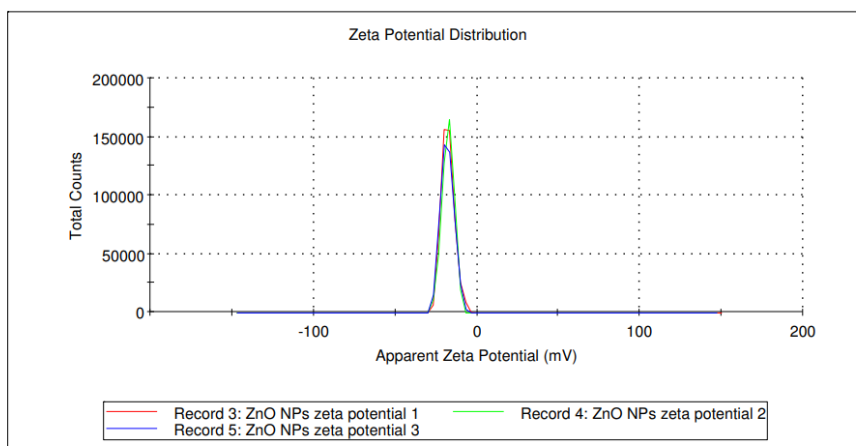


Figure 5.5: Zeta potential graph of green synthesized ZnO NPs obtained from Zetasizer.





5.4.2 In vitro antifungal effect of ZnO NPs

To assess the impact of various concentrations of green-synthesized ZnO NPs – prepared at concentrations of 0.5 g/L, 1.2 g/L, and 2.0 g/L – on *Colletotrichum sp.*, the growth and area of the fungal colony were monitored and quantified in Petri dishes. Tables 5.1 and 5.2 show the

effects of nanoparticle treatments on fungal growth, allowing for the determination of their antifungal efficacy compared to the control group. Following the experiment's initiation, two days post-seeding, *Colletotrichum sp.* showed rapid growth, forming a cottony colony in the control treatment. By day 7, the fungus had colonised almost the entire petri dish. In contrast, colonies treated with different concentrations of ZnO NPs displayed slower growth, with the most diminished growth observed at the 2.0 g/L concentration by day 7. At this point, the average area of fungal growth in the control treatment reached 1321.75 mm², while in the 0.5 g/L treatment it measured 924.14 mm² (30.04% inhibition), 667.85 mm² (49.41% inhibition), in the 1.2 g/L treatment, and 289.75 mm² (78.05% inhibition) in the 2.0 g/L treatment. Statistical analysis using analysis of variance and Tukey's test revealed a significant difference in growth area between the control samples and all treatments from day 3 onwards. While no significant difference was observed between effects of the 1.2 g/L and 2.0 g/L concentrations of ZnO NPs until day 6, the distinction became evident by day 7.

The findings presented in this study contribute to and expand upon existing knowledge regarding the antifungal properties of nanoparticles, as evidenced by previous research (Huang et al., 2023; Mosquera-Sánchez et al., 2020). ZnO NPs synthesized through environmentally friendly methods have consistently demonstrated antifungal efficacy in numerous studies discussed in Chapter 2. Although most studies suggest that smaller nanoparticles (< 100 nm) exhibit increased efficacy (Rasha et al., 2021), this experiment yielded nanoparticles with an average size of approximately 239.7 nm, which nonetheless exhibited significant antifungal activity against *Colletotrichum sp.* These synthesised nanoparticles effectively fulfilled the objective of controlling fungal growth, underscoring their utility. However, it is conceivable that smaller-sized nanoparticles and higher concentrations may yield even greater inhibitory effects, as indicated by previous research.

Table 5.1. Photographs of colonies of *Colletotrichum sp.* subjected to different treatments during 7 days incubation: control and ZnO NPs of concentrations 0.5g/L, 1.2g/L and 2.0g/L

Day	Control	0.5g/L	1.2g/L	2g/L
1				

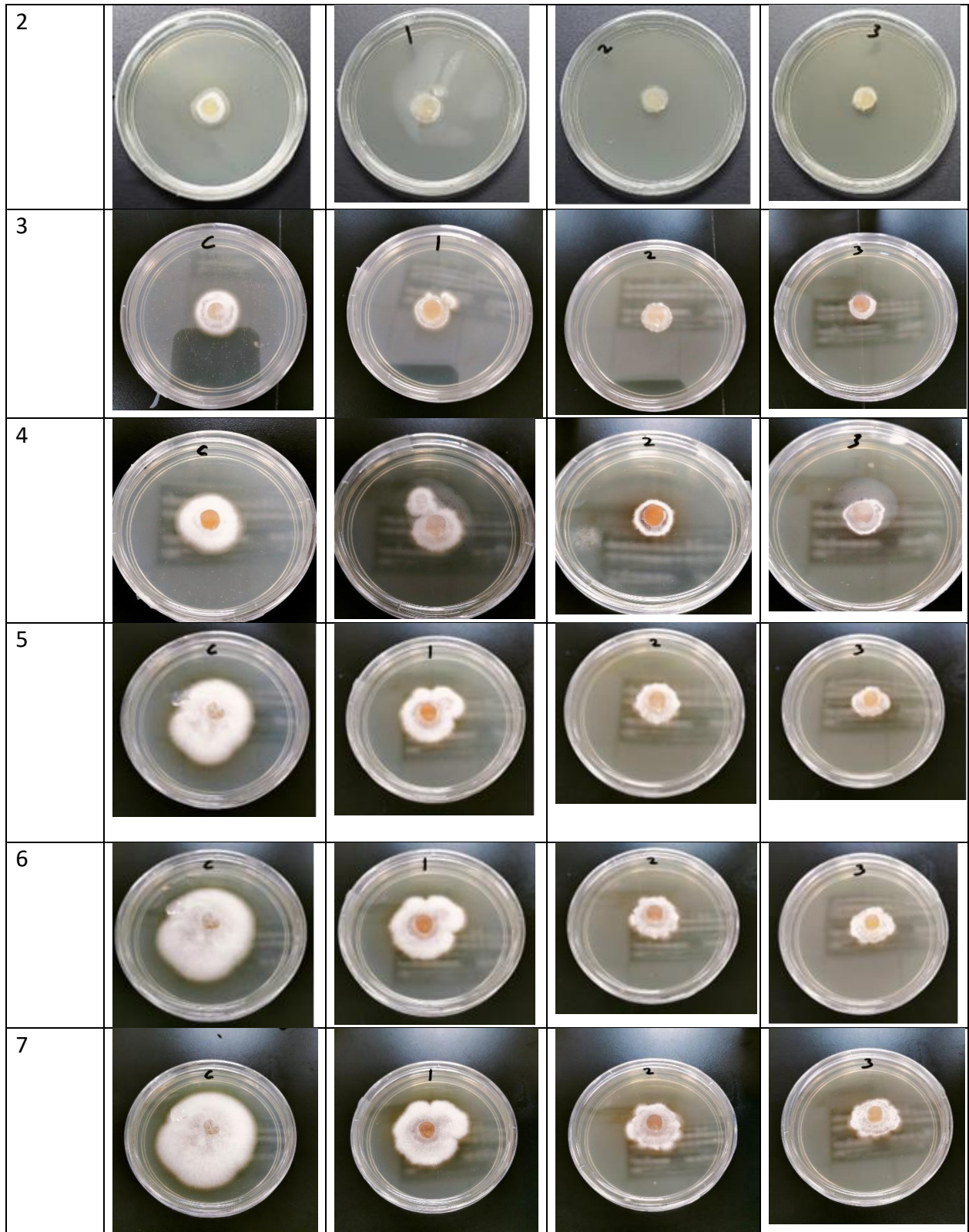


Table 5.2. Average fungal growth area (and standard deviations) of *Colletotrichum* sp. and percentage inhibition relative to the control across three treatments over the seven-day measurement period. Values in the same column with different letters are significantly different, ($p < 0.05$).

Day	Control	0.5g/L	1.2g/L	2.0g/L
1	3.1	3.1	3.1	3.1
2	37.83 ± 6.68 ^{ab}	21.42± 6.68 ^{bc}	17.64± 6.68 ^c	15.95± 6.68 ^c
3	175.13 ± 12.36 ^a	54.42±12.36 ^b	18.45±12.36 ^c	18.07±12.36 ^c
4	383.98 ±46.19 ^a	169.74 ±46.19 ^b	60.18 ±46.19 ^b	41.08 ±46.19 ^b
5	700.74±82.08 ^a	345.24±82.08 ^b	99.79±82.08 ^c	81.36±82.08 ^c
6	984.21±77.75 ^a	492.09±77.75 ^b	246.02±77.75 ^c	180.87±77.75 ^c
7	1321.75±121.21 ^a	924.14±121.21 ^b	667.85±121.21 ^b	289.75±121.21 ^c

5.4.3 In vivo antifungal effect of Chitosan-ZnO NPs coating to control anthracnose disease in papayas.

In vivo experiments involving various treatments applied to papaya revealed significant findings. In the control group, 50% of papaya samples exhibited disease incidence by day 5, which increased to 100% by day 6 (Figure 5.6). Conversely, papayas subjected to different treatments demonstrated reduced disease incidence. Papayas treated solely with 0.5% chitosan exhibited a disease incidence of 42% by day 6, which increased to 83% by day 7, with all samples manifesting disease incidence from day 8 onwards. Treatment combining chitosan with varying concentrations of ZnO NPs showed further reductions in disease incidence. Notably, the treatment containing 0.5 g/L ZnO NPs exhibited disease incidence post day 6, similar to the chitosan-only treatment. By day 6, the disease incidence was 50%, with all papayas exhibiting symptoms after day 8. In contrast, the treatment containing 1.5 g/L ZnO NPs showed no disease incidence until day 6, increasing to 42% by day 7, and reaching 100% by day 8. Moreover, the 2.5g/L ZnO NPs treatment displayed 100% disease incidence only after day 10. Hence, in comparison to chitosan only coatings, the integration of 2.5g/L ZnO NPs with chitosan reduced the disease percentage of papaya by 63%. These findings underscore the efficacy of incorporating ZnO NPs into chitosan treatments, delaying the onset of disease symptoms when stored at room temperature.

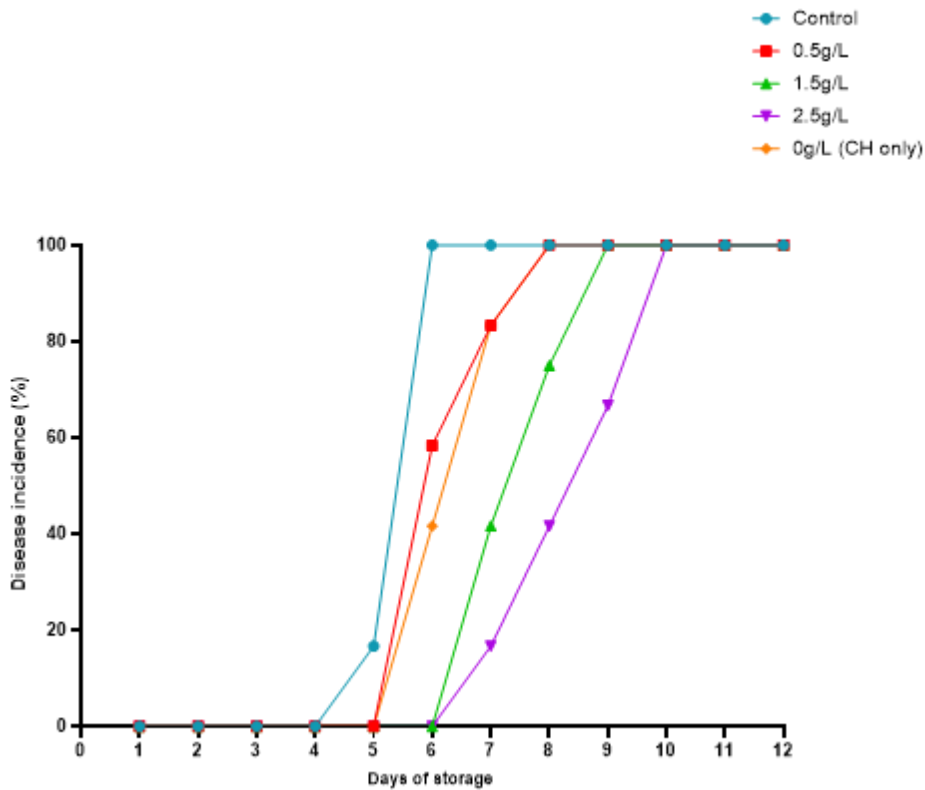


Figure 5.6: Effect of different concentrations of chitosan-ZnO NPs on disease incidence in inoculated Sekaki papaya fruits after storage for 12 days.

Disease severity measurements also showed consistent trends in the management of anthracnose disease in papaya fruits (Figure 5.7 and Table 5.3). While all papayas in the treatment groups exhibited disease incidence by the end of the storage period, there were significant differences in symptom severity among treatments. Analysis of variance and Tukey's test indicated that, initially, when symptoms began to appear on day 7, no significant differences were observed between the control and treatment groups. However, on days 8 and 9, treatments with 2.5 g/L ZnO NPs significantly reduced disease severity compared to the other treatments. By day 10, treatments with 1.5 g/L and 2.5 g/L ZnO NPs exhibited a significant decrease in disease severity. By the end of day 12, all treatments displayed a significant reduction in symptoms compared with the control. The disease severity was reduced by approximately 36.5% when chitosan was combined with 2.5 g/L of ZnO nanoparticles compared to using chitosan alone. This suggests that adding ZnO NPs to chitosan solutions can significantly reduce the symptoms of anthracnose disease in papayas. Photographs of the papaya samples from day 8, when significant differences were evident, are shown in Table 5.4.

Table 5.3. Disease severity average for each treatment group recorded for tested papayas over the storage of 12 days.

Day	Control	0.5g/L	1.5g/L	2.5g/L	0g/L (CH only)
1	1.00	1.00	1.00	1.00	1.00
2	1.00	1.00	1.00	1.00	1.00
3	1.00	1.00	1.00	1.00	1.00
4	1.00	1.00	1.00	1.00	1.00
5	2.17 ± 0.28 ^a	1.00±0.28 ^b	1.00 ±0.28 ^b	1.00 ± 0.28 ^b	1.00 ± 0.28 ^b
6	2.00 ± 0.27 ^a	1.58± 0.27 ^b	1.00 ± 0.27 ^c	1.00 ± 0.27 ^c	1.58± 0.27 ^b
7	2.00 ±0.26 ^a	1.83± 0.26 ^a	1.42±0.26 ^a	1.17±0.26 ^a	1.83±0.26 ^a
8	2.67 ± 0.34 ^a	2.58± 0.34 ^a	1.75± 0.34 ^{ab}	1.42±0.34 ^b	2.25± 0.34 ^{ab}
9	3.25 ± 0.39 ^a	2.75± 0.39 ^{ab}	2.33± 0.39 ^{ab}	1.67± 0.39 ^b	3.33± 0.39 ^a
10	3.67 ± 0.32 ^a	2.92± 0.32 ^{ab}	2.92± 0.32 ^b	2.17± 0.32 ^c	3.42± 0.32 ^{ab}
11	4.33± 0.35 ^a	3.17± 0.35 ^{bc}	2.42± 0.35 ^{bc}	2.17± 0.35 ^c	3.50± 0.35 ^{ab}
12	4.83± 0.42 ^a	3.25± 0.42 ^b	3.25± 0.42 ^b	2.33± 0.42 ^b	3.67± 0.42 ^{ab}

Table notes: CH- Chitosan

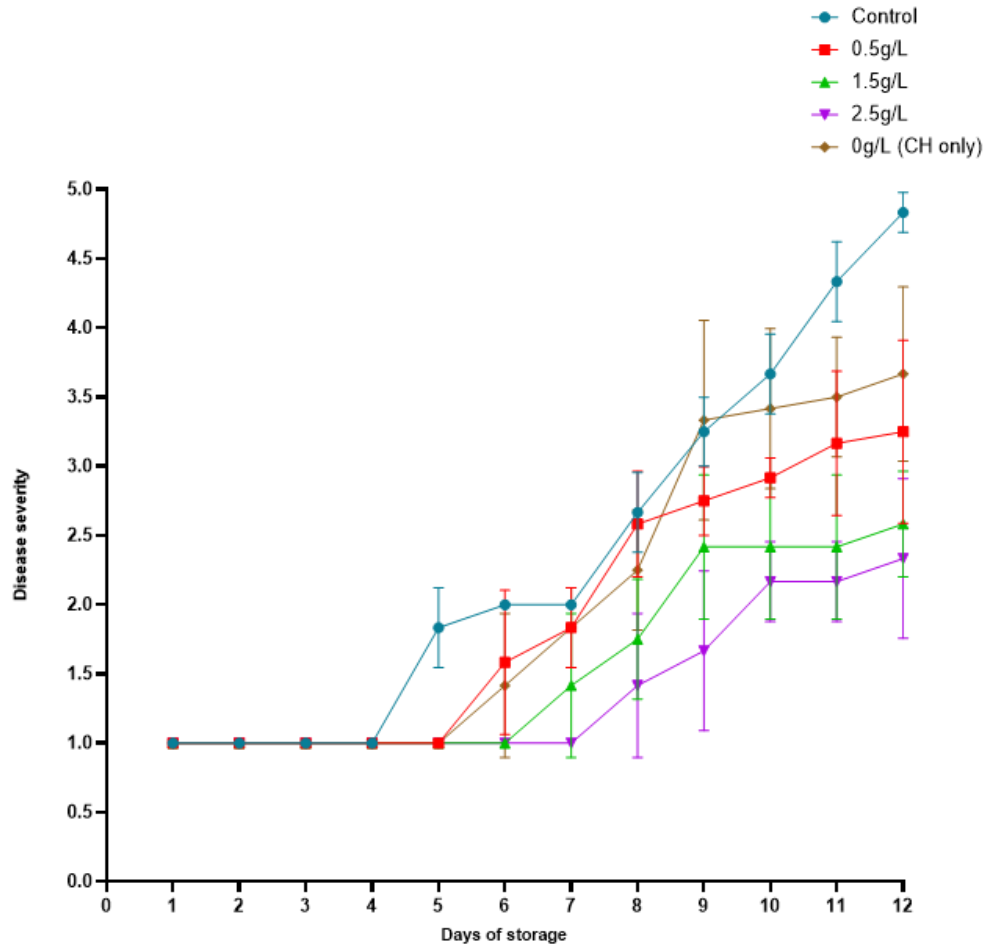






















Figure 5.7: Effect of different concentrations of chitosan-ZnO NPs on disease severity of inoculated Sekaki papaya fruits after storage for 12 d at room temperature. Vertical bars represent standard errors of the mean.

Table 5.4: Photographs of papaya samples showing significant differences in disease symptoms under different concentrations of ZnO NPs-0.5g/L, 1.5g/L, 2g/L, 0g/L (Chitosan only) and control, from 8 to 12th day of storage.

Day	Control	0.5g/L	1.5g/L	2.5g/L	0g/L
8					
9					
10					
11					



5.5 Chapter conclusion

This study highlighted the efficacy of chitosan-ZnO NPs in both in vitro and in vivo management of anthracnose in harvested papaya fruits. In vitro experiments revealed a dose-dependent increase in fungal growth inhibition with higher concentrations of ZnO NPs, whereas in vivo assessments demonstrated a corresponding decrease in disease incidence and severity with increasing ZnO NPs concentration. Notably, there is no published literature on the application of chitosan-ZnO NPs as a coating for freshly harvested whole papayas, although one study conducted on cut papayas explored the use of chitosan solutions mixed with varying concentrations of ZnO NPs (Lavinia et al., 2019). In that experiment, ZnO NPs exhibited antibacterial properties during storage at 10°C, with the highest concentration (0.027% w/v) effectively suppressing bacterial growth, thereby maintaining microbial counts below the safe consumption threshold. This study corroborates these findings and demonstrates similar microbial inhibition in whole uncut papayas. Additionally, this research aimed to develop a cost-effective and environmentally friendly coating for papayas to effectively combat one of the primary postharvest diseases. Using the eco-friendly biopolymer chitosan combined with ZnO nanoparticles synthesized from pandan leaves offers a low-cost, sustainable treatment solution. This approach minimizes the need for extensive use of laboratory chemicals, supporting a non-toxic and environmentally friendly method. This study paves the way for future research exploring different papaya cultivars and various postharvest fungal infections. Ultimately, such interventions hold promise for implementation in developing countries as viable and cost-effective solutions to mitigate food loss in the postharvest chain.

Limitations and Future Directions

The integration of EN technology into fruit quality control protocols offers a cost-effective and efficient alternative for the early detection of post-harvest diseases, potentially reducing reliance on labour-intensive and time-consuming methods. Similar to papaya, every other horticultural crop has wide varieties of cultivar, each might have their own unique biomarker. To offer a more precise assessment of EN's applicability, it is crucial to conduct field-based enquiries with a larger and more diverse sample size encompassing various fruit varieties collected from different geographical locations. Such an approach would facilitate continuous monitoring of volatile alterations in fresh produce across papaya farms and storage facilities. Further exploration at the genomic and proteomic levels is required to elucidate the precise role of volatile compounds in papaya ripening. Nonetheless, the results of this study underscore the potential of EN as a valuable asset for fruit quality control, emphasising the importance of integrating smart technologies into food production processes to meet the rising demand for high-quality food. Moreover, to further validate the accuracy and efficiency of CBR, future work should also explore comparisons with other well-established statistical models such as PCA, LDA, and SVM. These methods are widely used in classification tasks and can provide valuable benchmarks for evaluating CBR's performance. Comparing CBR with these models will allow researchers to confirm its ability to accurately classify diseases while ensuring that the system remains efficient for real-world applications in agriculture.

Conducting in-field assessments of EN technology presents an opportunity to evaluate its practicality and economic viability for farm usage, considering factors such as installation costs, user training, accuracy, time, and financial returns. Given papaya's significance as an affordable nutrient source in many developing countries and its susceptibility to severe postharvest losses, exploring novel technologies is imperative to achieve the United Nations Sustainable Development Goals (SDGs), such as Zero Hunger (SDG 1), Zero Poverty (SDG 2), and Sustainable Production and Consumption (SDG 12). If the results are promising, innovative technology can significantly enhance food security and promote sustainable agricultural practices in these regions.

Early detection enables timely intervention to control the spread of fruit diseases, thus prompting a third experiment focusing on the preparation of edible coatings using eco-friendly synthesised ZnO NPs incorporated into chitosan to offer a cost-effective solution. In this study, the application of chitosan-ZnO NP coatings to papaya was investigated. Results from storage experiments demonstrated that coated fruits exhibited a delayed onset of anthracnose disease and reduced disease severity compared to non-coated fruits. While several techniques exist to

prevent and control fungal infections in papayas, including hot water treatment, sanitiser washing, and chitosan and organic acid-based edible coatings, this study sheds light on the potential effectiveness of the chitosan-ZnO NP coating technique for papayas and possibly other perishable products. To gain comprehensive insights into the efficacy and applicability of nanoparticle-based coatings, further research should investigate various coating methods (e.g., spraying) across diverse papaya varieties and varying storage temperatures. Additionally, comparing these nanoparticle-based coatings to conventional chemical fungicides commonly used for postharvest disease control, such as Prochloraz, Thiabendazole (TBZ), Benomyl, and Imazalil, will help determine their effectiveness and safety in delaying disease onset relative to traditional treatments.

Conclusion

This study aimed to enhance postharvest management of papayas by using EN technology for early detection of ripening stages and fungal diseases, and by developing a sustainable anthracnose control method with green-synthesised ZnO nanoparticles in a chitosan coating.

This study demonstrated EN's effectiveness of EN in distinguishing ripening stages in Sekaki papaya by detecting changes in aroma profiles. CBR analysis showed notable differences in VOCs between days: 84.25% similarity between day 1 and day 3 samples, 82.81% between day 1 and day 5, and 94.19% between day 3 and day 5, all below the 98% threshold, indicating significant differences. This confirms EN's potential of EN for non-destructive monitoring of ripeness in papayas.

EN also proved effective in identifying early stage fungal diseases in papayas, reliably distinguishing volatile profiles of inoculated samples from controls over five days. For instance, CG-infected papayas showed 94.36% similarity between days 1 and 3, and 91.58% similarity between days 1 and 5, reflecting the progression of infection. Additionally, EN differentiated between fungal types. On day 1, CG-infected papayas had 94.27% similarity to FS-infected samples and 91.70% similarity to BC, with further distinctions by day 5, where BC exhibited the most distinct profile. The results confirm EN's potential of EN for identifying various fungal infections at both early and advanced stages. Moreover, by day 5, healthy and infected papayas showed increasing divergence, with CG, FS, and BC infections showing decreasing similarity to healthy controls.

Finally, an eco-friendly coating of 0.5% chitosan with green-synthesised ZnO NPs from pandan leaf extract, achieving a nanoparticle size of 239.7 nm, was effective in controlling anthracnose. Papayas treated with 2.5 g/L ZnO NPs saw a 63% reduction in disease incidence and a 36.5% reduction in severity compared to chitosan alone, highlighting the impact of the coating on delaying disease onset and progression.

In summation, EN technology, paired with an eco-friendly ZnO-chitosan coating, shows great promise for extending papaya shelf life and reducing postharvest losses.

List of Publications

1. Ali, A., Mansol, A.S., **Ayesha Ashraf Khan**, Kasturi Muthoosamy, and Siddiqui, Y. (2023). *Electronic nose as a tool for early detection of diseases and quality monitoring in fresh postharvest produce: A comprehensive review*. Comprehensive Reviews in Food Science and Food Safety. <https://doi.org/10.1111/1541-4337.13151>.
2. **Ayesha Ashraf Khan**, Yasmeen Siddiqui, Tan Guang Heng, and Asgar Ali. (2024). *Application of Electronic Nose to monitor the quality and ripening stages of papaya during postharvest storage*. ACS Food Science & Technology. <https://doi.org/10.1021/acsfoodscitech.4c00140>.

References

- Adak, M.F. and Yumusak, N. (2016) 'Classification of E-nose aroma data of four fruit types by ABC-based neural network', *Sensors*, 16(3), p. 304. <https://doi.org/10.3390/s16030304>
- Adedeji, A.A., Ekramirad, N., Rady, A., Hamidisepehr, A., Donohue, K.D., Villanueva, R.T. and Li, M. (2020) 'Non-destructive technologies for detecting insect infestation in fruit and vegetables under postharvest conditions: a critical review', *Foods*, 9(7), p. 927. <https://doi.org/10.3390/foods9070927>
- Agarwal, H., Kumar, S.V. and Rajeshkumar, S. (2017) 'A review on green synthesis of zinc oxide nanoparticles – an eco-friendly approach', *Resource-Efficient Technologies*, 3(4), pp. 406–413. <https://doi.org/10.1016/j.reffit.2017.03.002>
- Aghilinategh, N., Dalvand, M.J. and Anvar, A. (2020) 'Detection of ripeness grades of berries using an electronic nose', *Food Science & Nutrition*, 8(9), pp. 4919-4928. <https://doi.org/10.1002/fsn3.1788>
- A. Harikrishnan, Ramalingam, B., Nadeem, A., Ramachandran, B., Veena, V.K. and Muthupandian, S. (2023) 'Eco-friendly synthesis of zinc oxide nanoparticles (ZnO NPs) from *Piper betel* leaf extract: spectral characterization and its application on plant growth parameters in maize, fenugreek and red gram', *Materials Technology*, 39(1). <https://doi.org/10.1080/10667857.2023.2298547>
- Akhir, R., Umbaidillah, S.Z., Abdullah, N.A., Alrokayan, S.A.H., Khan, H.A., Soga, T., Rusop, M. and Khusaimi, Z., 2020. The Potential of *Pandanus amaryllifolius* Leaves Extract in Fabrication of Dense and Uniform ZnO Microrods. *Micromachines*, 11(3), p.299. <https://doi.org/10.3390/mi11030299>
- Alamdari, S., Mirzaee, O., Nasiri, F., Tafreshi, M.J., Sasani Ghamsari, M., Salmani Shik, S., Majles Ara, M.H., Lee, K.-Y. and Park, H.H., 2022. Green synthesis of multifunctional ZnO/chitosan nanocomposite film using wild *Mentha pulegium* extract for packaging applications. *Surfaces and Interfaces*, 34, p.102349. doi: <https://doi.org/10.1016/j.surfin.2022.102349>.

Al-Darwesh, M.Y., Ibrahim, S.S. and Mohammed, M.A. (2024) 'A review on plant extract mediated green synthesis of zinc oxide nanoparticles and their biomedical applications', *Results in Chemistry*, pp. 101368–101368. <https://doi.org/10.1016/j.rechem.2024.101368>.

Aldalbahi, A., Alterary, S., Ali Abdullrahman Almoghim, R., Awad, M.A., Aldosari, N.S., Fahad Alghannam, S., Nasser Alabdan, A., Alharbi, S., Ali Mohammed Alateeq, B., Abdulrahman Al Mohsen, A., Alkathiri, M.A. and Abdulrahman Alrashed, R. (2020). Greener Synthesis of Zinc Oxide Nanoparticles: Characterization and Multifaceted Applications. *Molecules*, 25(18), p.4198. [doi:https://doi.org/10.3390/molecules25184198](https://doi.org/10.3390/molecules25184198).

Al-Naamani, L., Dobretsov, S. and Dutta, J. (2016) 'Chitosan-zinc oxide nanoparticle composite coating for active food packaging applications', *Innovative Food Science & Emerging Technologies*, 38, pp. 231–237. <https://doi.org/10.1016/j.ifset.2016.10.010>

Ali, A., Mansol, A.S., Khan, A.A., Muthoosamy, K. and Siddiqui, Y. (2023) 'Electronic nose as a tool for early detection of diseases and quality monitoring in fresh postharvest produce: a comprehensive review', *Comprehensive Reviews in Food Science and Food Safety*. <https://doi.org/10.1111/1541-4337.13151>

Ali, M.M., Hashim, N., Abd Aziz, S. and Lasekan, O. (2020) 'Principles and recent advances in electronic nose for quality inspection of agricultural and food products', *Trends in Food Science & Technology*, 99, pp. 1-10. <https://doi.org/10.1016/j.tifs.2020.02.028>

Ali, M.M., Hashim, N., Abd Aziz, S. and Lasekan, O. (2020) 'An overview of non-destructive approaches for quality determination in pineapples', *Journal of Agricultural and Food Engineering*, 1, p. 0011. <http://dx.doi.org/10.37865/jafe.2020.0011>

Ali, A., Noh, N.M. and Mustafa, M.A. (2015) 'Antimicrobial activity of chitosan enriched with lemongrass oil against anthracnose of bell pepper', *Food Packaging and Shelf Life*, 3, pp. 56–61. <https://doi.org/10.1016/j.fpsl.2014.10.003>

Ali, M.M., Bachik, N.A., Muhadi, N.A.T., Yusof, T.N.T. and Gomes, C. (2019) 'Non-destructive techniques of detecting plant diseases: A review', *Physiological and Molecular Plant Pathology*, 108, p. 101426. <https://doi.org/10.1016/j.pmpp.2019.101426>

Anasontzis, G.E. and Christakopoulos, P. (2014) 'Challenges in ethanol production with *Fusarium oxysporum* through consolidated bioprocessing', *Bioengineered*, 5, pp. 393–395.

Aranaz, I., Alcántara, A.R., Civera, M.C., Arias, C., Elorza, B., Heras Caballero, A. and Acosta, N. (2021) 'Chitosan: an overview of its properties and applications', *Polymers*, 13(19), p. 3256. <https://doi.org/10.3390/polym13193256>

Arroyo, B.J., Bezerra, A.C., Oliveira, L.L., Arroyo, S.J., Melo, E.A. and Santos, A.M.P. (2020) 'Antimicrobial active edible coating of alginate and chitosan add ZnO nanoparticles applied in guavas (*Psidium guajava* L.)', *Food Chemistry*, 309, p. 125566. <https://doi.org/10.1016/j.foodchem.2019.125566>

Arthur, M.H.R., Lucas, C.G., Domingues, W.B., Silveira, T., Paschoal, J.D., Jornada, D.S., Corcine, C.D., Varela, A.S., Prado, W.A., Campos, V.F., Seixas, F.K., Guterres, S.S., Pohlmann, A.R. and Collares, T. (2017) 'Effects of chitosan-coated lipid-core nanocapsules on bovine sperm cells', *Toxicology in Vitro*, 40, pp. 214–222. <https://doi.org/10.1016/j.tiv.2017.01.017>

Azabou, S., Abid, Y., Sebi, H., Felfoul, I., Gargouri, A. and Attia, H. (2016) 'Potential of solid-state fermentation of tomato byproducts by *Fusarium solani* pisi for the enzymatic extraction of lycopene', *LWT - Food Science and Technology*, 68, pp. 280-287.

Badii, K. B., Billah, M. K., Afreh-Nuamah, K., Obeng-Ofori, D. & Nyarko, G. (2015). Review of the pest status, economic impact and management of fruit-infesting flies (Diptera: Tephritidae) in Africa. *African Journal of Agricultural Research*, 10, pp. 1488–1498. <http://dx.doi.org/10.5897/AJAR2014.9278>.

Baietto, M. & Wilson, A. D. (2015). Electronic-nose applications for fruit identification, ripeness and quality grading. *Sensors*, 15(1), pp. 899-931. <https://doi.org/10.3390/s150100899>.

Bajaj, K., Adhikary, T., Gill, P.P.S. & Kumar, A. (2023). Edible coatings enriched with plant-based extracts preserve postharvest quality of fruits: A review. *Progress in Organic Coatings*, 182, p.107669. doi:<https://doi.org/10.1016/j.porgcoat.2023.107669>.

Bandeira, M., Giovanela, M., Roesch-Ely, M., Devine, D.M. & da Silva Crespo, J. (2020). Green synthesis of zinc oxide nanoparticles: A review of the synthesis methodology and mechanism of formation. *Sustainable Chemistry and Pharmacy*, 15, p.100223. doi:<https://doi.org/10.1016/j.scp.2020.100223>.

Bano, A., Gupta, A., Prusty, M.R. & Kumar, M. (2023). Elicitation of fruit fungi infection and its protective response to improve the postharvest quality of fruits. *Stresses*, 3(1), pp.231–255. doi:<https://doi.org/10.3390/stresses3010018>.

Barragán-Iglesias, J., Méndez-Lagunas, L.L. & Rodríguez-Ramírez, J. (2018). Ripeness indexes and physicochemical changes of papaya (*Carica papaya* L. cv. Maradol) during ripening on-tree. *Scientia Horticulturae*, 236, pp. 272–278. doi:<https://doi.org/10.1016/j.scienta.2017.12.012>.

Basumatary, I.B., Mukherjee, A., Katiyar, V., Kumar, S. & Dutta, J. (2021). Chitosan-based antimicrobial coating for improving postharvest shelf life of pineapple. *Coatings*, 11(11), p.1366. doi:<https://doi.org/10.3390/coatings11111366>.

Bianchi, G., Falcinelli, B., Tosti, G., Bocci, L. & Benincasa, P. (2019). Taste quality traits and volatile profiles of sprouts and wheatgrass from hulled and non-hulled *Triticum* species. *Journal of Food Biochemistry*, 43(7), e12869. <https://doi.org/10.1111/jfbc.12869>.

Blancas-Benitez, F.J., Montañó-Leyva, B., Aguirre-Güitrón, L., Moreno-Hernández, C.L., Fonseca-Cantabrana, Á., Romero-Islas, L. del C. & González-Estrada, R.R. (2022). Impact of edible coatings on quality of fruits: A review. *Food Control*, 139, p.109063. doi:<https://doi.org/10.1016/j.foodcont.2022.109063>.

Boro, B., Boruah, J.S., Devi, C., Alemtoshi, Gogoi, B., Bharali, P., Reddy, P.V.B., Chowdhury, D. & Kalita, P. (2024). A novel route to fabricate ZnO nanoparticles using *Xanthium indicum* ethanolic leaf extract: Green nanosynthesis perspective towards photocatalytic and biological applications. *Journal of Molecular Structure*, 1300, p.137227. doi:<https://doi.org/10.1016/j.molstruc.2023.137227>.

Bouttier-Figueroa, D.C., Cortez-Valadez, M., Flores-Acosta, M. and Robles-Zepeda, R.E. (2024). Green Synthesis of Zinc Oxide Nanoparticles Using Plant Extracts and Their Antimicrobial Activity. *BioNanoScience*, 14(3), pp.3385–3400. doi:<https://doi.org/10.1007/s12668-024-01471-4>.

Brilli, F., Loreto, F. & Baccelli, I. (2019). Exploiting plant volatile organic compounds (VOCs) in agriculture to improve sustainable defense strategies and productivity of crops. *Frontiers in Plant Science*, 10, p.264.

Bruno, T. J. & Harries, M. E. (2019). Headspace analysis: Purge and trap. National Institute of Standard and Technology (NIST), pp. 379-384. <https://doi.org/10.3389/fpls.2019.00264>.

Bueno, M., Resconi, V. C., Campo, M. M., Ferreira, V. & Escudero, A. (2019). Development of a robust HS-SPME-GC-MS method for the analysis of solid food samples: Analysis of volatile

compounds in fresh raw beef of differing lipid oxidation degrees. *Food Chemistry*, 281, pp. 49-56. <https://doi.org/10.1016/j.foodchem.2018.12.082>.

Cellini, A., Blasioli, S., Biondi, E., Bertaccini, A., Braschi, I. & Spinelli, F. (2017). Potential applications and limitations of electronic nose devices for plant disease diagnosis. *Sensors*, 17(11), p.2596. <https://doi.org/10.3390/s17112596>.

Cellini, A., Spinelli, F., Donati, I., Ryu, C.M. & Kloepper, J.W. (2021). Bacterial volatile compound-based tools for crop management and quality. *Trends in Plant Science*, 26(9), pp.968-983. <https://doi.org/10.1016/j.tplants.2021.05.006>.

Chan-León, A.C., Estrella-Maldonado, H., Fuentes-Ortiz, G., Torres, L., Peraza Sánchez, S. & Santamaría, J.M. (2023). Ethylene-driven expression of genes involved in carotenoid biosynthesis during postharvest ripening is different in creole and commercial *Carica papaya* L. fruits. *Horticulture, Environment, and Biotechnology*. doi:<https://doi.org/10.1007/s13580-023-00568-1>.

Chauhan, R., Kumar, A., Tripathi, R. & Kumar, A. (2022). Advancing of zinc oxide nanoparticles for cosmetic applications. *Handbook of Consumer Nanoproducts*, pp.1057–1072. doi:https://doi.org/10.1007/978-981-16-8698-6_100.

Chawla, R., Sivakumar, S. & Kaur, H. (2021a). Antimicrobial edible films in food packaging: Current scenario and recent nanotechnological advancements—a review. *Carbohydrate Polymer Technologies and Applications*, 2, p.100024. doi:<https://doi.org/10.1016/j.carpta.2020.100024>.

Chawla, R., Sivakumar, S. & Kaur, H. (2021b). Antimicrobial edible films in food packaging: Current scenario and recent nanotechnological advancements—a review. *Carbohydrate Polymer Technologies and Applications*, 2, p.100024. doi:<https://doi.org/10.1016/j.carpta.2020.100024>.

Chen, H.Z., Zhang, M. & Guo, Z. (2019). Discrimination of fresh-cut broccoli freshness by volatiles using electronic nose and gas chromatography-mass spectrometry. *Postharvest Biology and Technology*, 148, pp.168-175. <https://doi.org/10.1016/j.postharvbio.2018.10.019>.

Chen, H.Z., Zhang, M., Bhandari, B. & Guo, Z. (2018). Evaluation of the freshness of fresh-cut green bell pepper (*Capsicum annuum* var. *grossum*) using electronic nose. *LWT*, 87, pp.77-84. <https://doi.org/10.1016/j.lwt.2017.08.052>.

Chen, L.Y., Wong, D.M., Fang, C.Y., Chiu, C.I., Chou, T.I., Wu, C.C., Chiu, S.W. & Tang, K.T. (2018). Development of an electronic-nose system for fruit maturity and quality monitoring. In *2018 IEEE International Conference on Applied System Invention (ICASI)* (pp. 1129-1130). IEEE. <https://doi.org/10.1109/ICASI.2018.8394481>.

Chilo, J., Pelegri-Sebastia, J., Cupane, M. & Sogorb, T. (2016). E-nose application to food industry production. *IEEE Instrumentation & Measurement Magazine*, 19(1), pp.27–33. doi:<https://doi.org/10.1109/mim.2016.7384957>.

Cissé, M., Polidori, J., Montet, D., Loiseau, G. & Ducamp-Collin, M.N. (2015). Preservation of mango quality by using functional chitosan-lactoperoxidase systems coatings. *Postharvest Biology and Technology*, 101, pp.10–14. doi:<https://doi.org/10.1016/j.postharvbio.2014.11.003>.

Cui, S., Ling, P., Zhu, H. & Keener, H.M. (2018). Plant pest detection using an artificial nose system: A review. *Sensors*, 18(2), p.378. <https://doi.org/10.3390/s18020378>.

da Silva Ferreira, M.V., de Moraes, I.A., Passos, R.V.L., Barbin, D.F. & Barbosa, J.L. (2023). Determination of pitaya quality using portable NIR spectroscopy and innovative low-cost electronic nose. *Scientia Horticulturae*, 310, p.111784. <https://doi.org/10.1016/j.scienta.2022.111784>.

Da Silva Vale, A., Balla, G., Rodrigues, L.R.S., De Carvalho Neto, D.P., Soccol, C.R. & De Melo Pereira, G.V. (2022). Understanding the effects of self-induced anaerobic fermentation on coffee beans quality: Microbiological, metabolic, and sensory studies. *Foods*, 12, p.37.

Daniel, A.I., Keyster, M. & Klein, A. (2023). Biogenic zinc oxide nanoparticles: A viable agricultural tool to control plant pathogenic fungi and its potential effects on soil and plants. *Science of The Total Environment*, 897, p.165483. doi:<https://doi.org/10.1016/j.scitotenv.2023.165483>.

Daud, S.M., Najib, M.S., Zahed, N., Jusof, M.H.M., Jusoh, M.F.C. & Hassim, M.I.I.N. (2018). Classification of lubricant oil adulteration level using case-based reasoning. *Journal of Fundamental and Applied Sciences*, 9(4S), p.256. doi:<https://doi.org/10.4314/jfas.v9i4s.15>.

Dawood Bin Fazal & Ahmad, I. (2024). A critical analysis of extracts of okra seeds and amla offering green chemistry for synthesis of zinc oxide nanoparticles and their promising role in reducing crude oil viscosity. *Materials Today Communications*, pp.108172–108172. doi:<https://doi.org/10.1016/j.mtcomm.2024.108172>.

Dong, W., Hu, R., Long, Y., Li, H., Zhang, Y., Zhu, K. & Chu, Z. (2019). Comparative evaluation of the volatile profiles and taste properties of roasted coffee beans as affected by drying method and detected by electronic nose, electronic tongue, and HS-SPME-GC-MS. *Food Chemistry*, 272, pp.723-731. <https://doi.org/10.1016/j.foodchem.2018.08.068>.

Dukare, A.S., Paul, S., Nambi, V.E., Gupta, R.K., Singh, R., Sharma, K. & Vishwakarma, R.K. (2019). Exploitation of microbial antagonists for the control of postharvest diseases of fruit: A review. *Critical Reviews in Food Science and Nutrition*, 59(9), pp.1498-1513. <https://doi.org/10.1080/10408398.2017.1417235>.

Gong, D., Bi, Y., Zong, Y., Li, Y., Sionov, E. & Prusky, D. (2022). Characterization and sources of volatile organic compounds produced by postharvest pathogenic fungi colonized fruit. *Postharvest Biology and Technology*, 188, p.111903. doi:<https://doi.org/10.1016/j.postharvbio.2022.111903>.

Elik, A., Yanik, D.K., Istanbulu, Y., Guzelsoy, N.A., Yavuz, A. & Gogus, F. (2019). Strategies to reduce postharvest losses for fruit and vegetables. *Strategies*, 5(3), pp.29-39. <http://dx.doi.org/10.7176/JSTR/5-3-04>.

Elshafie, H.S., Osman, A., El-Saber, M.M., Ippolito, C., Camele, I. & Abbas, E. (2023). Antifungal activity of green and chemically synthesized ZnO nanoparticles against *Alternaria citri*, the causal agent of citrus black rot. *Plant Pathology Journal (Suwon)*, 39(3), pp.265–274. doi:<https://doi.org/10.5423/ppj.oa.02.2023.0035>.

Establés-Ortiz, B., Romero, P., Ballester, A.R., González-Candelas, L. & Lafuente, M.T. (2016). Inhibiting ethylene perception with 1-methylcyclopropene triggers molecular responses aimed to cope with cell toxicity and increased respiration in citrus fruits. *Plant Physiology and Biochemistry*, 103, pp.154–166. doi:<https://doi.org/10.1016/j.plaphy.2016.02.036>.

FAO (2022). Tropical fruits | FAO | Food and Agriculture Organization of the United Nations. Available at: <https://www.fao.org/markets-and-trade/commodities/tropical-fruits/en/>.

FDA (2019). Guidelines for the Validation of Chemical Methods in Food, Feed, Cosmetics, and Veterinary Products. *Guidelines for the Validation of Chemical Methods in Food, Feed, Cosmetics, and Veterinary Products*, 23. Retrieved from <https://fda.report/media/121751/ValidationNucleicAcidSequenceBasedAnalysisFoodFeedCosmeticsVeterinary.pdf>.

Fabi, J.P. & do Prado, S.B.R. (2019). Fast and furious: Ethylene-triggered changes in the metabolism of papaya fruit during ripening. *Frontiers in Plant Science*, 10, p.535.

doi:<https://doi.org/10.3389/fpls.2019.00535>.

Fakhar-e-Alam, M., Amjad, I., Saadullah, M., Tahir, M., Jawad, M., Asif, M., Atif, M., Zara, S. and Rashad, M., 2024. Antitumor activity of Zinc oxide nanoparticles fused with Green Extract of *Nigella sativa*. *Journal of Saudi Chemical Society*, 28(2), pp.101814–101814.

<https://doi.org/10.1016/j.jscs.2024.101814>

Farhad, G.N., Chen, Z. & Mehdi, M. (2014). Monitoring mango fruit ripening after harvest using electronic nose (zNose™) technique. *International Proceedings of Chemical, Biological and Environmental Engineering (IPCBE)*, 65, pp.36-40.

Feliziani, E. & Romanazzi, G. (2016). Postharvest decay of strawberry fruit: Etiology, epidemiology, and disease management. *Journal of Berry Research*, 6(1), pp.47–63.

doi:10.3233/jbr-150113.

Félix, C., Libório, S., Nunes, M., Félix, R., Duarte, A.S., Alves, A. & Esteves, A.C. (2018). *Lasiodiplodia theobromae* as a producer of biotechnologically relevant enzymes. *International Journal of Molecular Sciences*, 19, p.29.

Forte, A., Zucaro, A., Basosi, R. & Fierro, A. (2016). LCA of 1,4-butanediol produced via direct fermentation of sugars from wheat straw feedstock within a territorial biorefinery. *Materials (Basel)*, 9.

Frank, L.A., Onzi, G.R., Morawski, A.S., Pohlmann, A.R., Guterres, S.S. & Contri, R.V. (2020). Chitosan as a coating material for nanoparticles intended for biomedical applications. *Reactive and Functional Polymers*, 147, p.104459.

doi:<https://doi.org/10.1016/j.reactfunctpolym.2019.104459>.

Gadewar, M., Prashanth, G.K., Babu, M.R., Dileep, M.S., Prashanth, P., Rao, S., Mahadevaswamy, M., Ghosh, M.K., Singh, N., Mandotra, S.K., Chauhan, A., Rustagi, S., Chinnam, S., Ali, B., Ercisli, S. and Orhan, E., 2024. Unlocking Nature's Potential: Green Synthesis of ZnO Nanoparticles and Their Multifaceted Applications - A Concise Overview. *Journal of Saudi Chemical Society*, 28(1), pp.101774–101774. <https://doi.org/10.1016/j.jscs.2023.101774>

Gaggiotti, S., Mascini, M., Pittia, P., Della Pelle, F. and Compagnone, D. (2019). Headspace volatile evaluation of carrot samples—Comparison of GC/MS and AuNPs-hpDNA-based e-nose. *Foods*, 8(8), p.293. <https://doi.org/10.3390/foods8080293>

García-García, D.J., Pérez-Sánchez, G.F., Hernández-Cocoletzi, H., Sánchez-Arzubide, M.G., Luna-Guevara, M.L., Rubio-Rosas, E., Krishnamoorthy, R. and Morán-Raya, C. (2023). Chitosan Coatings Modified with Nanostructured ZnO for the Preservation of Strawberries. *Polymers*, 15(18), p.3772. doi:<https://doi.org/10.3390/polym15183772>

Genva, M., Kenne Kemene, T., Deleu, M., Lins, L. and Fauconnier, M.L. (2019). Is It Possible to Predict the Odor of a Molecule on the Basis of its Structure?. *International Journal of Molecular Sciences*, 20(12), p.3018. <https://doi.org/10.3390/ijms20123018>

Ghasemi-Varnamkhasti, M., Mohammad-Razdaria, A., Yoosefiana, S.H., Izadi, Z. and Rabiei, G. (2019). Selection of an optimized metal oxide semiconductor sensor (MOS) array for freshness characterization of strawberry in polymer packages using response surface method (RSM). *Postharvest Biology and Technology*, 151, pp.53-60. <https://doi.org/10.1016/j.postharvbio.2019.01.016>

Gliszczyńska-Świgło, A. and Chmielewski, J. (2017). Electronic nose as a tool for monitoring the authenticity of food. A review. *Food Analytical Methods*, 10(6), pp.1800-1816. <https://doi.org/10.1007/s12161-016-0739-4>

Gopinath, K., Sarinthip Thanakkasaranee, Seesuriyachan, P. and Rachtanapun, P. (2023). One-pot synthesis of gold nanoparticles using *Pandanus amaryllifolius* leaf extract and their antibacterial, antioxidant, anticancer, and ecotoxicity assessment. *Biocatalysis and Agricultural Biotechnology*, 50, p.102695. doi:<https://doi.org/10.1016/j.bcab.2023.102695>

Guillaume, Qian, X., Yang, Q., Dhanasekaran, S., Ianiri, G., Ballester, A.R., Zhang, X., Castoria, R. and Zhang, H. (2021). Securing fruit production: Opportunities from the elucidation of the molecular mechanisms of postharvest fungal infections. *Comprehensive Reviews in Food Science and Food Safety*, 20(3), pp.2508-2533. doi:<https://doi.org/10.1111/1541-4337.12729>

Hanh Thi Nguyen, Boonyaritthongchai, P., Buanong, M., Supapvanich, S. and Wongs-Aree, C. (2020). Postharvest Hot Water Treatment Followed by Chitosan- and κ -Carrageenan-Based Composite Coating Induces the Disease Resistance and Preserves the Quality in Dragon Fruit (*Hylocereus undatus*). *International Journal of Fruit Science*, 20(sup3), pp.S2030-S2044. doi:<https://doi.org/10.1080/15538362.2020.1851342>

Hariharan, G. and Prasannath, K. (2021). Recent Advances in Molecular Diagnostics of Fungal Plant Pathogens: A Mini Review. *Frontiers in Cellular and Infection Microbiology*, 10. doi:<https://doi.org/10.3389/fcimb.2020.600234>

Hazarika, S., Choudhury, R., Montazer, B., Medhi, S., Goswami, M.P. and Sarma, U. (2020). Detection of citrus tristeza virus in mandarin orange using a custom-developed electronic nose system. *IEEE Transactions on Instrumentation and Measurement*, 69(11), pp.9010-9018.

<https://doi.org/10.1109/TIM.2020.2997064>

Hendrick, Efrizon, Yultrisna, Humaira, Botto-Tobar, M. and Silvia, Y. (2022). E-Nose Application for Detecting Banana Fruit Ripe Levels Using Artificial Neural Network Backpropagation Method. *International Journal of Data Science*, 3(1), pp.11-18. doi:10.18517/ijods.3.1.11-18.2022

Hermida-Montero, L.A., Paraguay-Delgado, F., Cruz, L.F., Carrillo, D., Mtz-Enriquez, A.I. and Pariona, N. (2021). The role of coating and size of ZnO nanoparticles on the antifungal activity against *Raffaelea* species. *Materials Letters*, 301, p.130314.

doi:<https://doi.org/10.1016/j.matlet.2021.130314>

Huang, T., Li, X., Maier, M., O'Brien-Simpson, N.M., Heath, D.E. and O'Connor, A.J. (2023). Using inorganic nanoparticles to fight fungal infections in the antimicrobial resistant era. *Acta Biomaterialia*, 158, pp.56-79. doi:<https://doi.org/10.1016/j.actbio.2023.01.019>

Huang, X., Yu, S., Xu, H., Aheto, J.H., Bonah, E., Ma, M., Wu, M. and Zhang, X. (2019). Rapid and nondestructive detection of freshness quality of postharvest spinaches based on machine vision and electronic nose. *Journal of Food Safety*, 39(6), e12708. <https://doi.org/10.1111/jfs.12708>

Huq, M.A., Islam, A., Ashrafudoulla, M., Rahman, M., Parvez, M.M., Balusamy, S.R., Akter, S. and Rahman, M.S., 2023. Bioactive ZnO Nanoparticles: Biosynthesis, Characterization and Potential Antimicrobial Applications. *Pharmaceutics*, [online] 15(11), pp.2634–2634.

<https://doi.org/10.3390/pharmaceutics15112634>

Ibrahim, H.M. and Zairy, E.M.R.E., 2015. Chitosan as a biomaterial — structure, properties, and electrospun nanofibers. [online] IntechOpen. Available at:

<https://www.intechopen.com/chapters/49246> [Accessed 26 Sep. 2024].

Islam, M.F., Islam, S., Miah, M.A.S., Huq, A.K.O., Saha, A.K., Mou, Z.J., Mondol, M.M.H. and Bhuiyan, M.N.I., 2024. Green synthesis of zinc oxide nanoparticles using *Allium cepa* L. waste peel extracts and its antioxidant and antibacterial activities. *Heliyon*, [online] 10(3), p.e25430. Available at: <https://doi.org/10.1016/j.heliyon.2024.e25430> [Accessed 26 Sep. 2024].

Iqbal, N., Khan, N.A., Ferrante, A., Trivellini, A., Francini, A. and Khan, M.I.R., 2017. Ethylene role in plant growth, development and senescence: interaction with other phytohormones.

Frontiers in Plant Science, 8, p.475. Available at: <https://doi.org/10.3389/fpls.2017.00475> [Accessed 26 Sep. 2024].

Kim, J.Y., Haque, F., Lee, J.H., Park, Y.J., Seo, J.H., Mativenga, M. and Walker, B., 2024. Practical organic electronic noses using semi-permeable polymer membranes. *Applied Materials Today*, 37, pp.102137-102137. Available at: <https://doi.org/10.1016/j.apmt.2024.102137> [Accessed 26 Sep. 2024].

Jafarzadeh, S., Mohammadi Nafchi, A., Salehabadi, A., Oladzad-abbasabadi, N. and Jafari, S.M., 2021. Application of bio-nanocomposite films and edible coatings for extending the shelf life of fresh fruits and vegetables. *Advances in Colloid and Interface Science*, 291, p.102405. Available at: <https://doi.org/10.1016/j.cis.2021.102405> [Accessed 26 Sep. 2024].

Jamdagni, P., Khatri, P. and Rana, J.S., 2018. Green synthesis of zinc oxide nanoparticles using flower extract of *Nyctanthes arbor-tristis* and their antifungal activity. *Journal of King Saud University - Science*, [online] 30(2), pp.168-175. Available at: <https://doi.org/10.1016/j.jksus.2016.10.002> [Accessed 26 Sep. 2024].

Jan, H., Shah, M., Andleeb, A., Faisal, S., Khattak, A., Rizwan, M., Drouet, S., Hano, C. and Abbasi, B.H., 2021. Plant-based synthesis of zinc oxide nanoparticles (ZnO-NPs) using aqueous leaf extract of *Aquilegia pubiflora*: Their antiproliferative activity against HepG2 cells inducing reactive oxygen species and other in vitro properties. *Oxidative Medicine and Cellular Longevity*, [online] 2021, p.e4786227. Available at: <https://doi.org/10.1155/2021/4786227> [Accessed 26 Sep. 2024].

Jasinski, G., Wozniak, L., Kalinowski, P. and Jasinski, P., 2018. Evaluation of the electronic nose used for monitoring environmental pollution. In *2018 XV International Scientific Conference on Optoelectronic and Electronic Sensors (COE)*, pp.1-4. Available at: <https://doi.org/10.1109/COE.2018.8435146> [Accessed 26 Sep. 2024].

Jayan, H., Pu, H. and Sun, D.W., 2020. Recent development in rapid detection techniques for microorganism activities in food matrices using bio-recognition: A review. *Trends in Food Science & Technology*, 95, pp.233-246. Available at: <https://doi.org/10.1016/j.tifs.2019.11.007> [Accessed 26 Sep. 2024].

Jia, W., Liang, G., Jiang, Z. and Wang, J., 2019a. Advances in electronic nose development for application to agricultural products. *Food Analytical Methods*, 12(10), pp.2226-2240. Available at: <https://doi.org/10.1007/s12161-019-01552-1> [Accessed 26 Sep. 2024].

Jia, W., Liang, G., Tian, H., Sun, J. and Wan, C., 2019. Electronic nose-based technique for rapid detection and recognition of moldy apples. *Sensors*, 19(7), p.1526. Available at: <https://doi.org/10.3390/s19071526> [Accessed 26 Sep. 2024].

Jia, W., Liang, G., Wang, Y. and Wang, J., 2018. Electronic noses as a powerful tool for assessing meat quality: A mini review. *Food Analytical Methods*, 11(10), pp.2916-2924. Available at: <https://doi.org/10.1007/s12161-018-1283-1> [Accessed 26 Sep. 2024].

Jiarpinijnun, A., Osako, K. and Siripatrawan, U., 2020. Visualization of volatonic profiles for early detection of fungal infection on storage Jasmine brown rice using electronic nose coupled with chemometrics. *Measurement*, 157, p.107561. Available at: <https://doi.org/10.1016/j.measurement.2020.107561> [Accessed 26 Sep. 2024].

Fracarolli, J.A., Dal Fabbro, I.M. and Nehmi de Oliveira, I., 2017. Papaya (*Carica papaya*) classification by software. *Journal of Agricultural Science and Technology B*, 7(4). Available at: <https://doi.org/10.17265/2161-6264/2017.04.004> [Accessed 26 Sep. 2024].

Zhang, J., Cheng, D., Wang, B., Khan, I. and Ni, Y., 2017. Ethylene control technologies in extending postharvest shelf life of climacteric fruit. *Journal of Agricultural and Food Chemistry*, 65(34), pp.7308-7319. Available at: <https://doi.org/10.1021/acs.jafc.7b02616> [Accessed 26 Sep. 2024].

Junior, J.R.d.S., Corrêa-Filho, L., Oliveira Pereira, V., Guimarães Barboza, H.T., Sá Ferreira, J.C., Gomes Soares, A., Tonon, R.V. and Cabral, L.M.C., 2024. Application of rosin resin and zinc oxide nanocomposites to chitosan coatings for extending the shelf life of passion fruits. *Sustainable Food Technology*. Available at: <https://doi.org/10.1039/D3FB00189J> [Accessed 26 Sep. 2024].

Kambale, E.K., Domingues, I., Zhang, W., Marotti, V., Chen, C., Hughes, K., Quetin-Leclercq, J. and Memvanga, P.B., 2024. 'Green' synthesized versus chemically synthesized zinc oxide nanoparticles: In vivo antihyperglycemic activity and pharmacokinetics. *International Journal of Pharmaceutics*, 650, p.123701. Available at: <https://doi.org/10.1016/j.ijpharm.2023.123701> [Accessed 26 Sep. 2024].

Kang, S.H., Cha, H.J., Jung, S.W. and Lee, S.J., 2022. Application of chitosan-ZnO nanoparticle edible coating to wild-simulated Korean ginseng root. *Food Science and Biotechnology*, 31(5), pp.579–586. doi: <https://doi.org/10.1007/s10068-022-01054-7>.

Kasampalis, D.S., Kalivas, A., Siomos, A., et al., 2020. Chlorophyll fluorescence, non-photochemical quenching and light harvesting complex as alternatives to color measurement, in classifying tomato fruit according to their maturity stage at harvest and in monitoring

postharvest ripening during storage. *Postharvest Biology and Technology*, 161, p.111036. Available at: <https://doi.org/10.1016/j.postharvbio.2019.111036> [Accessed 26 Sep. 2024].

Kashyap, P.L., Xiang, X. and Heiden, P., 2015. Chitosan nanoparticle-based delivery systems for sustainable agriculture. *International Journal of Biological Macromolecules*, 77, pp.36–51. Available at: <https://doi.org/10.1016/j.ijbiomac.2015.02.039> [Accessed 26 Sep. 2024].

Khan, R.U., Khan, K., Albattah, W. and Qamar, A.M., 2021. Image-based detection of plant diseases: From classical machine learning to deep learning journey. *Wireless Communications and Mobile Computing*, 2021, pp.1–13. Available at: <https://doi.org/10.1155/2021/5541859> [Accessed 26 Sep. 2024].

Kiani, S., Mineai, S. and Ghasemi-Varnamkhasti, M., 2016. Application of electronic nose systems for assessing quality of medicinal and aromatic plant products: A review. *Journal of Applied Research on Medicinal and Aromatic Plants*, 3(1), pp.1–9. Available at: <https://doi.org/10.1016/j.jarmap.2015.12.002> [Accessed 26 Sep. 2024].

Kołodziejczak-Radzimska, A. and Jesionowski, T., 2014. Zinc oxide—from synthesis to application: A review. *Materials*, 7(4), pp.2833–2881. Available at: <https://doi.org/10.3390/ma7042833> [Accessed 26 Sep. 2024].

Koul, B., Sharma, S., Kumar, N., Agarwal, S. and Prakash, A., 2022. Carica papaya L.: A tropical fruit with benefits beyond the tropics. *Diversity*, 14(8), p.683. Available at: <https://doi.org/10.3390/d14080683> [Accessed 26 Sep. 2024].

Kumar, A., Verma, L.M., Sharma, S. and Singh, N., 2023. Zinc oxide nanoparticles (ZnO NPs) stabilized by phyto cellulose derived biopolymer and their bipartite interaction studies with agriculturally important microbes/Raphanus sativus (L.) seeds. *Ceramics International*, 49(24), pp.39771–39787. Available at: <https://doi.org/10.1016/j.ceramint.2023.07.179> [Accessed 26 Sep. 2024].

Kumar, S., Bithel, N., Kumar, S., Kishan, Sen, M. and Banerjee, C., 2024. Phyto-mediated synthesis of zinc oxide nanoparticles from *Clerodendrum infortunatum* L. leaf extract and evaluation of antibacterial potential. *South African Journal of Botany*, 164, pp.146–151. Available at: <https://doi.org/10.1016/j.sajb.2023.11.029> [Accessed 26 Sep. 2024].

Kumar, S.D., Yasasve, M., Karthigadevi, G., Aashabharathi, M., Subbaiya, R., Karmegam, N. and Govarthan, M., 2021. Efficiency of microbial fuel cells in the treatment and energy recovery from food wastes: Trends and applications—A review. *Chemosphere*, 132439. Available at: <https://doi.org/10.1016/j.chemosphere.2021.132439> [Accessed 26 Sep. 2024].

Kumar, S. and Dutta, J., 2020. Chitosan-based nanocomposite films and coatings: Emerging antimicrobial food packaging alternatives. *Trends in Food Science & Technology*, 97, pp.196–209. Available at: <https://doi.org/10.1016/j.tifs.2020.01.002> [Accessed 26 Sep. 2024].

Kus, F., Altinkok, C., Zayim, E., Erdemir, S., Tasaltin, C. and Gurol, I., 2021. Surface acoustic wave (SAW) sensor for volatile organic compounds (VOCs) detection with calix[4]arene functionalized gold nanorods (AuNRs) and silver nanocubes (AgNCs). *Sensors and Actuators B: Chemical*, 330, p.129402. Available at: <https://doi.org/10.1016/j.snb.2020.129402> [Accessed 26 Sep. 2024].

Kushwaha, K., Saini, S.S., Waghmode, B., Gaid, M., Agrawal, P.K., Roy, P. and Sircar, D., 2021. Volatile components in papaya fruits are the non-invasive biomarkers to monitor the ripening stage and the nutritional value. *European Food Research and Technology*, 247(4), pp.907–919. Available at: <https://doi.org/10.1007/s00217-020-03673-y> [Accessed 26 Sep. 2024].

La, D. D., Nguyen-Tri, P., Le, K. H., Nguyen, P. T. M., Nguyen, M. D.-B., Vo, A. T. K., Nguyen, M. T. H., Chang, S. W., Tran, L. D., Chung, W. J., & Nguyen, D. D. (2021). Effects of antibacterial ZnO nanoparticles on the performance of a chitosan/gum arabic edible coating for post-harvest banana preservation. *Progress in Organic Coatings*, 151, 106057. <https://doi.org/10.1016/j.porgcoat.2020.106057>

Lakshmeesha, T. R., Murali, M., Ansari, M. A., Udayashankar, A. C., Alzohairy, M. A., Almatroudi, A., Alomary, M. N., Asiri, S. M. M., Ashwini, B. S., Kalagatur, N. K., Nayak, C. S., & Niranjana, S. R. (2020). Biofabrication of zinc oxide nanoparticles from *Melia azedarach* and its potential in controlling soybean seed-borne phytopathogenic fungi. *Saudi Journal of Biological Sciences*, 27(8), 1923–1930. <https://doi.org/10.1016/j.sjbs.2020.06.013>

Lakshmi, S., Rs, R., Ct, R., Nadagouda, S., & Nidoni, U. (2018). Effect of biosynthesized zinc oxide nanoparticles coating on quality parameters of fig (*Ficus carica* L.) fruit. *Journal of Pharmacognosy and Phytochemistry*, 7(3), 10–14. <https://www.phytojournal.com/archives/2018/vol7issue3/PartA/7-2-474-494.pdf> [Accessed 18 Mar. 2024]

Lavinia, M., Hibarturrahman, S.N., Harinata, H. and Wardana, A.A., 2019. Antimicrobial activity and application of nanocomposite coating from chitosan and ZnO nanoparticle to inhibit microbial growth on fresh-cut papaya. *Food Research*, 4(2), pp.307–311. [https://doi.org/10.26656/fr.2017.4\(2\).255](https://doi.org/10.26656/fr.2017.4(2).255)

Law, J. W.-F., Ab Mutalib, N.-S., Chan, K.-G., & Lee, L.-H. (2015). Rapid methods for the detection of foodborne bacterial pathogens: Principles, applications, advantages and limitations. *Frontiers in Microbiology*, 5, 770. <https://doi.org/10.3389/fmicb.2014.00770>

Le, K. H., Nguyen, M. D.-B., Tran, L. D., Nguyen Thi, H. P., Tran, C. V., Tran, K. V., Nguyen Thi, H. P., Dinh Thi, N., Yoon, Y. S., Nguyen, D. D., & La, D. D. (2021). A novel antimicrobial ZnO nanoparticles-added polysaccharide edible coating for the preservation of postharvest avocado under ambient conditions. *Progress in Organic Coatings*, *158*, 106339.

<https://doi.org/10.1016/j.porgcoat.2021.106339>

Levasseur-Garcia, C. (2018). Updated overview of infrared spectroscopy methods for detecting mycotoxins on cereals (corn, wheat, and barley). *Toxins*, *10*, 38.

<https://doi.org/10.3390/toxins10010038>

Li, C., Li, F., Wang, K., & Xie, D. (2024). Green and facile fabrication of multifunctional cellulose nanocrystal and carvacrol together reinforced chitosan bio-nanocomposite coatings for fruit preservation. *International Journal of Biological Macromolecules*, 130651.

<https://doi.org/10.1016/j.ijbiomac.2024.130651>

Li, J., Di, T., & Bai, J. (2019). Distribution of volatile compounds in different fruit structures in four tomato cultivars. *Molecules*, *24*(14), 2594.

Li, H., Brouwer, B., Oud, N., Verdonk, J. C., Tikunov, Y., Woltering, E., Schouten, R., & Pereira da Silva, F. (2021). Sensory, GC-MS and PTR-ToF-MS profiling of strawberries varying in maturity at harvest with subsequent cold storage. *Postharvest Biology and Technology*, *182*, 111719.

<https://doi.org/10.1016/j.postharvbio.2021.111719>

Li, M., Landahl, S., East, A. R., Verboven, P., & Terry, L. A. (2019). Optical coherence tomography—A review of the opportunities and challenges for postharvest quality evaluation. *Postharvest Biology and Technology*, *150*, 9–18.

<https://doi.org/10.1016/j.postharvbio.2018.12.005>

Li, Q., Gu, Y., & Wang, N. F. (2017). Application of random forest classifier by means of a QCM-based e-nose in the identification of Chinese liquor flavors. *IEEE Sensors Journal*, *17*(6), 1788–1794.

<https://doi.org/10.1109/JSEN.2017.2657653>

Li, Y., Zhou, Y., Wang, Z., Cai, R., Yue, T., & Cui, L. (2021). Preparation and characterization of chitosan–nano-ZnO composite films for preservation of cherry tomatoes. *Foods*, *10*(12), 3135.

<https://doi.org/10.3390/foods10123135>

Licen, S., Barbieri, G., Fabbris, A., Briguglio, S. C., Pillon, A., Stel, F., & Barbieri, P. (2018). Odor control map: Self-organizing map built from electronic nose signals and integrated by different instrumental and sensorial data to obtain an assessment tool for real environmental scenarios. *Sensors and Actuators B: Chemical*, *263*, 476–485.

<https://doi.org/10.1016/j.snb.2018.02.144>

- Lioutas, E. D., Charatsari, C., & De Rosa, M. (2021). Digitalization of agriculture: A way to solve the food problem or a trolley dilemma? *Technology in Society*, 67, 101744. <https://doi.org/10.1016/j.techsoc.2021.101744>
- Liu, C., Xiao, C., & Li, W. (2021). Zinc oxide nanoparticles as electron transporting interlayer in organic solar cells. *Journal of Materials Chemistry C*, 9(40), 14093–14114. <https://doi.org/10.1039/D1TC03434K>
- Liu, Q., Zhao, N., Zhou, D., Sun, Y., Sun, K., Pan, L., & Tu, K. (2018). Discrimination and growth tracking of fungi contamination in peaches using electronic nose. *Food Chemistry*, 262, 226-234. <https://doi.org/10.1016/j.foodchem.2018.04.100>
- Lou, Z., Wang, L., & Shen, G. (2018). Recent advances in smart wearable sensing systems. *Advanced Materials Technologies*, 3(12), 1800444. <https://doi.org/10.1002/admt.201800444>
- Luo, C.-X., Schnabel, G., Hu, M., & De Cal, A. (2022). Global distribution and management of peach diseases. *Phytopathology Research*, 4(1). <https://doi.org/10.1186/s42483-022-00134-0>
- Loutfi, A., Coradeschi, S., Mani, G. K., Shankar, P., & Rayappan, J. B. B. (2015). Electronic noses for food quality: A review. *Journal of Food Engineering*, 144, 103–111. <https://doi.org/10.1016/j.jfoodeng.2014.07.019>
- Madeshwari Ezhilan, Nesakumar, N., K. Jayanth Babu, Srinandan, C. S., & Bosco, J. (2018). An electronic nose for Royal Delicious apple quality assessment – A tri-layer approach. *Food Research International*, 109, 44–51. <https://doi.org/10.1016/j.foodres.2018.04.009>
- Madufor, N., Perold, W., & Opara, U. (2018). Detection of plant diseases using biosensors: A review. *Acta Horticulturae*, 1201, 83-90. <https://doi.org/10.17660/ActaHortic.2018.1201.12>
- Makarichian, A., Chayjan, R. A., Ahmadi, E., & Zafari, D. (2022). Early detection and classification of fungal infection in garlic (*A. sativum*) using electronic nose. *Computers and Electronics in Agriculture*, 192, 106575. <https://doi.org/10.1016/j.compag.2021.106575>
- Martinelli, F., Scalenghe, R., Davino, S., Panno, S., Scuderi, G., Ruisi, P., Villa, P., Stroppiana, D., Boschetti, M., Goulart, L. R., & Davis, C. E. (2015). Advanced methods of plant disease detection. A review. *Agronomy for Sustainable Development*, 35, 383–396. <https://doi.org/10.1007/s13593-015-0310-7>
- Mastilović, J., Kevrešan, Ž., Kukolj, D., Kovač, R., Samek, D.U., Stankovski, S., Ostojić, G. and Đerić, M., 2024. Sensors in postharvest technologies: Evidence from patent portfolio analysis.

Postharvest Biology and Technology, 208, p.112628. Available at:
<https://doi.org/10.1016/j.postharvbio.2023.112628> [Accessed 26 Sep. 2024].

Mohammad-Razdari, A., Rousseau, D., Bakhshipour, A., Taylor, S., Poveda, J. and Kiani, H., 2022. Recent advances in E-monitoring of plant diseases. *Biosensors and Bioelectronics*, 201, p.113953. <https://doi.org/10.1016/j.bios.2021.113953>

Mohd Israfi, N.A., Mohd Ali, M.I.A., Manickam, S., Sun, X., Goh, B.H., Tang, S.Y., Ismail, N., Abdull Razis, A.F., Ch'ng, S.E. and Chan, K.W., 2022. Essential oils and plant extracts for tropical fruits protection: From farm to table. *Frontiers in Plant Science*, [online] 13.
<https://doi.org/10.3389/fpls.2022.999270>

Mohd Yusof, H., Mohamad, R., Zaidan, U.H. and Abdul Rahman, N.A. (2019). Microbial synthesis of zinc oxide nanoparticles and their potential application as an antimicrobial agent and a feed supplement in animal industry: a review. *Journal of Animal Science and Biotechnology*, 10(1).
[doi:https://doi.org/10.1186/s40104-019-0368-z](https://doi.org/10.1186/s40104-019-0368-z).

Mehmood, S., Ahmed, W., Rizwan, M., Bundschuh, J., Elnahal, S.M.A. and Li, W., 2024. Green synthesized zinc oxide nanoparticles for removal of carbamazepine in water and soil systems. *Separation and Purification Technology*, 334, pp.125988–125988.
<https://doi.org/10.1016/j.seppur.2023.125988>

Mosquera-Sánchez, L.P., Arciniegas-Grijalba, P.A., Patiño-Portela, M.C., Guerra-Sierra, B.E., Muñoz-Florez, J.E. and Rodríguez-Páez, J.E., 2020. Antifungal effect of zinc oxide nanoparticles (ZnO-NPs) on *Colletotrichum* sp., causal agent of anthracnose in coffee crops. *Biocatalysis and Agricultural Biotechnology*, 25, p.101579. <https://doi.org/10.1016/j.bcab.2020.101579>

Mustika, R. and Wardana, A.A., 2020. Nanocomposite coating based on chitosan and ZnO nanoparticles to maintain the storage quality of meatball. *Food Research*, 4(6), pp.1867–1870.
[https://doi.org/10.26656/fr.2017.4\(6\).169](https://doi.org/10.26656/fr.2017.4(6).169)

Naiel, B., Fawzy, M., Halmy, M.W.A. and Mahmoud, A.E.D., 2022. Green synthesis of zinc oxide nanoparticles using *Limonium pruinatum* L. Chaz. extract: characterization, evaluation of anti-skin cancer, antimicrobial and antioxidant potentials. *Scientific Reports*, [online] 12(1), p.20370.
<https://doi.org/10.1038/s41598-022-24805-2>

Naseer, M., Aslam, U., Khalid, B. and Chen, B. (2020). Green route to synthesize Zinc Oxide Nanoparticles using leaf extracts of *Cassia fistula* and *Melia azadarach* and their antibacterial potential. *Scientific Reports*, 10(1). [doi:https://doi.org/10.1038/s41598-020-65949-3](https://doi.org/10.1038/s41598-020-65949-3).

Nataraj, K., Vanishree, S., Murali, M. and Amruthesh, K.N., 2024. Bio-fabrication, characterization and biological properties of zinc oxide nanoparticles (ZnO-NPs) from scarlet morning glory - *Ipomoea hederifolia*. *Materials Chemistry and Physics*, [online] 314, p.128873. <https://doi.org/10.1016/j.matchemphys.2023.128873>

Ncama, K., Magwaza, L.S., Mditshwa, A. and Tesfay, S.Z., 2018. Plant-based edible coatings for managing postharvest quality of fresh horticultural produce: A review. *Food Packaging and Shelf Life*, 16, pp.157–167. <https://doi.org/10.1016/j.fpsl.2018.03.011>

Nouri, B., Mohtasebi, S.S. and Rafiee, S., 2020. Quality detection of pomegranate fruit infected with fungal disease. *International Journal of Food Properties*, 23(1), pp.9–21. <https://doi.org/10.1080/10942912.2019.1705851>

Obianom, C., Romanazzi, G. and Sivakumar, D., 2019. Effects of chitosan treatment on avocado postharvest diseases and expression of phenylalanine ammonia-lyase, chitinase and lipoxygenase genes. *Postharvest Biology and Technology*, 147, pp.214–221. <https://doi.org/10.1016/j.postharvbio.2018.10.004>

Okon, W.I., et al., 2017. Nutritional Quality of Raw and Processed Unripe *Carica papaya* Fruit Pulp and Its Contribution to Dietary Diversity and Food Security in Some Peasant Communities in Nigeria. *International Journal of Biological and Chemical Sciences*, 11(3), p.1000. <https://doi.org/10.4314/ijbcs.v11i3.5>. Accessed 21 Nov. 2020.

Oladzabbasabadi, N., Mohammadi Nafchi, A., Ariffin, F. and Karim, A.A., 2023. Bioactive Nano-Based Packaging for Postharvest Storage of Horticultural Produce. In: *CRC Press eBooks*, pp.221–236. <https://doi.org/10.1201/9781003142287-11>

Palou, L. and Smilanick, J.L. (eds.) (2019) *Postharvest Pathology of Fresh Horticultural Produce*. CRC Press. doi: <https://doi.org/10.1201/9781315209180>.

Palumbo, M., Attolico, G., Capozzi, V., Cozzolino, R., Corvino, A., de Chiara, M.L.V., Pace, B., Pelosi, S., Ricci, I., Romaniello, R. and Cefola, M. (2022) ‘Emerging postharvest technologies to enhance the shelf-life of fruit and vegetables: An overview’, *Foods*, 11(23), p. 3925. doi: <https://doi.org/10.3390/foods11233925>.

Pan, L., Zhang, W., Zhu, N., Mao, S. and Tu, K. (2014) ‘Early detection and classification of pathogenic fungal disease in postharvest strawberry fruit by electronic nose and gas

chromatography–mass spectrometry’, *Food Research International*, 62, pp. 162–168. doi: <https://doi.org/10.1016/j.foodres.2014.02.020>.

Pan, Y., Jiang, Y., Huang, Q., Zhu, Y., Nie, Y., Yuan, R. and Zhang, Z. (2022) ‘Abnormal chilling injury of postharvest papaya is associated with the antioxidant response’, *Journal of Food Biochemistry*, 46(10). doi: <https://doi.org/10.1111/jfbc.14272>.

Panjaworayan, N., T-Thienprasert, J., Ruangtong, J., Jaithon, T., Huehne, P.S. and Piasai, O., 2021. Large Scale Synthesis of Green Synthesized Zinc Oxide Nanoparticles from Banana Peel Extracts and Their Inhibitory Effects against *Colletotrichum* sp., Isolate KUFC 021, Causal Agent of Anthracnose on Dendrobium Orchid. *Journal of Nanomaterials*, 2021, pp.1–10. <https://doi.org/10.1155/2021/5625199>

Parven, A., Sarker, Md.R., Megharaj, M. and Md. Meftaul, I. (2020) ‘Prolonging the shelf life of papaya (*Carica papaya* L.) using Aloe vera gel at ambient temperature’, *Scientia Horticulturae*, 265, p. 109228. doi: <https://doi.org/10.1016/j.scienta.2020.109228>.

Pascale, R., Bianco, G., Calace, S., Masi, S., Mancini, I.M., Mazzone, G. and Caniani, D. (2018) ‘Method development and optimization for the determination of benzene, toluene, ethylbenzene and xylenes in water at trace levels by static headspace extraction coupled to gas chromatography–barrier ionization discharge detection’, *Journal of Chromatography A*, 1548, pp. 10–18. doi: <https://doi.org/10.1016/j.chroma.2018.03.018>.

Patel, H.K. (2014) *The Electronic Nose: Artificial Olfaction Technology*. Biological and Medical Physics, Biomedical Engineering. New Delhi: Springer India. doi: 10.1007/978-81-322-1548-6.

Pattyn, J., Vaughan-Hirsch, J. and Van de Poel, B. (2020) ‘The regulation of ethylene biosynthesis: A complex multilevel control circuitry’, *New Phytologist*, 229(2), pp. 770–782. doi: <https://doi.org/10.1111/nph.16873>.

Peris, M. and Escuder-Gilabert, L. (2016) ‘Electronic noses and tongues to assess food authenticity and adulteration’, *Trends in Food Science & Technology*, 58, pp. 40–54. doi: <https://doi.org/10.1016/j.tifs.2016.10.014>.

Petrasch, S., Silva, C.J., Mesquida-Pesci, S.D., Gallegos, K., van den Abeele, C., Papin, V., Fernandez-Acero, F.J., Knapp, S.J. and Blanco-Ulate, B. (2019) ‘Infection strategies deployed by *Botrytis cinerea*, *Fusarium acuminatum*, and *Rhizopus stolonifer* as a function of tomato fruit ripening stage’, *Frontiers in Plant Science*, 10. doi: <https://doi.org/10.3389/fpls.2019.00223>.

- Pinnamaneni, R. (2017) 'Nutritional and medicinal value of papaya (*Carica papaya* Linn.)', *World Journal of Pharmacy and Pharmaceutical Sciences*, 6(8), pp. 2559–2578. doi: <https://doi.org/10.20959/wjpps20178-9947>.
- Prasad, K., Jacob, S. and Siddiqui, M.W. (2018) 'Fruit maturity, harvesting, and quality standards', *Preharvest Modulation of Postharvest Fruit and Vegetable Quality*, pp. 41–69. doi: <https://doi.org/10.1016/b978-0-12-809807-3.00002-0>.
- Pohanka, M. (2018) 'Overview of piezoelectric biosensors, immunosensors and DNA sensors and their applications', *Materials*, 11(3), p. 448. doi: <https://doi.org/10.3390/ma11030448>.
- Pölitiz, C. (2016) 'Supervised extraction of usage patterns in different document representations', in *Solving Large Scale Learning Tasks. Challenges and Algorithms*. Cham: Springer, pp. 346–361. doi: https://doi.org/10.1007/978-3-319-41706-6_19.
- Qiu, S. and Wang, J. (2015) 'Application of sensory evaluation, HS-SPME GC-MS, E-nose, and E-tongue for quality detection in citrus fruits', *Journal of Food Science*, 80(10), pp. S2296–S2304. doi: <https://doi.org/10.1111/1750-3841.13012>.
- Ragazou, K., Garefalakis, A., Zafeiriou, E. and Passas, I. (2022) 'Agriculture 5.0: A new strategic management mode for a cut cost and an energy efficient agriculture sector', *Energies*, 15(9), p. 3113. doi: <https://doi.org/10.3390/en15093113>.
- Rajin, S.A.K., Samad, S.A. and Muad, A.M. (2015) 'Postharvest quality evaluation of grapes using non-destructive electronic nose', *Journal of Electrical and Electronics Engineering*, 8(2), p. 35.
- Ramadan, N.S., Wessjohann, L.A., Mocan, A., C Vodnar, D., El-Sayed, N.H., El-Toumy, S.A., Abdou Mohamed, D., Abdel Aziz, Z., Ehrlich, A. and Farag, M.A. (2020) 'Nutrient and sensory metabolites profiling of *Averrhoa carambola* L. (starfruit) in the context of its origin and ripening stage by GC/MS and chemometric analysis', *Molecules*, 25(10), p. 2423.
- Rasha, E., Monerah, A., Manal, A., Rehab, A., Mohammed, D. and Doaa, E. (2021) 'Biosynthesis of zinc oxide nanoparticles from *Acacia nilotica* (L.) extract to overcome carbapenem-resistant *Klebsiella pneumoniae*', *Molecules*, 26(7), p. 1919. doi: <https://doi.org/10.3390/molecules26071919>.
- Ray, M., Ray, A., Dash, S., Mishra, A., Achary, K.G., Nayak, S. and Singh, S. (2017) 'Fungal disease detection in plants: Traditional assays, novel diagnostic techniques and biosensors', *Biosensors and Bioelectronics*, 87, pp. 708–723. doi: <https://doi.org/10.1016/j.bios.2016.09.032>.

Rodrigues, J.P., de Souza Coelho, C.C., Soares, A.G. and Freitas-Silva, O. (2021) 'Current technologies to control fungal diseases in postharvest papaya (*Carica papaya* L.)', *Biocatalysis and Agricultural Biotechnology*, 36, p. 102128. doi: <https://doi.org/10.1016/j.bcab.2021.102128>.

Romanazzi, G., Feliziani, E. and Sivakumar, D. (2018) 'Chitosan, a biopolymer with triple action on postharvest decay of fruit and vegetables: Eliciting, antimicrobial and film-forming properties', *Frontiers in Microbiology*, 9. doi: <https://doi.org/10.3389/fmicb.2018.02745>.

Roohallah Saberi Riseh, R., Vatankhah, M., Hassanisaadi, M. and Kennedy, J.F. (2023) 'Chitosan-based nanocomposites as coatings and packaging materials for the postharvest improvement of agricultural product: A review', *Carbohydrate Polymers*, 309, p. 120666. doi: <https://doi.org/10.1016/j.carbpol.2023.120666>.

Ruslan, R. and Roslan, N. (2016) 'Assessment on the skin color changes of *Carica papaya* L

Sanaeifar, A., Mohtasebi, S.S., Ghasemi-Varnamkhasti, M. and Ahmadi, H., 2016. Application of MOS based electronic nose for the prediction of banana quality properties. *Measurement*, 82, pp.105–114. doi: <https://doi.org/10.1016/J.MEASUREMENT.2015.12.041>.

Sanaeifar, A., ZakiDizaji, H., Jafari, A. and de la Guardia, M., 2017. Early detection of contamination and defect in foodstuffs by electronic nose: A review. *TrAC Trends in Analytical Chemistry*, 97, pp.257–271. doi: <https://doi.org/10.1016/J.TRAC.2017.09.014>.

Seesaard, T., Thippakorn, C., Kerdcharoen, T. and Kladsomboon, S., 2020. A hybrid electronic nose system for discrimination of pathogenic bacterial volatile compounds. *Analytical Methods*, 12(47), pp.5671–5683. doi: <https://doi.org/10.1039/d0ay01255f>.

Semagn, K., 2014. Leaf tissue sampling and DNA extraction protocols. In: *Molecular Plant Taxonomy*. Totowa, NJ: Humana Press, pp.53–67. doi: https://doi.org/10.1007/978-1-62703-767-9_3.

Shaikh, P.M.M., Butala, N., Sharma, S. and Sukumaran, S., 2017. Review on diagnosis the plant disease at early stage. *International Journal of Advanced Research in Computer and Communication Engineering*, 6, pp.321–324. doi: <http://dx.doi.org/10.17148/IJARCCCE.2017.6372>.

Sharma, N., Aggarwal, N., Kumari, S., Patial, P., Kumar, N., Ali, D. and Tripathi, S., 2023. Exploring physicochemical characteristics and antimicrobial efficacy of biosynthesized Zinc

- oxide nanoparticles using Lantana Camara leaf extract. *Journal of Molecular Structure*, p.137396. doi: <https://doi.org/10.1016/j.molstruc.2023.137396>.
- Shen, F., Wu, Q., Liu, P., Jiang, X., Fang, Y. and Cao, C., 2018. Detection of *Aspergillus* spp. contamination levels in peanuts by near infrared spectroscopy and electronic nose. *Food Control*, 93, pp.1–8. doi: <https://doi.org/10.1016/j.foodcont.2018.05.039>.
- Shi, C., Xiang, L. and Guo, J., 2024. Exploring the frontier of fruit diseases management: Advances in nano-based and biocontrol strategies and underlying action mechanism. *South African Journal of Botany*, 166, pp.612–623. doi: <https://doi.org/10.1016/j.sajb.2024.01.060>.
- Shi, H., Zhang, M. and Adhikari, B., 2019. Advances of electronic nose and its application in fresh foods: A review. *Critical Reviews in Food Science and Nutrition*, 58(16), pp.2700–2710. doi: <https://doi.org/10.1080/10408398.2017.1327419>.
- Singh, A., Rahman, Md.A., Sharma, R. and Yemmireddy, V., 2021. Papaya ripeness and post-harvest storage conditions affect growth, survival and death kinetics of *Salmonella* and spoilage organisms. *Postharvest Biology and Technology*, 181, p.111659. doi: <https://doi.org/10.1016/j.postharvbio.2021.11165>.
- Singh, D. and Sharma, R.R., 2018. Postharvest Diseases of Fruits and Vegetables and Their Management. In: *Postharvest Disinfection of Fruits and Vegetables*. pp.1–52. doi: <https://doi.org/10.1016/b978-0-12-812698-1.00001-7>.
- Singh, K., Nancy, Singh, G. and Singh, J., 2022. Sustainable synthesis of biogenic ZnO NPs for mitigation of emerging pollutants and pathogens. *Environmental Research*, p.114952. doi: <https://doi.org/10.1016/j.envres.2022.114952>.
- Song, J., Chen, Q., Bi, J., Meng, X., Wu, X., Qiao, Y. and Lyu, Y., 2020. GC/MS coupled with MOS e-nose and flash GC e-nose for volatile characterization of Chinese jujubes as affected by different drying methods. *Food Chemistry*, 331, p.127201. doi: <https://doi.org/10.1016/j.foodchem.2020.127201>.
- Sucharitha, K.V., Beulah, A.M. and Ravikiran, K., 2018. Effect of chitosan coating on storage stability of tomatoes (*Lycopersicon esculentum* Mill). *International Food Research Journal*, 25(1), pp.93–99.
- Suchorab, Z., Frąc, M., Guz, Ł., Oszust, K., Łagód, G., Gryta, A., Bilińska-Wielgus, N. and Czerwiński, J., 2019. A method for early detection and identification of fungal contamination of

building materials using e-nose. *PLoS ONE*, 14(4), p.e0215179. doi: <https://doi.org/10.1371/journal.pone.0215179>.

Sundaram, S. and Prabhakaran, J., 2017. Effect of 1-methylcyclopropene (1-MCP) on volatile compound production in papaya (*Carica papaya* L.) fruit. *Pharmaceutical Innovation Journal*, 6, pp.532–536.

Tait, E., Perry, J.D., Stanforth, S.P. and Dean, J.R., 2014. Use of volatile compounds as a diagnostic tool for the detection of pathogenic bacteria. *TrAC Trends in Analytical Chemistry*, 53, pp.117–125. doi: <https://doi.org/10.1016/j.trac.2013.08.011>.

Taghipour, S., Ehtesham Nia, A., Hokmabadi, H. and Martínez-Gómez, P., 2024. Physicochemical and quality characters of fresh pistachio (*Pistacia vera* L.) cultivars in response to chitosan/ZnO nanocomposite coating. *Food Chemistry*, 435, p.137136. doi: <https://doi.org/10.1016/j.foodchem.2023.137136>.

Tan, G.H., Ali, A. and Siddiqui, Y., 2022. Current strategies, perspectives and challenges in management and control of postharvest diseases of papaya. *Scientia Horticulturae*, 301, p.111139. doi: <https://doi.org/10.1016/j.scienta.2022.111139>.

Tan, G.H., Ali, A. and Siddiqui, Y., 2023. Major fungal postharvest diseases of papaya: Current and prospective diagnosis methods. *Crop Protection*, 174, p.106399. doi: <https://doi.org/10.1016/j.cropro.2023.106399>.

Udavatha Premchand, Mesta, R.K., Venkatappa Devappa, M.P., Basavarajappa, V., Venkataravanappa, Reddy, L. and Shankarappa, K.S., 2023. Survey, Detection, Characterization of Papaya Ringspot Virus from Southern India and Management of Papaya Ringspot Disease. *Pathogens*, 12(6), p.824. doi: <https://doi.org/10.3390/pathogens12060824>.

Ungureanu-Comanita, E.D., Cosbuc, E.L., Cozma, P., Smaranda, C. and Gavrilesu, M., 2020. Human Health Risks Concerning Food Waste Management. In: 2020 *International Conference on e-Health and Bioengineering (EHB)*. IEEE. doi: <https://doi.org/10.1109/EHB50910.2020.9280298>.

Utpala, R., Yadav, S., Rawat, S.S. and Sundaram, S., 2021. Effect of edible coating of chitosan-ZnO nanoparticles on postharvest quality and storage life of papaya (*Carica papaya* L.). *International Journal of Fruit Science*, 21(1), pp.1186–1201. doi: <https://doi.org/10.1080/15538362.2021.1946355>.

- Vasco, C., Torres, B., Jácome, E., Torres, A., Eche, D. and Velasco, C., 2021. Use of chemical fertilizers and pesticides in frontier areas: A case study in the Northern Ecuadorian Amazon. *Land Use Policy*, 107, p.105490. doi: <https://doi.org/10.1016/j.landusepol.2021.105490>.
- Venkatesan, S., Suresh, S., Arumugam, J., Ramu, P., Pugazhenthiran, N., Jothilakshmi, R. and Prabu, K.M., 2024. Sunlight assisted degradation of methylene blue by zinc oxide nanoparticles green synthesized using *Vitex negundo* plant leaf extract. *Results in Chemistry*, 7, pp.101315–101315. doi: <https://doi.org/10.1016/j.rechem.2024.101315>.
- Ventura-Aguilar, R.I., Bautista-Baños, S., Hernández-López, M. and Llamas-Lara, A., 2021. Detection of *Alternaria alternata* in tomato juice and fresh fruit by the production of its biomass, respiration, and volatile compounds. *International Journal of Food Microbiology*, 342, p.109092. doi: <https://doi.org/10.1016/j.ijfoodmicro.2021.109092>.
- Viejo, C.G., Fuentes, S., Godbole, A., Widdicombe, B. and Unnithan, R.R., 2020. Development of a low-cost e-nose to assess aroma profiles: An artificial intelligence application to assess beer quality. *Sensors and Actuators B: Chemical*, 308, p.127688. doi: <https://doi.org/10.1016/j.snb.2020.127688>.
- Vinod, B.R., Ram, A., Sethi, S., Prakash, J., Meena, N.K., Menaka, M., Mishra, S.S. and Shivaswamy, G., 2023. Recent advances in physical treatments of papaya fruit for postharvest quality retention: A review. *eFood*, 4(2). doi: <https://doi.org/10.1002/efd2.79>.
- Vishnu Sankar Sivasankarapillai, V., Krishnamoorthy, N., Eldesoky, G.E., Wabaidur, S.M., Islam, A., Dhanusuraman, R. and Ponnusamy, V.K., 2022. One-pot green synthesis of ZnO nanoparticles using *Scoparia dulcis* plant extract for antimicrobial and antioxidant activities. *Applied Nanoscience*, 13(9), pp.6093–6103. doi: <https://doi.org/10.1007/s13204-022-02610-7>.
- Voss, H.G.J., Ayub, R.A. and Stevan, S.L., 2020. E-nose prototype to monitor the growth and maturation of peaches in the orchard. *IEEE Sensors Journal*, 20(20), pp.11741–11750. doi: <https://doi.org/10.1109/JSEN.2020.3000070>.
- Voss, H.G.J., Stevan Jr, S.L. and Ayub, R.A., 2019. Peach growth cycle monitoring using an electronic nose. *Computers and Electronics in Agriculture*, 163, p.104858. doi: <https://doi.org/10.1016/j.compag.2019.104858>.
- Wang, M. and Chen, Y., 2023. Electronic nose and its application in the food industry: a review. *European Food Research and Technology*. doi: <https://doi.org/10.1007/s00217-023-04381-z>.

Wei, L. and Guohua, H., 2015. Kiwi fruit (*Actinidia chinensis*) quality determination based on surface acoustic wave resonator combined with electronic nose. *Bioengineered*, 6(1), pp.53–61. doi: <https://doi.org/10.1080/21655979.2014.996430>.

Wen, T., Zheng, L., Dong, S., Gong, Z., Sang, M., Long, X., Luo, M. and Peng, H., 2019. Rapid detection and classification of citrus fruit infestation by *Bactrocera dorsalis* (Hendel) based on electronic nose. *Postharvest Biology and Technology*, 147, pp.156–165. doi: <https://doi.org/10.1016/j.postharvbio.2018.09.017>.

Wilson, A.D., 2018. Application of electronic-nose technologies and VOC-biomarkers for the noninvasive early diagnosis of gastrointestinal diseases. *Sensors*, 18(8), p.2613. doi: <https://doi.org/10.3390/s18082613>.

Xu, S., Sun, X., Lu, H., Yang, H., Ruan, Q., Huang, H. and Chen, M., 2018. Detecting and monitoring the flavor of tomato (*Solanum lycopersicum*) under the impact of postharvest handlings by physicochemical parameters and electronic nose. *Sensors*, 18(6), p.1847. doi: <https://doi.org/10.3390/s18061847>.

Yakubu, H.G., Kovacs, Z., Toth, T. and Bazar, G., 2021. Trends in artificial aroma sensing by means of electronic nose technologies to advance dairy production – a review. *Critical Reviews in Food Science and Nutrition*, pp.1–15. doi: <https://doi.org/10.1080/10408398.2021.1945533>.

Yang, X., Hameed, U., Zhang, A., Zang, H., Gu, C., Chen, Y. and Xu, Y., 2017. Development of a nested-PCR assay for the rapid detection of *Pilidiella granati* in pomegranate fruit. *Scientific Reports*, 7(1). doi: <https://doi.org/10.1038/srep40954>.

Ying, X., Liu, W. and Hui, G., 2015. Litchi freshness rapid non-destructive evaluating method using electronic nose and non-linear dynamics stochastic resonance model. *Bioengineered*, 6(4), pp.218–221. doi: <https://doi.org/10.1080/21655979.2015.1011032>.

Zakaria, L., 2021. Diversity of *Colletotrichum* species associated with anthracnose disease in tropical fruit crops—A review. *Agriculture*, 11(4), p.297. doi: <https://doi.org/10.3390/agriculture11040297>.

Zakaria, L., 2023. *Fusarium* species associated with diseases of major tropical fruit crops. *Horticulturae*, 9(3), p.322. doi: <https://doi.org/10.3390/horticulturae9030322>.

Zeghoud, S., Hemmami, H., Ben Seghir, B., Ben Amor, I., Kouadri, I., Rebiai, A., Messaoudi, M., Ahmed, S., Pohl, P. and Simal-Gandara, J., 2022. A review on biogenic green synthesis of ZnO

nanoparticles by plant biomass and their applications. *Materials Today Communications*, 33, p.104747. doi: <https://doi.org/10.1016/j.mtcomm.2022.104747>.

Zhang, H., Huang, D., Pu, D., Zhang, Y., Chen, H., Sun, B. and Ren, F., 2020. Multivariate relationships among sensory attributes and volatile components in commercial dry porcini mushrooms (*Boletus edulis*). *Food Research International*, 133, p.109112. doi: <https://doi.org/10.1016/j.foodres.2020.109112>.

Zhang, L., Huang, C., Zhao, Y., Zheng, C. and Hu, C., 2023. Post-ripening and senescence behavior of atemoya (*Annona cherimola* × *A. squamosa*) under two typical storage temperatures. *Postharvest Biology and Technology*, 200, p.112336. doi: <https://doi.org/10.1016/j.postharvbio.2023.112336>.

Zhang, M., Wu, J., Shi, Z., Cao, A., Fang, W., Yan, D., Wang, Q. and Li, Y., 2022. Molecular methods for identification and quantification of foodborne pathogens. *Molecules*, 27(23), pp.8262–8262. doi: <https://doi.org/10.3390/molecules27238262>.

Zhang, Z., Chen, T., Li, B., Qin, G. and Chen, Y., 2021. Molecular basis of pathogenesis of postharvest pathogenic fungi and control strategy in fruits: progress and prospect. *Molecular Horticulture*, 1(2). doi: <https://doi.org/10.1186/s43897-021-00004-x>.

Zhao, X., Lin, C.W., Wang, J. and Oh, D.H., 2014. Advances in rapid detection methods for foodborne pathogens. *Journal of Microbiology and Biotechnology*, 24(3), pp.297–312. doi: <https://doi.org/10.4014/jmb.1310.10013>.

Zhao, X., Zhang, J., Ming, H., Zou, W.E., Wang, Y., Zhao, C., Mu, S., Zhang, H.A. and Qiu, L.I., 2016. Research on pork jerky obtained through fermentation with *Pediococcus acidilactici*. *Polish Journal of Food and Nutrition Sciences*, 66, pp.25–29.

Zheng, Z. and Zhang, C., 2022. Electronic noses based on metal oxide semiconductor sensors for detecting crop diseases and insect pests. *Computers and Electronics in Agriculture*, 197, p.106988. doi: <https://doi.org/10.1016/j.compag.2022.106988>.

Zheng, X., Su, Y., Chen, Y., Wan, R., Liu, K., Li, M. and Yin, D., 2014. Zinc oxide nanoparticles cause inhibition of microbial denitrification by affecting transcriptional regulation and enzyme activity. *Environmental Science & Technology*, 48(23), pp.13800–13807. doi: <https://doi.org/10.1021/es504251v>.

Zhou, X., Li, X., Zhao, B., Chen, X. and Zhang, Q., 2022. Discriminant analysis of vegetable oils by thermogravimetric-gas chromatography/mass spectrometry combined with data fusion and

chemometrics without sample pretreatment. *LWT*, 161, p.113403. doi: <https://doi.org/10.1016/j.lwt.2022.113403>.

Zhou, X.Q., Hayat, Z., Zhang, D.D., Li, M.Y., Hu, S., Wu, Q., Cao, Y.F. and Yuan, Y., 2023. Zinc oxide nanoparticles: synthesis, characterization, modification, and applications in food and agriculture. *Processes*, 11(4), p.1193. doi: <https://doi.org/10.3390/pr11041193>.

Zhu, W., Hu, C., Ren, Y., Lu, Y., Song, Y., Ji, Y., Han, C. and He, J., 2021. Green synthesis of zinc oxide nanoparticles using *Cinnamomum camphora* (L.) Presl leaf extracts and its antifungal activity. *Journal of Environmental Chemical Engineering*, 9(6), p.106659. doi: <https://doi.org/10.1016/j.jece.2021.106659>.